Development of a full process simulation package for tail gas cleaning from melamine production with ionic liquids

Duan, Yuanmeng

Publication date:
2023

Document Version
Publisher's PDF, also known as Version of record

Process and System Engineering Center

Department of Chemical and Biochemical Engineering

Technical University of Denmark

Development of a full process simulation package for tail gas cleaning from melamine production with ionic liquids

PhD Thesis by

Yuanmeng Duan

April 2023

Development of a full process simulation package for tail gas cleaning from melamine production with ionic liquids

PhD Thesis

April 2023

By

Yuanmeng Duan

Published by: Process and System Engineering Center
Department of Chemical and Biochemical Engineering
Technical University of Denmark
Søltofts Plads, 228A, 2800 Kgs. Lyngby, Denmark

PhD thesis

Process and System Engineering Center

Department of Chemical and Biochemical Engineering

Technical University of Denmark

Development of a full process simulation package for tail gas cleaning from melamine production with ionic liquids

This thesis was prepared by

Yuanmeng Duan

Supervised by

Associate Professor Jakob Kjøbsted Huusom (main supervisor)

Associate Professor Jens Abildskov (co-supervisor)

Professor Xiangping Zhang (co-supervisor)

Assessment committee

Associate Professor Xiaodong Liang

Senior Lecture Isuru Udugama

Principal Scientist Eirini Karakatsani

Preface

This thesis is the result of my Ph.D. project conducted at PROSYS, Department of Chemical and Biochemical Engineering, Technical University of Denmark, and Beijing Key Laboratory of Ionic Liquids Clean Process, Institute of Process Engineering, Chinese Academy of Sciences. This Ph.D. project was carried out from October 2019 to April 2023, under the supervision of Professor Jakob Kjøbsted Huusom and co-supervisors Professor Jens Abildskov, and Professor Xiangping Zhang. The work was funded by grants jointly provided by the Department of Chemical and Biochemical Engineering, Technical University of Denmark, Denmark, and the Institute of Process Engineering, Chinese Academy of Sciences, China.

Yuanmeng Duan

April 2023

Kgs. Lyngby, Denmark

Acknowledgements

I owe a big thanks to my parents for their unlimited patient support and never-ending love for me.

I would like to express my special appreciation to my supervisors, professor Jakob Kjøbsted Huusom and co-supervisors, Professor Jens Abildskov, and Professor Xiangping Zhang, for giving me the chance of this position. Their patient help and valuable guidance always support me during these difficult three years. Thanks to professor Shaojuan Zeng and Haifeng Dong for the external stay in China, and I cherish the cooperation experience of the industrial application of this work in IPE.

I sincerely thank my former and current colleagues at PROSYS at DTU and the cleaning energy group in IPE. Thanks to Jess, Paul, Joachim, Jesper, Mads, Peter and Adam for helpful suggestions in my project and my staying in Denmark. Special thanks to Joachim for the translation of Danish abstract. Thanks to Guoxiong Zhan, Fei Chang, Sensen Shi, Zongyuan Hu, and Zhixing Wu for their help and support on my project during my external stay in IPE. A special thanks to Anja, Gitte, Ditte and Qiu.

Thanks to the good friends I made during my PhD for helping me get the best out of life possible. Name a few I would like to thank (in no particular order): Jingyu, Ziran, Fa, Chonghui, Yuchen, Ruru, Zhiwei, Zhaoqing and other friends. You all brighten my life in Denmark, and I will cherish the days we have.

I would like to thank my best friend Xiaobin, who light on my life over these three years, and Jingju, my previous colleague in Aspen, with a lot of help in my simulation work. Thanks to all my friends in China, especially Jia, Jun, Chengxiang, Yitu and Jianjun, for your encouragement to me.

Thanks to everybody else who has been a part of my life and work at DTU and IPE for all of your help and support.

Yuanmeng Duan

April 2023

Kgs. Lyngby, Denmark

Abstract

Melamine production is known to produce a tail gas with a significant amount of NH_3 and CO_2. The most common separation methods applied to melamine tail gas are water scrubbing and urea co-production technology. With good stability, non-volatility and tailored properties, ionic liquids (ILs) are regarded as vital potential solvents for gas separation. Therefore, two new process technologies, one is the ionic liquid-based process (IL-0), and the other is the enhanced ionic liquid process (IL-En) were employed and evaluated for energy and cost efficiency. The IL-En employs stripping on the treatment of melamine tail gas. The protic ionic liquid named 1-butyl imidazolium bis (trifluoromethylsulfonyl) imide ([Bim][NTf_2]) was selected for the evaluation of the melamine tail gas cleaning process. Thermodynamic data were fitted to the NRTL equations. Three full process flowsheets were simulated in Aspen Plus V11 ^{TM}. A basic and an enhanced ionic liquid process (IL-0 and IL-En), a conventional water scrubbing (WS) technology as a comparison, process sensitivity analysis and energy/economic evaluation were carried out. The results showed that the total separation cost of the IL-En can be reduced by 61% compared to that of the WS process. Moreover, the IL-based flowsheet is simpler than WS and avoids wastewater discharge.

In order to give deep analysis of the proposed technology, a detailed multi-objective optimization (MOO) for the NH_3/CO_2 separation of the tail gas by IL in technical-energy-economic evaluation. According to the optimization results, specific cases with different objective functions were chosen, and the relationship between key parameters was analyzed. The results showed that the ionic liquid-based technology could realize a better performance regarding the technical-energy-economic than the base case. Deeper analyses with the influence of operation parameters with evaluation index were carried out, thus providing support to the industrial application of the new separation technology.

On the basis of the process steady-state design and multi-objective optimization work, the dynamic control behavior and evaluation of balanced IL-based NH_3/CO_2 separation were carried out. In order to analyze the dynamic behavior of this new technology, the two step test were considered: the tail gas flowrate and composition fluctuation were introduced to the process. With the procedure of definition of control problem, conversion from steady-state to dynamic mode and successful inventory control, the simulation results showed that NH_3 concentration and NH_3 recovery have a positive response with more tail gas and NH_3 in the system. With the analysis of the parameter behavior on the different tail gas fluctuations, basic dynamic control could be built to guarantee

stabilization with different fluctuations. Based on the detailed investigation about this process's dynamic behavior, this new technology is fairly easy and simple to operate. Finally, the full-scale simulation package for the IL- based NH_3/CO_2 separation process will be established and provide strong support to this novel and new technology industrial application.

摘要

三聚氰胺生产会产生含有大量NH_3和CO_2的尾气。目前较为常用的三聚氰胺尾气分离方法为水洗法和尿素联产技术。离子液体(IL)具有良好的稳定性、不易挥发性和结构可设计等特点，被认为是气体分离领域重要的潜在溶剂。在此基础上，本研究设计了两种基于离子液体的新工艺技术，一种是基于离子液体的基础工艺(IL-0)，另一种是增强型离子液体工艺 (IL-En)。在工艺设计完成的基础上，分别对两种工艺过程进行了能耗与经济评估。结果显示，IL-En工艺具有更好的能耗与经济效果。本研究选用质子型离子液体：1-丁基咪唑双(三氟甲基磺酰基)亚胺([Bim][NTf_2])对三聚氰胺尾气氨碳分离工艺进行模拟评价。首先，通过回归NRTL方程得到可靠的热力学数据，该模拟回归结果与实验值符合。其次，在Aspen Plus V11^{TM}中进行了三种工艺流程的模拟，并进行了三种工艺（1 基础离子液体氨碳分离工艺，2 汽提强化离子液体氨碳分离工艺，3 传统水洗氨碳分离工艺）的稳态流程模拟，工艺灵敏度分析及能耗经济评价。结果表明，与传统水洗工艺相比，汽提强化的离子液体工艺单位氨回收成本相比传统水洗工艺可降低61%。此外，基于离子液体的工艺在工艺流程上比传统水洗工艺更为简单且可避免废水排放。

为进一步对上述基于离子液体的氨碳分离新技术进行深入分析，通过分离指标-能耗-经济三个维度进行该新工艺的多目标优化。通过选取不同的工艺目标函数，并对关键参数之间的耦合关系进行分析。多目标优化结果表明，汽提强化的离子液体三聚氰胺尾气氨碳分离工艺在分离指标-能耗-经济方面比基础离子液体分离工艺表现更为优异。通过多目标优化，筛选出基于不同工艺目标函数的具体案例，根据不同评价指标对各个操作参数的影响进行进一步分析，为该新技术的工业化应用提供更为有利的数据与技术支持。

在上述离子液体三聚氰胺尾气氨碳分离工艺的稳态研究及多目标优化工作基础上，进一步对该工艺的动态控制表现进行了分析与详细评估。引入三聚氰胺尾气流量及氨气组成波动两种不同的阶跃测试序列验证该工艺的动态稳定性。本工作通过定义动态控制目标、稳态到动态模式的转换以及系统设备液位储量控制，进行了工艺动态开环控制模拟。结果表明，随着工艺尾气流量与氨气组成的波动，净化气中的氨气浓度以及氨气回收率均呈现正响应。通过分析全流程工艺参数在不同尾气扰动序列下的变化，能够建立基本的动态控制方案以保证工艺在不同波动下的动态稳定。基于对该过程动态控制的详细分析，确认了新技术的可操作性。最后，本工作通过建立基于离子液体的NH_3/CO_2分离过程的全流程模拟工艺数据包，为该新技术的工业应用提供强有力的支持。

Resumé

Melaminproduktion producerer en restgas med en betydelig mængde NH_3 og CO_2. De mest almindelige separationsmetoder, der anvendes til melamin-halegas, er vandskrubning og urea-koproduktionsteknologi. Med god stabilitet, begrænset flygtighed og skræddersyede egenskaber betragtes ioniske væsker (IL'er) som potentielle opløsningsmidler til gasseparation. Derfor er to nye procesteknologier, ioniske væskebaserede proces (IL-0) og forbedrede ioniske væskeproces (IL-En), blev anvendt og evalueret for energi- og omkostningseffektivitet. IL-En anvender stripping til behandling af melaminhalegas. Den protiske ioniske væske kaldet 1-butylimidazolium-bis (trifluormethylsulfonyl)-imid ([Bim][NTf_2]) blev udvalgt til evaluering af melamin-halegasrensningsprocessen. Termodynamiske data blev tilpasset til NRTL-ligningerne. Tre fulde procesdiagrammer blev simuleret i Aspen Plus V11 ^{TM}. En grundlæggende og en forbedret ionisk væskeproces (IL-0 og IL-En), og en konventionel vandskrubbeteknologi (WS) som sammenligning, procesfølsomhedsanalyse og energi/økonomisk evaluering blev udført. Resultaterne viste, at de samlede separationsomkostninger ved brug af IL-En kan reduceres med 61% sammenlignet med WS-processen. Desuden er det IL-baserede flowsheet enklere end WS og undgår spildevandsudledning.

For at give en omfattende analyse af den foreslåede teknologi udføres en detaljeret multi-objektiv optimering (MOO) for NH_3/CO_2-separering af restgassen ved IL i teknisk-energi-økonomisk evaluering. I henhold til optimeringsresultaterne blev specifikke cases med forskellige objektfunktioner valgt, og sammenhængen mellem nøgleparametre blev analyseret. Resultaterne viste, at den ioniske væskebaserede teknologi har bedre energiøkonomi end basisscenariet. Analyser med indflydelse af driftsparametre med evalueringsindeks blev udført, hvilket understøttede af den industrielle anvendelse af den nye separationsteknologi.

På basis af steady-state design og multi-objektiv optimeringsarbejde evaluerede vi dynamiske kontrol og balanceret IL-baseret NH_3/CO_2-separation. For at analysere den dynamiske opførsel af denne nye teknologi udførtes trin ændringer: Ændringer i gasstrømningshastigheden og sammensætning blev introduceret i processen. Med definition af kontrolproblem, konvertering fra

steady-state til dynamisk tilstand og vellykket lagerstyring, viste simuleringsresultaterne, at NH_3-koncentration og NH_3-genvinding har en positiv respons med mere restgas og NH_3 i systemet. Med analysen af parametrenes indflydelse på de forskellige restgasudsving kunne grundlæggende dynamisk styring sættes op, som garanterer stabilisering ved udsving i restgassen. Den detaljerede undersøgelse af denne proces' dynamiske adfærd viste, at denne nye teknologi er relative nem og enkel at operere. Endelig giver fuldskala-simuleringer af IL-baseret NH_3/CO_2-separationsprocessen stærk støtte til anvendelse af denne nye teknologi i industrien.

Nomenclature

IL	Ionic liquid
IL-0	Ionic liquid-based
IL-En	Enhanced ionic liquid
NRTL	Non-random two liquid model
WS	Water scrubbing
ILs	Ionic liquids
[Bim][NTf_2]	1-butyl imidazolium bis(trifluoromethylsulfonyl)imide
R^2	Correlation coefficient
AARD	Average absolute relative deviation
TSC	Total separation cost
ACC	Annual capital cost
TOC	Total operating cost
TCI	Total capital investment
PEC	Purchased equipment cost
VOC	Variable operating cost
FOC	Fixed operating cost
TPEC	Total process energy consumption
SPEC	Specific process energy consumption
HEN	Heat exchange network
MOO	Multi-objective optimization
PIL-Tas	cobaltous thiocyanate functionalized poly ionic liquids
NSGA-II	Nondominated Sorting Genetic Algorithm II
y_{NH3}	NH_3 concentration in the purified gas stream
MOGA	Multi Objective Genetic Algorithm
MEA	6-Ethyl-o-toluidine
MDEA	Methyl diethanolamine
PZ	Piperazine
TAC	Total annual cost
TPC	Total purification cost
TPCOE	Total process CO_2 emission
η_{eff}	Process thermodynamic efficiency
F_{NH3}	Mole flowrate of NH_3 in purified gas stream
$F_{Purified}$	Mole flowrate of total purified gas stream
x_{NH3}	NH_3 mass fraction in the product stream
P_{ab}	Pressure of absorption column
R_{LT}	Ratio of lean to total solvent
F_{total}	Flow rate of total solvents
T_{F12}	Temperature of Flash 1 and 2
$P_{F1,}$	Pressure of Flash 1
P_{F2}	Pressure of Flash 2
F_{air}	Flow rate of air
P_{st}	Pressure of stripping column

$y_{NH3,min}$	Minimum NH_3 concentration in purified gas
$y_{NH3,max}$	Maximum NH_3 concentration in purified gas
$y_{NH3,no}$	Normalized NH_3 concentration in purified gas
$TSC_{, min}$	Minimum TSC
$TSC_{, max}$	Maximum TSC
$TSC_{, no}$	Normalized TSC

Contents

1 Introduction

In this chapter, the scope of the PhD project is presented. A background and motivation for the ionic liquid based gas separation technology presented in this thesis is given. Then an overview of the contribution of the thesis is introduced. This chapter concludes with an outline of the dissertation and a list of the scientific contributions disseminated during the PhD project in the form of conference presentations and journal articles. This chapter is partially based on the published articles:" Process simulation and evaluation for NH_3/CO_2 separation from melamine tail gas with protic ionic liquids", Separation and purification Technology, 288 (2022) 120680 [1] and" Multi-objective optimization of NH_3 and CO_2 separation with ionic liquid process", 14th International Symposium on Process Systems Engineering, Computer Aided Chemical Engineering, 49, 2022,1147-1152, [2].

1.1 Background

Environment issues have attracted more and more attention from the whole society with the background of the three major problems of “population, resources, and environment” in global sustainable development. Chemical engineering plays an essential role in producing raw materials for social and economic development. However, the chemical industry will unavoidably release some waste gases that harm the environment during production. These pollutants will have a negative impact on plant and animal growth when they enter the natural environment, endangering both the ecological balance and the long-term advancement of human society. Reduced pollution discharge from the source will lessen the environmental impact of the production process, which is required to regulate and control environmental pollution.

In recent years, the environmental problems caused by NH_3 tail gas emission have been paid more and more attention. NH_3-containing tail gas, as a kind of alkaline tail gas with strong pungent smell and will have reaction with other components in the atmosphere such as sulfur oxides SO_X, nitrogen oxides NO_X and other components to form solid particles, which is the formation of particulate aerosols in the atmosphere. Such particulate matter cause serious environmental pollution to the air. In view of the high pollution of NH_3-containing tail gas, strict emission requirements have been put forward for the discharge of NH_3-containing tail gas all over the world. In chemical fertilizers, livestock and pharmaceutical production, most industrial processes such as melamine plants generates NH_3, CO_2 and other gases that were discharged directly, which will cause serious pollution to the atmosphere [3] [4].

The emission of NH_3-containing tail gas from industrial tail gas threatened the environment increasingly [5]. The emission of NH_3 in European countries from 1990 to 2020 are shown in Figure 1 with the data provided by European Environment Agency (EEA) [6]. From Figure 1, the NH_3 emission is decreasing but went stable from 2010 with the proposal of National Emission reduction Commitments Directive (EU 28 NEC). EEA33 ammonia emissions have decreased by 25% between 1990 and 2011. It is obvious that the declines in NH_3 emission from 1990 to 2010 but improvements slowed down after 2010. It is urgent that more new gas cleaning technologies should be invented to realize much lower NH_3 emission.

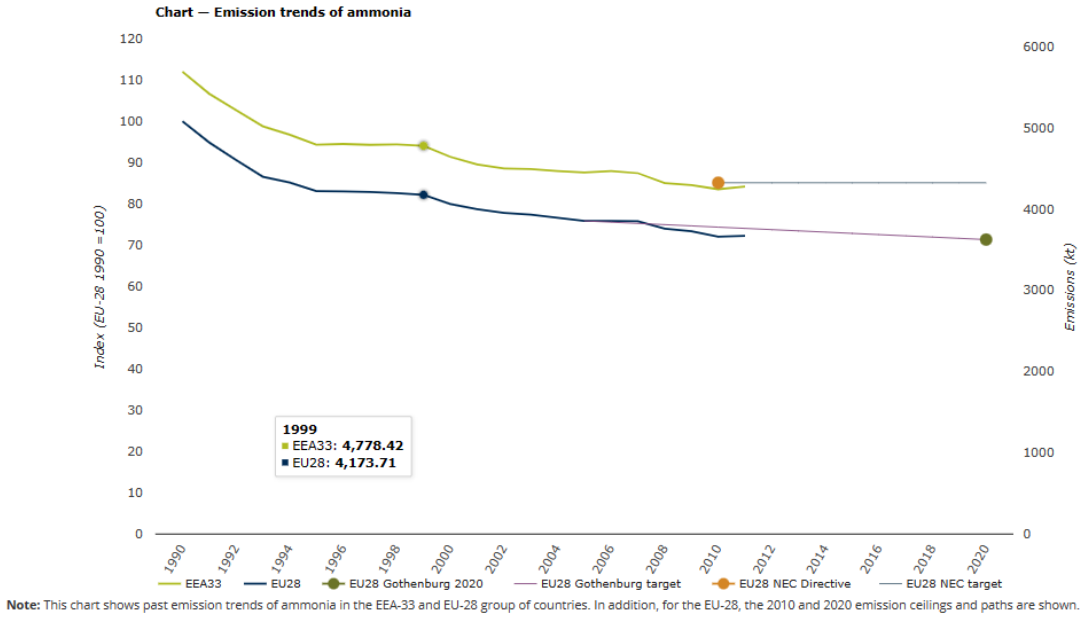

Figure 1 The emission of NH_3 in European countries from 1990 to 2020 [6].

For the other main area of NH_3 emission worldwide, in the United States totaled 4.54 million tons in 2021[7] . NH_3 emissions have leveled out in recent years. China is a global hotspot of atmospheric NH_3 emissions, according to 2020 China Ecological Environment Statistical Annual Report[8], the emission of waste gas are SO_2, NO_X, PM emissions and VOCs. Current estimates of Chinese NH_3 emissions still have large uncertainties. In order to have a detail and accurate estimation of the total NH_3 emission in China, Kong et al. [9] used the ground ammonia concentration observation data in China, the inversion and optimization of the national-scale atmospheric ammonia emissions (monthly, 15 km) was carried out, and the monthly ammonia emissions in China from September 2015 to August 2016 were obtained. In terms of total emissions, the total ammonia emissions in China estimated by the improved inventory are about 13.1 million tons per year which is higher than US and European. China's waste gas situation is even more severe. Some other researchers also reported different estimation output with the close value. Zhang et al. [10] reported total NH_3 emissions in China increased from 12.1 ± 0.8 million tons per year in 2000 to 15.6 ± 0.9 million tons per year in 2015 at an annual rate of 1.9%, which is approximately 40% higher than existing studies suggested. China's NH_3 emissions need to be taken into account in any future plans to clean up the air.

For the emission contribution made by different sections of the NH_3, Figure 2 shows the different sector share in EU, US and China. The agriculture denotes most of the NH_3 emission in the three regions which is around 80%. For the industrial processes, EU has contribution of 1.3%. The contributor index is 1.40% in US that is close to the value of 1.30% in Europe. As another big NH_3 emission area, China also has the same contribution compared with USA and Europe countries, large amount of NH_3 are emitted from the agriculture activities as a large agriculture country, at this part account for 18% of the global ammonia emissions [11]. For the contribution in China, because of the huge population, human contribute more than EU and US. For the industrial process, 1.8% of the index in China with more of the chemical process than the other two.

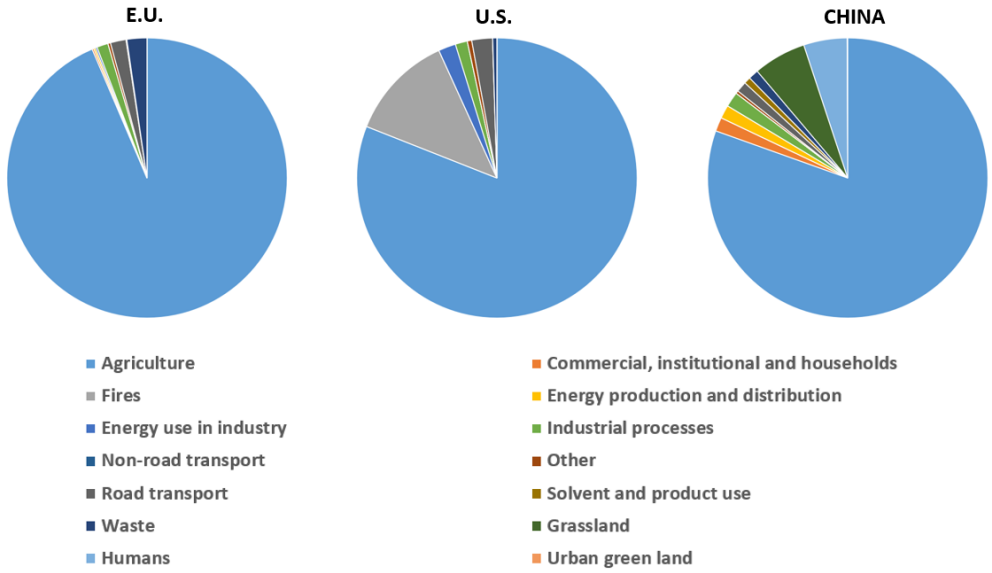

Figure 2 The contribution made by different sectors to emission of NH_3 in EU, US and China in 2011. [6] [7] [10].

The discharge of NH_3 will not only cause serious environmental problems, but also cause serious damage to human life and health [12]. According to recent study, ammonium nitrate and ammonium sulphate are the most prevalent secondary inorganic aerosols in many places. [13]. In addition, $PM_{2.5}$ contributed to the largest. According to current estimates, 82% to 97% of the EU-28 urban population was exposed to $PM_{2.5}$ concentrations higher than the WHO AQG threshold in 2015, resulting in 399,000 (35%) early deaths. [14]. As a colorless alkaline gas with a strong pungent odor, NH_3 can irritate and corrode human respiratory mucosa and damage human health. At the same time, exposure to high-concentration NH_3 environment can also cause cardiac arrest and respiratory arrest, seriously threatening human life.

Regarding on the severe NH_3 pollution, as reported of the European Environment Agency, in 2001, the European Community implemented the National Emission Ceilings Directive 2001/81/EC (NECD). The NECD establishes tight emission targets for four major air pollutants (NH_3, SO_2, NO_X, and non-methane volatile organic compounds (NMVOCs)) for each Member State in Europe beginning in 2010. For example, as regulated in 2020 CLRTAP Gothenburg Protocol ceiling for Denmark in 63 kt [6].With the severe environment regulation recent years, take industrial process as example, the NH_3 emission have decreased about 26% that the potential of the emission fallen is expected in the future [6].

Recently, the Chinese government announced plans to increase agricultural NH_3 emission control efforts through a variety of abatement strategies. It is hoped that NH_3 emissions would decrease significantly in the near future, bringing $PM_{2.5}$ concentrations [8] close to WHO guidelines (5 $\mu g/m^3$). As reported in 2021, the $PM_{2.5}$ emission in 2020 is 30 $\mu g/m^3$ and decreased 36.17% compared with 2017 is 47 $\mu g/m^3$ that there is still a long way to improve the air quality in China.

For the NH_3 emission standard in China, NH_3 control has been called for as a possible measure by policy makers, as regulated in 2015, the "National Standard for Discharge of Inorganic Chemical Industrial Pollutants" (GB31573-2015) was promulgated, which stipulated that the minimum value of industrial emissions containing NH_3 tail gas was 10 mg/m^3). At the same time, the 2018 draft for comments proposed that the concentration of NH_3 odor pollutants in the perimeter should be lower than 0.2 mg/m^3 [15].

In addition, in different provinces, for example in the Shandong province with most of the chemical factories, Shandong issued the "Emission Standards of Air Pollutants for Thermal Power Plants (DB37/664-2019 instead of DB37/664-2013)".The concentration of ammonia at the factory boundary should meet the limit requirement of 1.0 mg/m^3 in GB14554 [16]. For the melamine industry in China, the emission standard (T/CNFAGS 2-2121) of pollutants by the China Nitrogen Fertilizer Industry Association Melamine Branch with the 0.6 mg/m^3, and they encourage all the melamine production companies to self-monitoring and implement voluntary.

For the industrial process NH_3 emission in China, Figure 3 showed the different chemical process contribution. From Figure 3, the synthesis NH_3 denote the most of the total NH_3 emission, the second is the melamine production process with 3.6 billion Nm^3 per year.

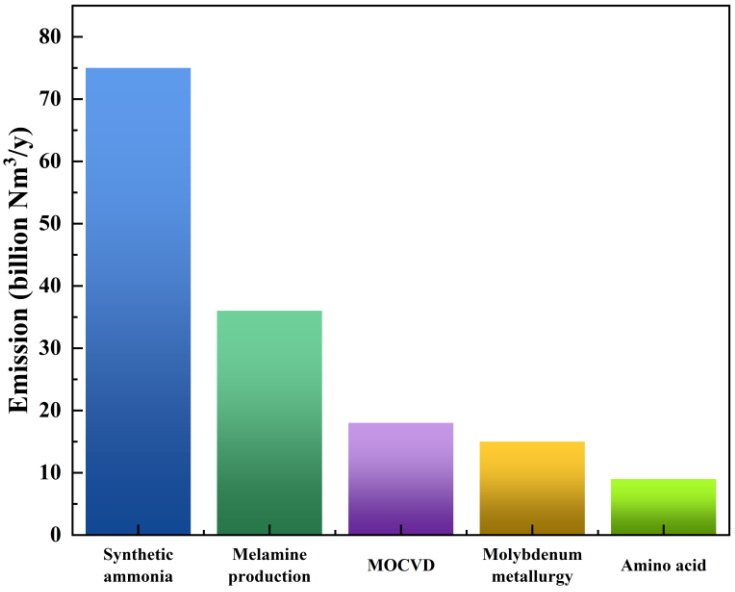

Figure 3 NH_3-containing waste gas emissions from different industries.

This project focus on the melamine tail gas cleaning as the cleaning object. Melamine is an organic chemical product with urea as the primary raw material. It is mainly used in sheet materials, melamine powder, and impregnated paper. It can also be used in coatings, resins, and flame-retardant materials. In addition, for anti-folding and anti-shrinkage treatment of textiles agents, synthetic fireproof laminate bonding, fixing agent or hardening agent for waterproofing agents, etc.

The melamine market size was evaluated at more than 1,600 kilotons in 2021. It is projected to register a compound annual growth rate of around 4% during the forecast period. The Asia-Pacific region controlled the majority of the market. Melamine usage is expanding in the region as construction activities expand and demand for laminates, wood adhesives, and paints and coatings rises in China, India, and Japan. More than one-fourth of the worldwide coatings market is accounted for by China. According to the China National Coatings Industry Association, the industry has grown by 7% in the last few years [17]. The melamine market is highly fragmented, with the top five firms accounting for around 40% of total production capacity. OCI NV, Borealis AG, Henan Xinlianxin Chemicals Group Co. Ltd, Prefere Resins Holding GmbH, and Grupa Azoty are among these companies [17].

The modest global expansion will be driven by China's mainland, which accounts for nearly half of global melamine consumption and nearly three-quarters of global capacity. In the future years, the European melamine market is predicted to grow at a 3% annual rate, Asia Pacific at a 5% annual rate, and North America at a 2% annual rate[18] [19].

Taking melamine production in China as an example, China's melamine industry started in the 1950s. After years of development, China has become the world's most extensive production base. In China, 2021, the total annual output of melamine in 2021 was about 1.5 million tons, an increase of 15% from 1.3 million tons in 2020. In addition, China produces four times more melamine than the second largest producer, the Netherlands. The third place in this ranking is Germany with a 8.8% share. In recent years, domestic melamine production capacity has increased rapidly, and the supply exceeds demand. According to statistics, at the end of 2019, melamine's domestic adequate production capacity reached 1.945 million tons per year, the total national output of melamine was about 1.3 million tons, a year-on-year increase of 1%, and the ability operating rate was 66.53% [20]. In addition, this project's cooperated melamine factory Shandong Shuntian has the productivity of 90,000 tons per year as the 9th ranking in China.

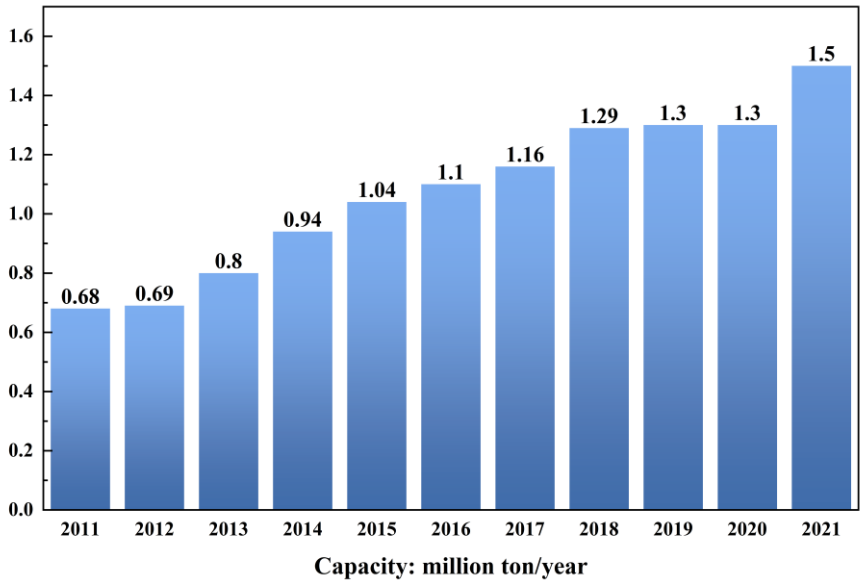

Figure 4 Production of China's melamine industry from 2011 to 2020.

From the above background, the purification treatment of NH_3-containing gas is a common technical requirement in the fields of chemical industry, environment, energy, etc. The emission of NH_3-

containing gas has large volume, which has a serious impact on the environment. As the melamine industry that emits a large amount of NH_3-containing gas in China, there is an urgent need for efficient and economical ammonia-containing gas recovery technology. NH_3 is widely used as an important chemical raw material in fertilizer, metallurgy and refrigeration industries. Separation and recovery simulation, optimization evaluation and process dynamics of NH_3-containing gas in industrial tail gas have significant economic benefits for the development of green chemical industry. If the new technology can recover NH_3 with high efficiency and low energy consumption, the efficient recovery of NH_3 will produce significant economic and social benefits.

The most used NH_3-containing tail gas cleaning methods include conventional solvent absorption method [21] [22] [23], biological filtration method [24] [25], catalytic oxidation method [26], adsorption method [27], membrane separation [28], and other purification processes. The absorption method absorbs and purifies NH_3-containing tail gas by using solvents with a higher NH_3 absorption capacity as an absorbent. At present, the most common methods are the conventional solvent method, ionic liquid method, deep eutectic solvent method, and so on.

At present, water scrubbing and acid washing [29] [30] method are the main representative technology dealing with the tail gas. The acid washing method employs acidic solvents such as sulfuric acid and phosphoric acid solution to react with NH_3 in the tail gas to be treated, then convert the NH_3 to NH_4+ and achieve the tail gas purification. However, because of the acidity of the solvent, this method will corrode the pipeline and equipment, raising the overall anti-corrosion standard of the process and increasing the equipment investment costs. The absorbed rich solvent needs complex operations such as high-temperature evaporation and dehydration, drying, and granulation to obtain ammonium salt products with low economic value. As a result, this purification technology not only has complex processes, high energy consumption, and is incapable of recovering NH_3 resources effectively, but it also has issues such as low added value of the obtained products. The water scrubbing employs water with high NH_3 solubility as the absorption solvent to achieve tail gas separation and purification. However, this process has disadvantages including high water consumption, high energy consumption for NH_3 treatment and low NH_3 recovery rate. The issues severely limit the industrial application of the traditional acid/water scrubbing process. Simultaneously, it is critical that the existing conventional solvent NH_3 absorption process need to be modified to meet the increasingly stringent environmental protection requirements.

At ambient temperature, the ionic liquid consists of positive and negative ions and is a liquid organic salt. Due to its programmable structure, extraordinarily low vapor pressure, and high gas solubility, it has attracted considerable interest in gas separation. One of the earliest room temperature ionic liquids was ethylammonium nitrate, reported by Paul [31] in 1914. In the 1970s and 1980s [33], potential battery electrolytes based on alkyl-substituted imidazolium and pyridinium cations with halide or tetrahalogenoaluminate anions were devised [32]. In 1992, Wilkes and Zawarotko [34] obtained ionic liquids with 'neutral' weakly coordinating anions such as hexafluorophosphate (PF_6) and tetrafluoroborate (BF_4), enabling a vastly expanded range of applications. In fact, ILs as new types of fluids have only gotten a lot of attention in the past 20 years. Few SCI papers were written about ILs in 1996, but more than 120,000 were written about them in 2023 [35]. This is a faster rate of growth than other popular scientific fields. This means that more and more researchers are looking into this interesting area, with lots of good results.

It has recently become a focus of NH_3 removal studies to combine high-viscosity ionic liquids with porous channel adsorption materials. Conventional and functional ionic liquids are the two types of ionic liquids that can be used for NH_3 absorption. Figure 5 showed some typical ionic liquid's cationic and anionic structure for NH_3 absorption. Sulfonic acid functionalized ionic liquids, hydroxyl functionalized ionic liquids, metal ionic liquids, and proton ionic liquids are the most common types of functionalized ionic liquids [36].

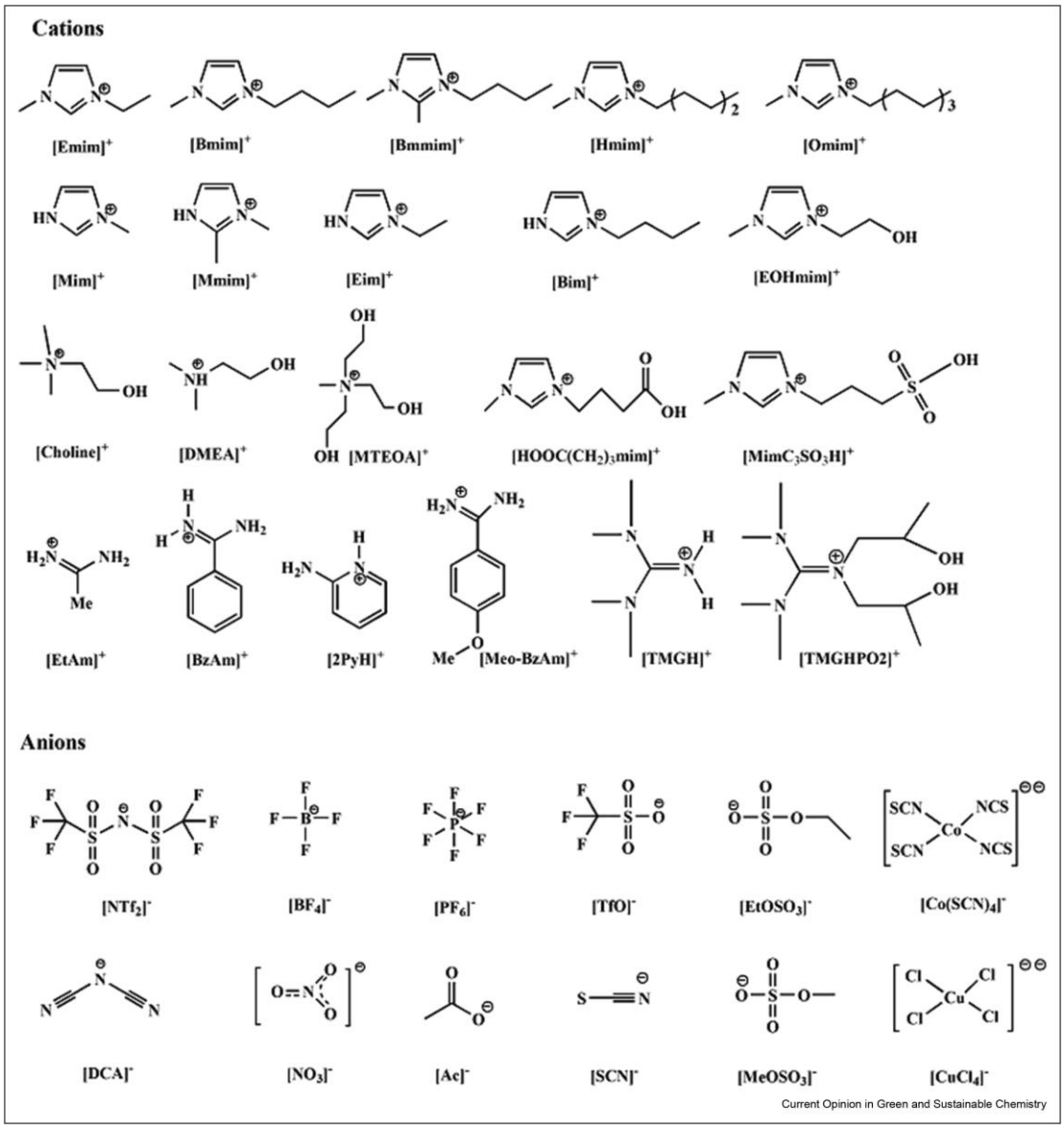

Figure 5 The typical cationic and anionic structure of ILs for NH_3 separation[37].

Ionic liquids have a wide range of industrial applications, and many researchers are working to promote ionic liquid absorption processes. To facilitate the industrial application of this technology on a large scale, it is necessary to use process simulation technology to derive the process characteristic value, which serves as a data reference for industrial design and process analysis. Computational simulation can reduce experimental investment, identify potential bottlenecks in the process in real-time, and propose feasible solutions while evaluating the process's application prospect and potential.

The reported literature has researched the process simulation and evaluation of the ionic liquid-based process, and most work is related to the carbon capture process. Basha et al. [38] used the Peng-Robinson (PR) equation to fit the CO_2 solubility data of [HMIm][Tf_2N], and designed an absorption process to study the separation performance of ionic liquids. Shiflett et al. [39] used the Redlich-Kwong (RK) model to regress the solubility data of CO_2 in [C_4Mim][Ac], obtained well-correlated RK model parameters, and simulated the process of CO_2 absorption by ionic liquids. Through the sensitivity analysis of process parameters, the process with the least energy consumption is obtained, and the energy consumption is reduced by about 16% compared with traditional MEA. Huang et al. [40] used the NRTL model to establish a gas-liquid equilibrium model suitable for [Bmim][BF_4], [Bmim][DCA] and [Bpy][BF_4] IL-CO_2 systems, and compounded MEA-IL of CO_2 absorption. The study found that when the compounding ratio of [Bpy][BF_4] is 0.2, the process has the smallest separation energy consumption (3.17 GJ/t CO_2), which can reduce operating costs compared with the MEA process about 18%. Based on the COSMO method, Ruiz et al. [41] established a cyclic process of ionic liquid-NH_3 absorption-refrigeration, and investigated the cycle performance of seven ionic liquids including [Choline][NTf_2], [Emim][Ac], [Emim][$EtSO_4$], [Emim][SCN], [Emim][NTf_2], [Hmim][Cl] and [HOemim][BF_4]. The results showed that the ionic liquids with high NH_3 absorption solubility exhibited better cycle performance.

As one of the major players in the ionic liquid field in the academic area, the Institute of Process Engineering plays a vital role in this area. The Ionic Liquid Research Department of the Institute of Process Engineering, centering on ionic liquids, has done frontier work on the gas absorption mechanism of ionic liquids, the design of functional ionic liquids, the development of new ionic liquid-based processes, and engineering scale-up. In terms of technology transformation, the problems of high-performance ionic liquid absorbent design and low mass transfer efficiency of ionic liquids have been broken through, and the 130 million Nm^3/year ionic liquid ammonium molybdate tail gas cleaning industrial pilot plant has been upgraded and operated stably [42].

This PhD project is co-funded by the Department of Chemical and Biochemical Engineering, Technical University of Denmark, Denmark, and the Institute of Process Engineering, Chinese Academy of Sciences, China, in order to improve academic collaboration. During the period of external study at IPE, some related works in academic and industrial application work are also included in this PhD project. The low concentration NH_3 tail gas cleaning with ionic liquids and green degree analysis for chemical engineering work were included in the academic work, and as

co-author with four publications with process design contribution. For the industrial application, this project also includes the in-depth participation in the industrialization of ionic liquids-based process design. During the promotion of the industrialization project, mainly responsible for the regression of the physical properties of ionic liquids and process design, including process optimization, equipment calculation and selection, etc., and completed the preliminary process simulation data package of the process. The industrialization project is currently under construction with the scale of 1.5 billion Nm^3/year melamine tail gas cleaning process by ionic liquids.

The United Nations has released a list of 17 sustainable development goals (SDG), with 169 goals in aspect of the social, economic and environmentally development in a global perspective [43]. Among 17 SDGs, the goal 12 and 13 are relevant for the green gas separation process. Goal 12: Responsible consumption and production. This is related to establishing and ensuring sustainable production in all industries. For the gas separation process, this translates to making the separation greener, reducing energy consumption and reducing the usage of waste such as solvents. Goal 13: Climate Action. This is to take urgent action to combat climate change. For the tail gas cleaning process, a high-performance separation process with low energy consumption could be more efficient and thus reduce energy requirements, the process would be more environmentally friendly. Therefore, a more environmentally friendly gas cleaning and separation process can reduce the release of harmful gas emissions.

1.2 Motivation

For the traditional melamine tail gas cleaning technology, most are faced with high energy consumption and low product value, for example, the ammonia bicarbonate in the ammonia bicarbonate co-producing method. The traditional treatments of melamine tail gas are water scrubbing (WS), solvent absorption, urea and ammonium bicarbonate co-producing methods.

Ionic liquid (IL) was composed of positive and negative ions and was regarded as a potential solvent. Because of its designable structures, extremely low vapor pressure, and high gas solubility, it has received wide attention in the field of gas separation. There is already much research regarding the synthesis of different ionic liquids, thermodynamic analysis, and process simulation in various gas separation areas. However, detailed process simulation and analysis of NH_3 and CO_2 separation is rare. To facilitate the large-scale application of new technology in the industry, it is necessary to use process simulation to provide data for industrial design and process analysis.

The motivation for this PhD project is to further develop a full simulation package of the melamine tail gas cleaning with ionic liquids. As a newly developed technology, it is necessary to have detailed analysis and results in aspects of the thermodynamics of chosen ionic liquids, process simulation, evaluation, and dynamic control. In order to let this new technology become a viable alternative to industrial gas separation processes and thus reduce energy consumption. With the potential high gas absorption performance of ionic liquids, it is urgent and vital to develop the full simulation package of the new technology:

1. The rigorous process design needs to be carried out with simulation software. The internal operation parameter affection to the energy and economic evaluation also needs to be researched.
2. The initial steady-state design is unsuitable for high technology and energy-economic-friendly requirements. Reasonable optimization methods should be employed for the new process, for example, the multi-objective optimization method. Different scenarios based on the various objectives will be gained and analyzed based on the optimization result.
3. As the requirement of future industrial application, the new ionic liquid-based gas separation process should be robust and able to deal with the fluctuation in the tail gas as flow rate and composition.

1.3 Project objectives

The objective of this project is to develop a full simulation package of the ionic liquid-based melamine tail gas cleaning new technology. Other technologies are employed for energy-efficient and cost economic gas processing. Dynamic control strategy is design for one of the ionic liquid-based process. This covers the following:

- To develop a physical model containing information on gas solubility in ILs.
- To develop steady-state design for the traditional water scrubbing and two IL-based process.
- To evaluate the different technology with energy-economy index for the NH_3/CO_2 gas separation problem.
- To perform process multi-optimization and analysis for IL-based separation technology.
- To perform process dynamic control design for IL-based separation technology.

1.4 Thesis structure

The thesis is divided into the following chapters, for each with a chapter summary:

- **Chapter 2: Full simulation package of IL-based tail gas cleaning technology:** A brief literature review of the technology development of the IL-based gas separation is given. The current melamine tail gas cleaning technology, the current development of high NH_3 performance ionic liquids, the thermodynamic regression of ionic liquids, the process and evaluation of ionic liquid-based gas separation are summarized.
- **Chapter 3: Case study: Process design, simulation and evaluation of IL-based technology:** Based on the rigorous regression of the thermodynamic of the chosen ionic liquids, two IL-based processes are designed and simulated in Aspen Plus. Detailed comparison in aspect of the energy and economic are carried out with the traditional water scrubbing method of the melamine tail gas cleaning.
- **Chapter 4: Case study: Process optimization of IL-based technology:** In order to give a detailed analysis of the two IL-based processes, multi objective optimization are employed with the process and after the optimization, different cased based on different evaluation are obtain and detailed performance for the two IL-based gas separation processes are carried out in this chapter.
- **Chapter 5: Case study: Dynamic evaluation and regulatory control of IL-based technology:** On the basis of the results of a previous work, the dynamic control behavior and evaluation of balanced IL-based NH_3/CO_2 separation were carried out in this chapter. Two step test were considered: the tail gas flowrate and composition fluctuation were introduced in the process. The regulatory control were carried out to show the stability and operability of the new IL-based technology. The proposing dynamic control strategy is tested with tail gas flow rate and NH_3 concentration fluctuation.
- **Chapter 6: Discussion:** The summarizing, discussion and limitation of the thesis was given of the gas cleaning technology with ionic liquids.
- **Chapter 7: Conclusion and future work:** The thesis conclusion and considerations for future perspectives for the progress in ionic liquid-based gas separation technology.
- **Appendix:** Detailed calculation method, stream result, and published articles are shown in Appendix.

1.5 Publication can conference contributions

The journal publications and conference contributions that have been a part of this PhD project are listed below.

1.5.1 Journal publications

Duan Y, Zhan G, Chang F, Shi S, Zeng S, Dong H, Abildskov J, Huusom J K, Zhang X. Process simulation and evaluation for NH_3/CO_2 separation from melamine tail gas with protic ionic liquids. *Sep. Purif. Technol.* 2022;288:120680.

Duan Y, Zhan G, Shi S, Zeng S, Dong H, Abildskov J, Huusom J K, Zhang X. Technical-energy-economic multi-objective optimization of ionic liquid-based CO_2 /NH_3 separation from melamine tail gas. Finished. (23-12-2022).

Shi S, **Duan Y**, Zhan G, Chang F, Zeng S, Ji X, Liu Z, Meng X, Zhang X. Simulation and energetic assessment of the ammonia synthesis loop with ionic liquid-Based ammonia recovery from recycle gas. *Sep. Purif. Technol.* 2022;301:121951.

Zhan G, Cao F, Bai L, Chang F, Zhou B, **Duan Y**, Zeng S, Dong H, Li Z, Zhang X. Process Simulation and Optimization of Ammonia-Containing Gas Separation and Ammonia Recovery with Ionic Liquids. *ACS Sustainable Chem. Eng*. 2021, 9, 1, 312–325.

Zhan G, Bai L, Wu B, Cao F, **Duan Y**, Chang F, Bai Y, Shang D, Li Z, Zhang X, Zhang S. Dynamic process simulation and optimization of CO_2 removal from confined space with pressure and temperature swing adsorption. *Chem. Eng. J*. 2021,416,129104.

Chang F, Zhang X, Zhan G, **Duan Y**, Zhang S. Review of Methods for Sustainability Assessment of Chemical Engineering Processes. *Ind. Eng. Chem. Res*. 2021, 60, 1, 52–66.

Chang F, Zhan G, Wu Z, **Duan Y**, Shi S, Zeng S, Zhang X, Zhang S. Techno-economic analysis and process design for the electroreduction of CO_2 to CO production using ionic liquid as electrolyte. *ACS Sustainable Chem. Eng.* 2021,9,27,9045-9052.

1.5.2 Conference contributions

Duan Y, Zhan G, Chang F, Shi S, Abildskov J, Huusom J K, Zhang X. Multi-objective optimization of NH_3 and CO_2 separation with ionic liquid process. *Part of volume: 14th International Symposium on Process Systems Engineering. Computer Aided Chemical Engineering.* 2022;49:1147-1152.

Duan Y, Zeng S, Abildskov J, Huusom J K, Zhang X, Zhang S. Process simulation and evaluation for melamine tail gas cleaning with protic ionic liquids. 7th Asia-Pacific conference on ionic liquids and green process-Suzhou, China, 2021(poster)

Duan Y, Zhan G, Chang F, Zeng S, Abildskov J, Huusom J K, Zhang X. Process simulation and evaluation for NH_3/CO_2 separation in melamine tail gas with ionic liquids. 13th European congress of chemical engineering and 6th European congress of applied biotechnology-Berlin, Germany,2021(poster)

Duan Y, Abildskov J, Huusom J K, Zhang X. Process simulation and optimization of NH_3/CO_2 separation with ionic liquids. 23th Nordic Process Control Workshop-Lulea, Sweden, 2022(poster)

Duan Y, Zhan G, Chang F, Shi S, Abildskov J, Huusom J K, Zhang X. Multi-objective optimization of NH_3 and CO_2 separation with ionic liquid process. 14th International Symposium on Process Systems Engineering-Kyoto, Japan, 2022(Oral)

Duan Y, Abildskov J, Huusom J K, Zhang X. Process simulation and optimization for melamine tail gas separation with ionic liquids. 9th International Conference on Engineering for Waste and Biomass Valorisation-Kgs. Lyngby, Denmark, 2022(poster)

2 Literature review of the IL-based tail gas cleaning technology

This chapter introduces the research status of ionic liquid-based gas cleaning and separation technology, providing the readers with general knowledge of the state-of-the-art research on gas separation and cleaning with the new green solvents as ionic liquids. This chapter was divided into three parts from the aspect of the simulation package of new technology in chemical engineering. The first part introduces the research status of the process design and simulation of the ionic liquid-based gas cleaning and separation technology. The newly synthesized functional ionic liquids dealing with NH_3 and CO_2 were introduced. The process design and simulation literature were classified correspondingly. The second part concentrated on the optimization of the ionic liquid-based technology, different multi-objective optimization method was introduced, and some research about the optimization based on the ionic liquids was employed. In the last part, the new dynamic control scheme of the ionic liquid was given. In conclusion, this chapter was a total literature review based on this PhD project. This chapter is partially based on the published articles:" Process simulation and evaluation for NH_3/CO_2 separation from melamine tail gas with protic ionic liquids", Separation and purification Technology, 288 (2022) 120680 [1] and" Multi-objective optimization of NH_3 and CO_2 separation with ionic liquid process", 14th International Symposium on Process Systems Engineering, Computer Aided Chemical Engineering, 49, 2022,1147-1152, [2].

2.1 IL based process design and simulation

In this section, first, a brief introduction to the NH_3 and CO_2-containing tail gas cleaning method will be introduced, and second, the development of NH_3 absorption ionic liquids will be summarized. Last, the state quo about the ionic liquid-based process design and evaluation will be introduced.

2.1.1 The traditional cleaning method for NH_3, CO_2 and NH_3 /CO_2 separation

The main methods for the NH_3-containing tail gas cleaning method are solvent absorption, biological filtration, catalytic oxidation, adsorption, electrocatalysis, and membrane separation. For the solvent absorption method, the current common method is the solvent (water or acid solvent) method, ionic liquids method, deep eutectic solvent method, and so on. This method employs the reaction principle between NH_3 and acid or water, converting the NH_3 to ammonium salt [29] [30]. However, this process faced some disadvantages, including relatively high solvent consumption, high energy consumption for NH_3 treatment, and low NH_3 recovery rate. The issues severely limit the industrial application of the traditional acid/water washing process. As the new green solvent, ionic liquid has been widely used in catalysis, gas separation, extraction, and other fields. IL has unique character such as extremely low vapor pressure, non-flammability, good thermal stability, and designable structure. In recent years, many researchers have applied ionic liquids to the absorption and separation of NH_3 and have conducted systematic research on the NH_3 separation performance of ionic liquids [44]. A detailed introduction will be shown in section 2.1.2.

For the deep eutectic solvents, this solvent has the benefits of inexpensive and easily obtained raw materials, a variety of types, a simple synthesis process, and non-toxicity. They are widely used in gas separation, organic molecular catalysis, and the synthesis of nanomaterials. Jiang et al. [45] created a deep eutectic solvent from ethylamine hydrochloride and glycerol, discovered that the solvent's NH_3 absorption capacity can reach 9.631 mol/kg when the temperature was 298.2 K and pressure was both 106.7 kPa. The solvent's NH_3 absorption capacity remained essentially unchanged following the absorption-desorption cycle experiment. Li et al. [46] used NH_4SCN and imidazole (Im) as raw materials to synthesize deep eutectic solvents. The influence of absorption temperature, pressure, flow rate, water content, and molar ratio on the physical properties and absorption capacity of deep eutectic solvents was researched. The study found that the deep eutectic solvent composed of NH_4SCN/Im can capture NH_3 quickly, has good absorption-desorption cycle performance, and shortens the absorption saturation time as the gas flow rate increases. Under the normal absorption

pressure, and the absorption temperature is 303.15 K, the NH_4SCN/Im (1:2) solvent can absorb up to 9.65 mol NH_3/kg, which is mainly due to the hydrogen bond between NH_4+ and NH_3. The effect caused the deep eutectic solvent of NH_4SCN/Im to have a higher NH_3 absorption capacity. The deep eutectic solvents have the advantage of high absorption capacity in NH_3 absorption and will be the potential solvent for the future NH_3-containing tail gas purification processes.

To achieve the goal of NH_3 absorption, degradation, and removal, the biological filtration method employs the chemical decomposition of NH_3 by microorganisms to pass the NH_3-containing tail gas through multi-layer biological filter membranes or fillers. However, because the process involves microorganisms, strict temperature and humidity control is required, which increases the difficulty of applying and implementing biofiltration [47].

Catalytic oxidation technology of NH_3-containing tail gas is classified into two types: catalyst catalytic oxidation and electrocatalytic oxidation. These two catalytic methods convert NH_3 to other components such as (N_2, H_2O, NO_2, and so on) and then achieve tail gas purification after further treatment [48]. Mustafa et al. [49] investigated the catalytic oxidation of NH_3 using atomic oxygen on Ag and Au catalysts. According to the research, catalysts can completely convert NH_3 to N_2. On the other hand, the purification process has issues such as high operating temperature (> 900 K), high process energy consumption, and limited NH_3 concentration after the purification.

The adsorption method employs a porous material with a large specific surface to adsorb it via physical or weak chemical interaction between the adsorbent and NH_3, with the goal of purifying the NH_3-containing tail gas. Ruckart et al. [50] used the loading method to modify the SBA-15 molecular sieve. The experiment found that under the extremely low partial pressure of NH_3 (P_{NH3} < 0.01 kPa), the adsorption capacity of the modified adsorption material for NH_3 can reach 1.5 mol/kg, which is much higher than that of the unmodified SBA-15 molecular sieve (0.07 mol/kg).

Membrane separation method uses materials such as NH_3-friendly and hydrophobic membranes to realize the permeation of NH_3 under the condition of pressure difference on both sides, so as to achieve the purpose of enriching and purifying NH_3 in tail gas. Yang et al. [28] prepared a material with good NH_3 separation performance using ionic liquid [Eim][NTf_2] and membrane material Nexar to achieve the goal of efficient separation of NH_3-containing tail gas. Experiments have shown that the membrane material's NH_3 permeability and NH_3/N_2 selectivity can reach 2711 Barrer and 1407, respectively, at room temperature and normal pressure.

The most used CO_2 capture methods include solvent absorption and membrane separation [51]. The low temperature methanol washing method [52] use the methanol with temperature 323-333 K, and absorb the light oil, CO_2 and H_2S. Because of the high absorption performance and selectivity, the concentration in purified gas can be 10-20 ppm and the sulfur compounds can be removed less than 0.1 ppm. However, this method faces the difficulty that the whole process in the operation with low temperature and the flow chart is complex. The material equipment should be low temperature steel material with high capital cost.

The Selexol method [53] employed the polyethylene glycol dimethyl ether (NHD) to capture CO_2 in the fuel gas. The solvent has the better stability and low vapor pressure, and the flow chart is simple. However, the absorption is physical way and this technology is suitable for the CO_2 with high partial pressure. Currently, the most mature solvent absorption method employes the decarbonization solvent: 30 wt% ethanolamine (MEA) solution [54]. To lower the energy consumption with high absorption performance, the mixed amine process is investigated. Veawab et al. [55] studied the reboiler heat consumption in the mixed amine process versus a single alcohol amine solution for CO_2 capture. The results show that the heat consumption of a single alcohol amine solution is MEA, DEA, and MDEA from high to low. The energy consumption of the process is closely related to the loading of rich liquid and lean liquid. The influence of the mixed amine ratio on the heat consumption of the reboiler mainly lies in the heat consumed by the evaporation of water in the solvent.

For the melamine tail gas, CO_2 and NH_3 can react with each other at specific conditions of temperature and pressure, leading to the production of ammonium bicarbonate crystals. These ammonium bicarbonate crystals have negative impact on the operation conditions and will lead to equipment malfunctioning.

The processing principle of the solvent absorption separation method is to use sulfuric acid or another acidic solvent to chemically react with the NH_3 in the tail gas to form ammonium salt. In the ammonia recovery system, Xue et al. [56] absorb the ammonia in the tail gas with dilute sulfuric acid to produce dilute ammonium sulfate. The main drawback of adopting this approach to treat melamine tail gas is the generation of ammonium salt-containing dust particles during the ammonium salt drying process, as well as the complexity and difficulty of operating the succeeding processing section. Additionally, because acid solvents are so easily corrosive and cause equipment and pipelines to corrode, they raise the cost of equipment.

At present, the conventional melamine tail gas treatment methods mainly include water scrubbing method, melamine tail gas co-production urea method, co-production of ammonium bicarbonate method, etc., but the water vapor contained in the melamine tail gas will condensed into liquid water during the pressurization process, and further will produce ammonia ammonium crystallization with NH_3 and CO_2, which will have impact on working conditions.

Many factories currently use various co-production treatment techniques because many melamine plants are situated near urea and ammonium bicarbonate plants. [57], mainly including melamine tail gas co-production urea method and co-production ammonium bicarbonate method etc. Melamine tail gas co-production urea method is through the co-production of melamine tail gas with the original urea device. Many large-scale melamine producers have urea production equipment that uses recovered melamine tail gas to create urea and achieve recycling. The technology of using high pressure to recover melamine tail gas is relatively mature.

The method of co-producing ammonium bicarbonate from melamine tail gas [58] has the advantages of low investment, and less impact on the melamine system. The co-production method does involve some inert gases, albeit they tend to form minute crystals in the carbonization tower that the centrifuge cannot separate to produce quality goods.

2.1.2 The ionic liquids for NH_3 absorption

Ionic liquids have attracted much attention in the field of gas separation due to its structure designable, extremely low vapor pressure and high gas solubility. The use of ionic liquids to clean NH_3-containing tail gas has advantages about high ammonia absorption, good selectivity, no wastewater discharge, operational energy and low cost. The currently reported ionic liquids for separating ammonia mainly include conventional ionic liquids, functional ionic liquids (hydroxyl, protons, and metals), etc.

For the conventional ionic liquids, Yokozeke et al. [44] tested the solubility of NH_3 in seven common imidazole ionic liquids and found that the solubility of NH_3 in conventional imidazole ionic liquids is limited, and the solubility difference between different types of ionic liquids is low. Li et al. [59] studied the relationship between the alkyl side chains on imidazole ionic liquids with the NH_3 absorption. The same anion [BF_4] was fixed as control variables. The study found that with increasing the length of the alkyl side chain, the absorption of NH_3 by the ionic liquid can be

effectively improved. However, the reason for the low absorption performance is that the interrelationship with NH_3 and ionic liquids is physical.

Functional ionic liquids were synthesized in order to improve the solubility of NH_3. Palomar et al. [41] employed the molecular simulation methods to study the solubility difference of NH_3 in hydroxyl functional and conventional ionic liquids. The simulation results show that hydroxyl groups can enhance the solubility of NH_3 in ionic liquids. Then, Chen et al. [60] measured the solubility of NH_3 in metal ionic liquids $[C_4Mim][Zn_2Cl_5]$, and found that the presence of metal ions $[Zn_2Cl_5]$ can increase the solubility performance of NH_3 in ionic liquids. Zeng et al. [61] studied the solubility of NH_3 in $[Cnmim]_2[Co(NCS)_4]$, and found that the ionic liquid has excellent NH_3 absorption properties, and the solubility can reach 6.09 mol NH_3/mol IL, which is about more than 30 times that of conventional ionic liquid [Cnmim][SCN]. Zhang et al. [62] synthesized a protic IL: 1-butyl imidazolium bis (trifluoromethylsulfonyl) imide ([Bim][NTf_2]) that has high NH_3 absorption performance (2.69 mol NH_3/mol IL at 313 K, 100 kPa) compared with conventional ILs.

Based on Zhang's work, more research about the protic ionic liquids were carried out. Li et al. [63] synthesized three pyridinium-based protic ILs with single protic H showing higher NH_3 absorption capacity with the maximum of 3.078 mol NH_3/mol IL at 313 K, 100 kPa. However, there was an apparent reduction in NH_3 capacity for pyridinium-based protic ionic liquids during the absorption-desorption cycles. Luo et al. [64] reported a porous PIL-TAs (cobaltous thiocyanate functionalized poly ionic liquids) for superhigh capacity and reversible NH_3 uptake, whose capacity of 13.2-20.1mmol/g at 298 K and 1 bar is higher than most of the reported sorbents. Deng et al. [65] studied the physical properties and NH_3 absorption performance of six proton ethanolamine-based ionic liquids from the molecular structure. The experimental study found that [EtAN][SCN] had the smallest viscosity, which was 78.18 mPa. The molar absorption capacity of NH_3 reaches 0.296 and 0.0802 g NH_3/g PILs under the absorption pressure of 100.0 and 4.5 kPa, respectively, and the reason for the high NH_3 absorption capacity of the ionic liquid is the multiple hydrogen bonds between NH_3 and proton hydrogen, hydroxyl and thiocyanate in the molecule. At the same time, the ideal selectivity of the ionic liquid for NH_3/CO_2 was as high as 365. Yuan et al. [66] designed and synthesized a variety of bifunctional protic ionic liquids ([CnOHim]X (n = 1, 2; X = [NTf_2]-, [BF_4]-, [SCN]-)), which have weakly acidic and hydroxyl to enhance the NH_3 absorption performance of ionic liquids. It is found that [EtOHim][NTf_2] has the highest NH_3 solubility, which is 3.11 mol NH_3/mol IL, and the highest NH_3 mass solubility is [EtOHim][SCN] with a value of 0.221 g NH_3/g

IL. At the same time, these ionic liquids can select NH_3/CO_2 and NH_3/N_2 up to 65 and 104 respectively.

2.1.3 The process simulation and evaluation of ionic liquids for NH_3 absorption and NH_3/CO_2 separation

There will be many uncertainties and risks in emerging technologies from the laboratory to the industrial application. Through the process simulation and system integration of the entire purification process, the purification and separation performance of the process can be obtained, and the technical development potential can be evaluated, which will help reduce development costs and reduce or even avoid possible technical risks. At the same time, simulation methods are also conducive to improving the quality and efficiency of existing processes. With simulation and evaluation of the existing process, process bottlenecks can be discovered and possible solutions and optimization strategies can be proposed. To support the large-scale use of this technology in the industry, process simulation technology needs to be used to produce the process characteristic value, which serves as a data reference for industrial design and process analysis.

For the process simulation about the NH_3 containing tail gas cleaning with ionic liquids. Ruiz et al. [41] used the COSMO-SAC model to simulate the process of ionic liquid ammonia absorption refrigeration and proved that ionic liquid has high ammonia absorption performance. Simulation studies show that ionic liquids have great potential as absorbents in NH_3 refrigeration cycles. Chen et al. [67] regressed the NRTL model parameters based on the experimental solubility data of NH_3-[Bmim][BF_4] and obtained good NRTL fitting parameters. Based on the obtaining accurate physical property parameters, the Aspen Plus software was used to build a synthetic ammonia purge gas purification process based on ionic liquid. The sensitivity analysis method was used to obtain the suitable operating parameters of the process. The simulation results show that the energy consumption of the ionic liquid process can be reduced by about 14% compared with the conventional process under the condition that the recovery rate and purity of NH_3 reach 93.3 % and 95.2 %, respectively.

In terms of the process simulation and evaluation of NH_3/CO_2 separation by ILs, Liu et al. [68] screened 10 a hydroxyl-functionalized imidazolium-based IL by a systematic computer-aided IL design. The IL-based process was evaluated by technical-economical assessment. The simulation

results showed that compared with the traditional water scrubbing processes, the IL-based process represents a 45%, 35% and 19% reduction in overall equivalent energy, separation cost and net CO_2 emission, respectively. But this screening didn't include strict thermodynamic modeling with experimental data from the synthetic IL. In addition, the purified gas in this simple flowsheet don't meet the ppm NH_3 requirement. This work et al. [1] performed two IL-based NH_3/CO_2 separation process simulation and evaluation based on energy and economic assessment. The result showed that IL-based technology has a better financial cost than water scrubbing, in which the total separation cost of the IL-based process can be reduced by 61% than water scrubbing. It is important to note that as a novel new technology, deep analyzation of the relationship between operation parameters with objective functions, gaining higher separation performance, lower energy and economical consumption via rigorous optimization are necessary. For the industrial application of NH_3/CO_2 separation, the first industrial test pilot plant with 50 Nm^3/h of IL-based NH_3 recovery from melamine tail gas worldwide was constructed by the Institute of Process Engineering, Chinese Academy of Sciences, with 3500 h stable running[69].

2.2 IL-based process optimization

2.2.1 The introduction of multi-objective optimization in chemical engineering

Process simulation can also construct a multivariate process model for process optimization and evaluation, aiming at energy, economy, and environment, and use optimization algorithms to solve the process operation plan to obtain the best optimization target. It is important to note that as a novel new technology, deep analysis of the relationship between operation parameters with objective functions, gaining higher separation performance, lower energy, and economical consumption via rigorous optimization are necessary.

Single-objective optimization (SOO) methods typically maximize economics by directing raw materials through a process to produce products with the highest sales margins. However, there is always more than one objective. Typically in the chemical engineering process, multi-objective optimization is the problem of proving the trade-off between at least two different objectives or evaluation criteria [70]. The objective functions were always fundamental performance (recovery rate, product purity, and so on), energy, economy, environment, control, safety, etc. A systematic procedure of the MOO consists of 5 steps: 1 Process model development and simulation; 2

Formulation of the optimization problem; 3 Solution of the optimization problem; 4 Review of optimization results obtained; 5 Selection of optimal solution [71].

In step 1, the models can be established based on the fundamental principles as the first principles model. Another way of the model is using a suitable simulator (Aspen Plus or PRO II) with internal models and equations for the complex chemical process. After the correct model is gained, there is a need to define the optimization problem, and the operation parameters, objective functions, and constraints should be defined. Then select the operation parameters, sensitivity analysis was employed and changing one operation parameter with a reasonable range at a time to see the affection to the process objective functions. Constraints can be equality or inequality type. Some operation parameters were always set as constraints for the safe operation of the process. In addition, the recovery rate or the product purity was considered a constraint if the process was designed with simulation software.

For the solution of the optimization problem in step 3, the most commonly used MOO platform is Excel or Matlab [72]. If the process uses the simulator model, the interface of the simulation software should be designed (ActiveX) [73]. After obtaining the result of the MOO, the MOO will give many solutions known as Pareto front [74]. Suppose the Pareto front is sufficiently broad and smooth, and the variation of the objective functions with the operation parameters can be explained based on some principle of the application. In that case, the different solutions based on objective functions can be found and analyzed.

The technologies for solving MOO problems can be divided into two ways. One is to convert the MOO problem to a series of SOO problems and then solve SOO by an established technique for SOO. Weighted sum [75] [76] and ε-constraint [77] are two common techniques. The other approach is the modification of the SOO to solve the problems with various objectives. any multi-objective approaches (MOA) are metaheuristics, most of which are population-based and include evolutionary algorithms. In general, evolutionary algorithms have been widely employed in the chemical engineering process for MOO applications. The main steps are divided into four steps: 1 Initialization of the population; 2 Generation of child population; 3 Choosing individuals for the next generation; 4 Checking stopping criteria. The most typical algorithm used in chemical engineering is the Nondominated sorting genetic algorithm II (NSGA-II) [78]. There is also some research on open-source and commercial software for solving MOO problems. Lin [79] presented NGPM (NSGA-II Program in Matlab), a strong MOO solver, on the Matlab file exchange community. It uses reference-point-based NSGA-II and features a GUI. Recent years, Python is

becoming increasingly popular in academic for the character of completely open source. PyGMO [80] is a robust scientific library for massively parallel optimization that can address restricted, unconstrained, single-objective, multi-objective, continuous, and integer optimization problems, as well as stochastic and deterministic issues.

In recent years, more attention has been given to multi-objective optimization (MOO) in the chemical engineering process [81] [82] [70]. For the MOO application in gas utilization area, there is some multi-objective optimization research work on CO_2 utilization technologies, Wang et al. [83] took the CO_2 capture and separation process from syngas as an example to make comprehensive energy-economic-environmental analysis and multi-objective optimization. The CO_2 escape flow rate and total annual cost were the multi-objective optimization scheme's objective functions, with values that were 5.9% and 1.5% greater than their minimal values, respectively. Hosseini et al. [84] used methyl diethanolamine (MDEA) and piperazine (PZ) bi-solvent as solvents and then carried out MOO for the post combustion CO_2 capture. CO_2 capture efficiency and reboiler heat duty were used as the objective functions and main decision variables are solvent flowrate and MDEA/PZ concentration. The optimization values showed a higher energy efficiency compared to MEA and MDEA/PZ in conventional process configuration. Panu et al. [85] used bi-objective optimization to develop carbon-hydrogen-oxygen symbiosis networks with the goal of minimizing both cost and CO_2 emissions. The goal of this network is to improve existing plant integration by adding new plants for capturing and converting CO_2 into chemicals used by existing plants. In some ways, the installation of additional plants is like revitalizing an existing eco-industrial park. They found a number of trade-off solutions between cost and CO_2 emissions using the ε-constraint technique. Manuele et al. [86] used multi-objective optimization to remove CO_2 and H_2S selectively from coal-derived syngas. The results showed that the Selexol method is critical for optimizing the pressures of the flash cascade releasing the CO_2-rich stream to store, because the compression power and steam required for reboiling are the highest energy penalties. Hence, to obtain the optimal scenario of the melamine tail gas separation process, it is necessary to employ an optimization method to achieve better process performance and give a detailed process analysis.

2.2.1 Research about the multi-objective optimization with ionic liquid process

Taking the ionic liquid NH_3/CO_2 separation process as an example, the separation process includes various unit processes, including absorption columns/desorption columns, vacuum pumps, heat exchangers, etc. The operation between different units will not only affect the separation

performance of tail gas, but also affect the process cost and energy consumption. The separation process is a multi-unit coupling system, and the improvement of the processing efficiency and performance of a single sub-unit does not lead to the improvement of the processing efficiency and performance of the whole system. At the same time, the operating parameters and evaluation indicators of each processing unit in the system are mutually coupled, restricted and weighed. Therefore, it is necessary to comprehensively examine the coupling relationship between the units in the entire system from the perspective of system engineering, and to optimize the process using relevant optimization algorithms (such as genetics, ant colony, etc.) Under the premise of obtaining a certain purification effect, so as to obtain treatment with the best purification solution for cost, energy consumption, environment and other indicators. Ionic liquids have broad prospects in industrial applications, and many researchers are committed to promoting the application of ionic liquid absorption processes. The simulation calculation can reduce the experimental investment, discover possible bottlenecks in the process in time and propose feasible solutions, and at the same time evaluate the application prospect and potential of the process.

In the ionic liquid application area, some research deals with two or more objectives to give a more detailed understanding of the new technology. Ma et al. [87] optimize the separation process of isopropanol-water azeotrope using ionic liquid as extractant, TAC, energy consumption per product flow rate and efficiency indicator of extractive section as main object functions. The results indicated that compared with the process using 1 evaporator, the process with 2 evaporators could reduce TAC by about 4 %. Tian et al. [88] proposed and performed a MOO for ionic liquids based producing 1,3-butadiene both the energy consumption and environmental impact of this new process, the result showed that the energy consumption of the IL-containing process could be reduced by 22 % and that its green degree could be improved by 9.2 %. Zhan et al. [89] employed MOO for the treatment of NH_3-containing tail gas with ionic liquids and after optimization, a series of solutions satisfying the constraints were provided by the Pareto front. The lowest objective functions can achieve 0.0211 \$/Nm^3 (TPC), 265.67 kg CO_2/h (TPCOE), and 48.05% (η_{eff}). Hence, to obtain the optimal scenario of the melamine tail gas separation process, it is necessary to employ an optimization method to achieve better process performance and give a detailed process analysis.

2.3 IL-based process dynamic control

The steady-state design and multi-objective optimization process provide a comprehensive technological process design and parameter analysis. However, the actual production process

constantly changes over time in both the load and composition of the tail gas. Hence, a steady-state simulation is only an ideal assumption and does not reflect the actual production process. Investigating process parameter behavior in response to process disturbances is important for a new and novel technology in future industrial applications. Dynamic simulation is one approach to analyze the behavior, includes definition of operational objectives and consideration of degrees of freedom available, bottom-up design of the control system, and starting with the stabilizing control layer[90]. On this basis, a plant-wide control strategy could be formulated and implemented to reject disturbances and maintain emission levels of harmful gases within acceptable bounds in the plan for industrial application.

For the bottom-up design, the regulatory control layer needs the process should realize stabilization through low-complexity controllers, for example, some single-loop PID controllers [91]. Regulatory control is a control strategy that regulates a process to the steady-state despite disturbances and set point changes. Inventory stabilization is a primary objective for the design of a regulatory control strategy for the process. Inventory control guarantees the set point by adjusting the manipulated variables which is an essential aspect of process control in chemical engineering. Inventory stabilization control involves maintaining the level of product in a storage tank or vessel at a desired set point or range, despite variations in the input and output flow rates. Inventory stabilization control aims to ensure that the equipment does not overflow or become empty, which could lead to process disruptions, safety hazards, and product quality issues. Level control, pressure control, and flow control are some common control strategies to achieve inventory stabilization control.

Robust control [92] ensures that chemical engineering processes are reliable, efficient, and safe. Developing and implementing robust control systems requires a thorough and detailed understanding of the process dynamics. Robust control maintained the process's stability within acceptable limits in operating conditions and disturbances in industrial applications. The system should be designed to be insensitive to variations in the process dynamics and external disturbances through robust regulator control. It is achieved by selecting appropriate control algorithms, tuning control parameters, and implementing suitable control strategies. Robust regulator control is crucial for ensuring a process’s smooth and reliable operation, achieving optimal product quality, and maximizing resource utilization.

Simple decentralized PID can meet the control requirements of simple processes, and for complex and integrated processes, it is necessary to select a suitable predictive dynamic control scheme or build a suitable dynamic model prediction scheme for the process. From the perspective of development trends, predictive control can focus on economic performance while considering control performance, such as economical MPC [93] [94], adding economic performance indicators to the objective function, and the controller can optimize process economic performance in real time, but the validity of its engineering applications still needs to be verified.

There is some research about the IL-based extraction process for the dynamic control research of the IL-based process. Sun et al. [87] studied the control structures of the extraction process for the separation of isopropanol-water using IL as extractant and the dynamic control result showed that when a fluctuation of ± 10% flow rate and composition variation is introduced after the system runs smoothly for 0.5 h. The control findings show that the control structure can withstand disturbances in feed flow and feed composition, and the product purity can be corrected to the specified value within 4 hours. Li et al. [95] set the process' conditional number as the objective function of the multi-objective optimization and the dynamic simulation of two IL-based extractive distillation of ethanol/THF separation were carried out to compare their dynamic responses based on the same dynamic control structure, and the best trade-off between objective functions solution shows better performance in the aspects which include maximum deviation and residual error of dynamic response. Darinel et al. [96] performed the dynamic analysis for the IL-based CO_2 capture process and provided insight into the degree of nonlinearity and the dynamics of the process. The results show that the plant can accommodate perturbations in the flue gas flow rate up to ±10% while meeting CO_2 recovery and purity targets. However, for the dynamic control of IL-based NH_3/CO_2 separation process, there are limited published research results.

As a traditional technology for the separation of NH_3/CO_2, the dynamic control research of water scrubbing is not quite much. As discussed in the previous chapter, the water scrubbing process has several distillation columns and a complex heat exchange network. The dynamic control problems will be more difficult than the simple flow chart technologies such as IL-based processes. Although there is limited published research about the dynamic control of separation of NH_3/CO_2 by the water scrubbing process, the dynamic control of water scrubbing has some similarities with the CO_2 capture process by amine solvents. In recent years, some research has been done on the dynamic control of gas separation [97]. Gao et al. [98] employed multi-objective optimization and carried

out dynamic control for the biogas pressurized water scrubbing process. The result showed that the designed dynamic control scheme is effective for the parameter disturbance and the process parameters can go back to the set value, and the quality of products gas can meet the requirement. Sahraei et al. [99]proposed an advanced model-based control strategy for the CO_2 capture plant. The MPC-based control scheme could resist disturbances with better performance compared with the decentralized control strategy. Lin et al. [100] investigated the dynamic simulation of plantwide control of an absorption/stripping CO_2 capture process employing monoethanolamine solvents. The proposed control scheme can stabilize quickly, and in order to keep the minimum energy consumption, the optimizing control can be carried out by adjusting the set point of the reboiler temperature of the stripping column. Turton et al. [101] employed MPC strategies for the different stripping configurations for the CO_2 capture process. The proposed nonlinear MPC can improve the performance by 95% compared with the PID controller. In addition, the proposed lean vapor compression CO_2 capture configurations have a 5.5% economic improvement compared to the traditional PID controller configuration.

2.4 Summary

This chapter summarized the current state of art from the aspect of NH_3, CO_2 containing tail gas cleaning and separation of NH_3/CO_2 in chemical engineering process, the optimization of IL-based process and dynamic control of IL-based process, gives an overview of the development of the IL-based gas separation technology and the background of this PhD project.

3 Case study: Process design, simulation and evaluation of IL-based techonology

This chapter gives a case study of the detailed IL-based gas separation process design, simulation and evaluation. This chapter was divided into three parts. The first part gives the IL thermodynamic property model and the validation of regression models with experiment data. The second part concentrated on the process design and simulation of the new technology in Aspen Plus. In the last part, the evaluation of this process was carried out in aspect of the energy consumption and economic analysis. In conclusion, this chapter was a detailed process design, simulation and evaluation of the new technology in this PhD project. This chapter is partially based on the published articles: ”Process simulation and evaluation for NH_3/CO_2 separation from melamine tail gas with protic ionic liquids”, Separation and purification Technology, 288 (2022) 120680 [1]

3.1 IL thermodynamic property model

The reliability of the ionic liquid processing of ammonia-containing gases in process simulation depends on the basic data and the accuracy of the thermodynamic model. The thermodynamic model can predict the phase equilibrium parameters, and the NRTL equation can calculate the properties of the multi-component solution from the data of the binary solution. The outstanding advantage of this method is that it can be used in partially miscible systems.

The COSMO-RS model [102] uses quantum chemistry to predict the phase equilibrium of a multi-component system, because it is regarded as an effective method for predicting the thermodynamic properties of ionic liquids. Lei [103] et al. used the UNIFAC model to estimate the solubility of CO_2 and $CO(H_2)$ in ionic liquids, then linked the model results with experimental data to determine the relationship between CO_2, $CO(H_2)$, and ionic liquid group parameter. Anantharaj et al. [104] screened ionic liquids with COSMO-RS-based in denitrification studies, the result showed that cations lacking aromatic rings, such as [EPYRO], [EMPIP], and [EMMOR], demonstrated greater selectivity and capacity regardless of the nitrogen heterocycle. Lee [105] and others not only used the COSMO-SAC model to predict the solvent's activity coefficient, but also developed a simple model to predict the fugacity coefficients of the four gases CO_2, CH_4, N_2, and H_2, and calculated the CO_2 in the ionic liquid, with the prediction results agreeing well with the experimental results.

According to the reference, Shang [106] synthesized a new functional protic IL([Bim][NTf_2]) which shows much higher NH_3 capacity than conventional ILs, in this work we choose this IL as the solvent. Accurate thermodynamic models are required to create the thermodynamic model of the ionic liquid, which includes single value component properties, temperature-dependent functional pure component properties, and the phase equilibrium relationship.

3.1.1 Critical properties of ionic liquids

The critical properties of the chosen ionic liquid ([Bim][NTf_2]) are computing using Huang's [40] fragment contribution-corresponding states (FC-CS) approach. Reliable thermodynamic models of ionic liquids are essential for obtaining reliable steady-state simulation data. The rigorous and correct thermodynamic model will be carried out in this section as a new component in process simulation software that lacks a detailed databank. Table 1 displays the critical property data.

Table 1 The critical properties of [Bim][NTf_2].

Parameter	[Bim][NTf_2]	Unit
Tc	1120.17	K
Pc	2205.00	kPa
Vc	641.35	Ml/mol
Tb	745.07	K
Mw	405.34	g/mol
ω	0.14	-

*: *Tc* is the critical temperature, *Pc* is the critical pressure, *Vc* is the critical volume, *Tb* is the boiling temperature, *Mw* is the molecular weight and ω is the acentric factor.

3.1.2 Physical property model of ionic liquids

Process simulation begins with the physical properties of ionic liquids. Table 2 displays the model equations for the properties of ionic liquids. Physical property data from the literature and the calculation result of the ionic fragments contribution COSMO-SAC (IFC-COSMO-SAC) method in Tu's work [107] are used to regress the model parameters. The IFC-COSMO-SAC approach predicts the thermodynamic parameters of IL in a quick and reliable manner. The model parameters are regressed using equations in Table 2 based on experimental ionic liquid property data. The corresponding parameters of the correlation equation for each of the main properties are shown in Table 2.

Table 2 Equation of main physical properties of [Bim][NTf_2].

Properties	Correlated Equation	Correlated Equation with parameters	Unit	Ref. of Exp. data
Viscosity	$\ln \mu = c_1 + \frac{c_2}{T} + c_3 \ln T$	$\ln \mu = -457.44 + \frac{24536.8}{T} + 65.43 \ln T$	Pa·s	[62] [108]
Heat capacity	$C_p = c_1 + c_2 T + c_3 T^2$	$C_p = -106.2 + 2.93T - 0.01T^2$	kJ/K/kmol	[107] [109]
Density	$\frac{M_w}{\rho} = c_1 + c_2 T$	$\frac{M_w}{\rho} = 0.21928 + 0.00019T$	m^3/kmol	[107] [106]
Surface tension	$\sigma = c_1 \times (1 - (\frac{T}{T_c}))^{(c_2 + c_3(\frac{T}{T_c}) + c_4(\frac{T}{T_c})^2 + c_5(\frac{T}{T_c})^3)}$	$\sigma = 43.84 \times (1 - (\frac{T}{T_c}))^{(0.43 + 3.89(\frac{T}{T_c}) - 8.02(\frac{T}{T_c})^2 + 6.09(\frac{T}{T_c})^3)}$	Dyne/cm	[107]
Thermo Conductivity	$\lambda = c_1 + c_2 T + c_3 T^2 + c_4 T^3$	$\lambda = 0.198 - 0.0004T$	W/m/k	[106]

*: μ is the viscosity, Cp is the heat capacity, ρ is the density, σ is the surface tension, λ is the thermo conductivity, Mw is the relative molecular weight, Tc is the critical temperature of the ionic liquid, c_i is the parameter of each correlated equation.

3.1.3 Validation of Main Thermodynamic Property Models

The model parameters are regressed using the equations in Table 2 based on experimental property data of the ionic liquid. Figure 6 depicts the main properties of the ionic liquid based on the experiment and the regression calculation results. The regression values agree well with the experimental data. This can be used to validate the dependability of physical property models and their suitability for process simulation. Following the acquisition of all model parameters via regression, these properties were entered into the corresponding location in simulation software. The *AARDs* and the corresponding location in Aspen software is shown in Table 3.

Table 3 *AARDs* of correlation equation and corresponding location of equation in Aspen software.

[Bim][NTf_2]	*AARD*	Aspen Models
Viscosity	2.72%	Liquid Viscosity (MULAND)
Tension	0.00%	Liquid Surface Tension (SIGDIP)
Density	0.01%	Liquid Molar Volume (VLPO)
Heat capacity	0.00%	Liquid Hear Capacity (CPLIKC)
Thermo conductivity	0.00%	Liquid Thermal Conductivity (KLDIP)

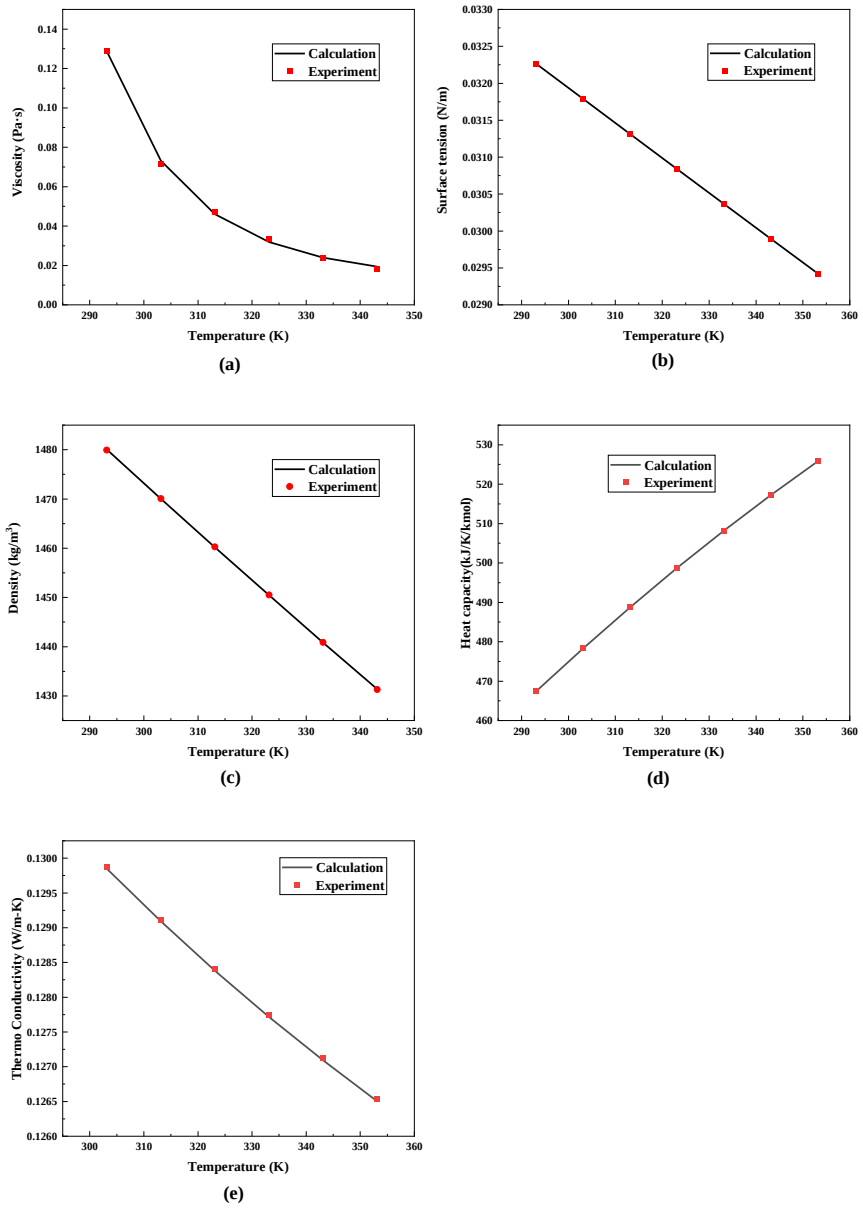

Figure 6 Experimental and calculated (a) viscosities, (b) surface tension, (c) densities, (d) heat capacity, (e) thermal conductivity of [Bim] [NTf_2] in Aspen Plus V11^{TM}. Points and lines indicate experimental data from literature and calculated data, respectively.

3.1.4 Vapor-liquid phase equilibria

The relationship of vapor-liquid equilibria is critical for the separation's performance in the process simulation of this system. The volatile components in the binary system of NH_3/CO_2 with an ionic liquid will be NH_3 and CO_2. The activity coefficient model describes the activity coefficients of NH_3 and CO_2 in an ionic liquid. The ideal gas state equation can be used to generalize the gas phase for vapor-liquid equilibrium at low or ambient pressure, which can be used to calculate the partial pressures of NH_3 and CO_2 in equation 1 [110]

$$Py_i = p_i = p_i^{sat} x_i \gamma_i \quad \text{Equation 1}$$

Where P is total pressure, yi is mole fraction of volatile component i, p_i^{sat} is the saturated vapor pressure of component i, γ_i is the activity coefficient and x_i is the mole faction of component i in liquid phase;

Activity coefficient is calculated by NRTL model and shown as Equation (2~5) [111] :

$$\ln \gamma_i = \frac{\sum_{j=1}^{\delta} \tau_{ji} G_{ji} x_j}{\sum_{j=1}^{\delta} G_{ji} x_j} + \sum_{j=1}^{\delta} \frac{G_{ij} x_j}{\sum_{k=1}^{\delta} G_{kj} x_k} \left[\tau_{ij} - \frac{\sum_{k=1}^{\delta} \tau_{kj} G_{kj} x_k}{\sum_{k=1}^{\delta} G_{kj} x_k} \right] \quad \text{Equation 2}$$

$$G_{ij} = \exp(-\alpha_{ij} \tau_{ij}) \quad \text{Equation 3}$$

$$\tau_{ij} = \left(g_{ij} - g_{jj} \right) / RT = a_{ij} + \frac{b_{ij}}{T} \quad \text{Equation 4}$$

$$\alpha_{ij} = \alpha_{ji} = \alpha \quad \text{Equation 5}$$

Where x is the mole fraction in liquid phase, δ is the number of components in vapor-liquid phase, R is the gas constant, T is the absolute temperature in K, α_{ij} is the factor of nonrandom parameters of system characteristics which is fixed at 0.2 for NH_3 and 0.3 for CO_2 [112], G_{ij} is the action energy between component i and component j in solution, g_{ij} is the energy interaction parameter.

3.1.5 Validation of Vapor-liquid phase equilibria Thermodynamic Property Models

The statistics of correlation coefficient (R^2) and average absolute relative deviation ($AARD$) were used as evaluation indices to validate the thermodynamic property models. The R^2 and $AARD$ are expressed as given equations:

$$R^2 = 1 - \frac{\sum_{i}^{N_p} (y_i^{cal} - y_i^{\exp})^2}{\sum_{i}^{N_p} (y_i^{\exp} - \frac{1}{N_p} \sum_{i}^{N_p} y_i^{\exp})^2} \quad \text{Equation 6}$$

$$AARD(\%) = 100 \times \sum_{i=1}^{N_p} \left| \frac{y_i^{cal} - y_i^{\exp}}{y_i^{\exp}} \right| / N_p \quad \text{Equation 7}$$

Where y_i^{cal} and $y_i^{\exp}$ are the calculation value and experiment value, respectively; *Np* is the number of experiment point.

Using experimental data from the literature, the NRTL parameters of NH_3/CO_2-IL in a binary system are regressed[106] [62], then the phase equilibrium models of NH_3/CO_2-ionic liquid are established. The parameters of NRTL model are shown in Table 4. The model estimated and experimental results for NH_3/CO_2-ionic liquid are compared on Figure 7. In Table 4, since *AARD* value being below 10% (8.32% of NH_3 and 4.79% of CO_2 ([Bim][NTf_2])), it is shown that The estimated outcomes fit in with the experimental data in the literature. This suggests that the NRTL model is sufficiently reliable for the NH_3/CO_2-ionic liquid system to be employed for process modeling. For the selectivity of NH_3 and CO_2 of [Bim][NTf_2], it is reported as shown in [62] that it has a high selectivity of the two gases which can be used in the separation of this system.

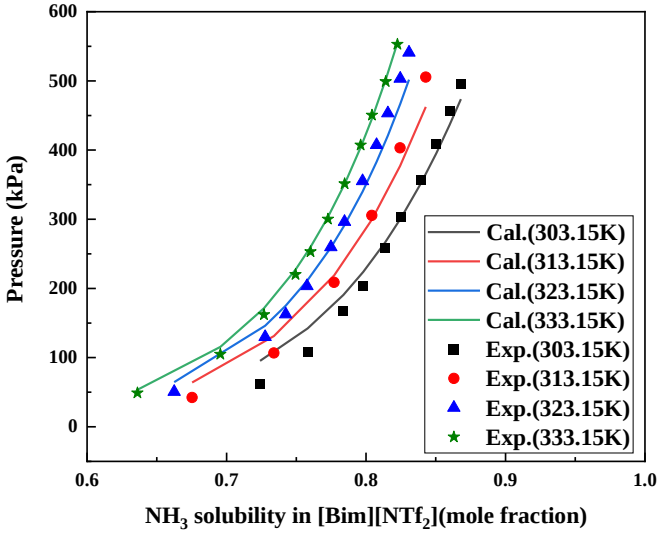

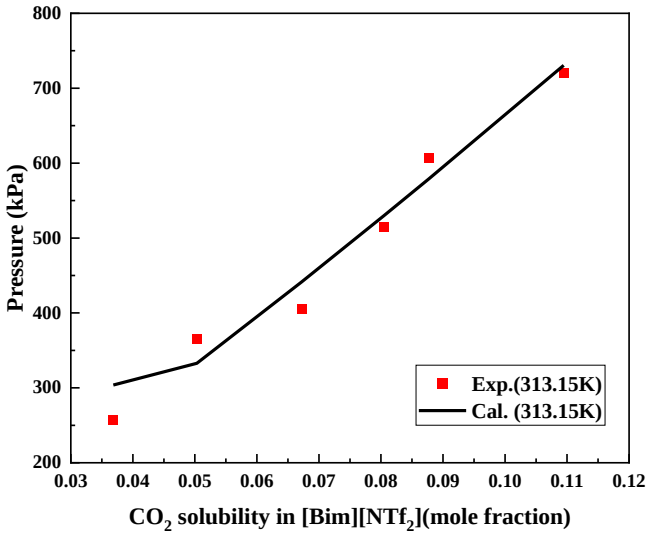

Figure 7 Comparison of the estimated and experimental values of total pressure values for NH_3/CO_2 [Bim][NTf_2] system.

Table 4 Regressed NRTL parameters for NH_3-[Bim][NTf_2] binary systems.

Gas	IL	a_{ij}	a_{ji}	b_{ij}	b_{ji}	c_{ij}	R^2	*AARD* (%)
NH_3	[Bim][NTf_2]	-8	-10.3	476.1	1259.4	0.2	0.995	8.32
CO_2	[Bim][NTf_2]	-3	19.7	867.9	-0.03	0.3	0.995	4.79

3.2 Process design and simulation

In this study, the feed stream of melamine tail gas information is getting from a Chinese melamine factory with the tail gas consists of 7.6 % nitrogen (N_2), 0.4 % water (H_2O), 55 % NH_3 and 37 % CO_2 in mole fraction. Raw feed flow in volume is 4480 Nm^3/h. The pressure and temperature of the raw stream flow are 200.00 kPa and 393.15 K, respectively. The process operation time is set as 8000 h per year. The purified gas of NH_3 concentration is about 6000 ppm (mole fraction) with gas separation. NH_3 purity in product stream is set over 0.996 mass fraction refers to the requirement of China national liquid ammonia product standard and factory demand. The pressure drop of column tray is set as 0.69 kPa per tray [113].

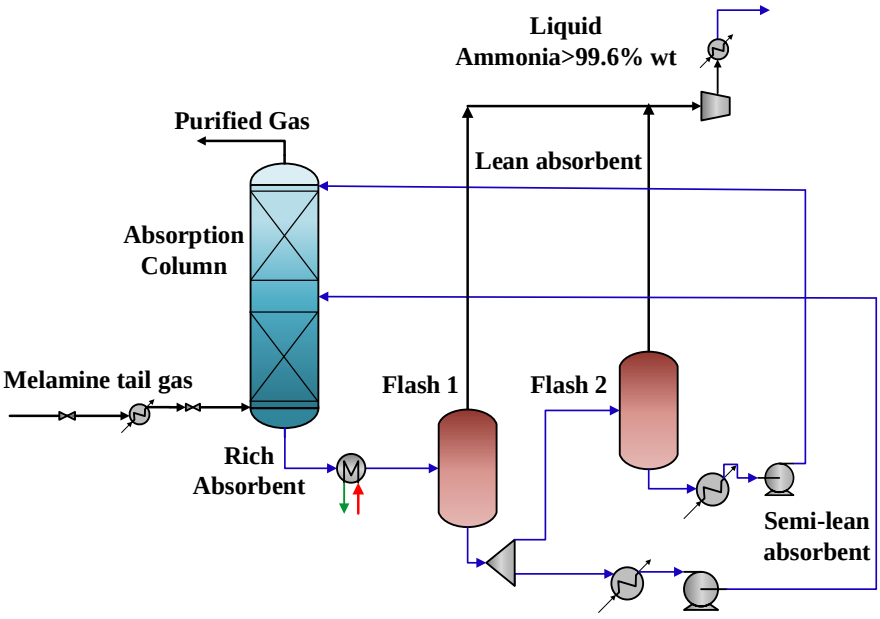

Figure 8 Flow chart of NH_3/CO_2 separation by [Bim][NTf_2] (IL-0).

Figure 8 depicts the design of the NH_3/CO_2 separation process. This procedure consists of two sections: NH_3 absorption and absorbent regeneration. The melamine tail gas is heated to 348.15 K before the gas

flows to the bottom of absorber at absorption temperature and pressure, contacting with the IL counter-currently. At certain conditions of temperature and pressure, NH_3 and CO_2 are able to react with one another. with the calculation of this reaction, the critical crystallization temperature with the tail gas composition in 200 kPa is 345.4 K and the gas temperature should large than this value to avoid the crystallization. Rich absorbent flowed into Flash 1, and NH_3 was released in Flash 1 as the temperature and pressure were slightly increased. The semi-lean absorbent liquid is divided into two parts after being regenerated in Flash 1. The remaining semi-lean adsorbent flows back into the Absorption tower and the partial liquid flows into Flash 2 and NH_3 is released again at a lower pressure and higher temperature than in Flash 1. Finally, for cyclic solvent utilization, the lean and semi-lean adsorbents are cooled to absorption temperature and pumped to absorption pressure.

For the requirement of new technology process intensification, energy-economic friendly process is the development trend of the new technology. For the absorption process, strengthening solvent purity is an effective way to achieve better absorption performance. Stripping column is a powerful equipment to deep purify the solvent, reduce energy and economic cost. An enhanced ionic liquid method (IL-En) is presented in order to reduce the cost of energy and separation when compared to the ionic liquid process. This enhanced ionic liquid process (IL-En) involves the addition of a stripping column in order to reduce the amount of NH_3 that is present in the lean solvent, which in turn reduces the amount of ILs that are used in comparison to the prior process. Figure 9 illustrates the conceptual design of NH_3/CO_2 absorption by the IL-En process.

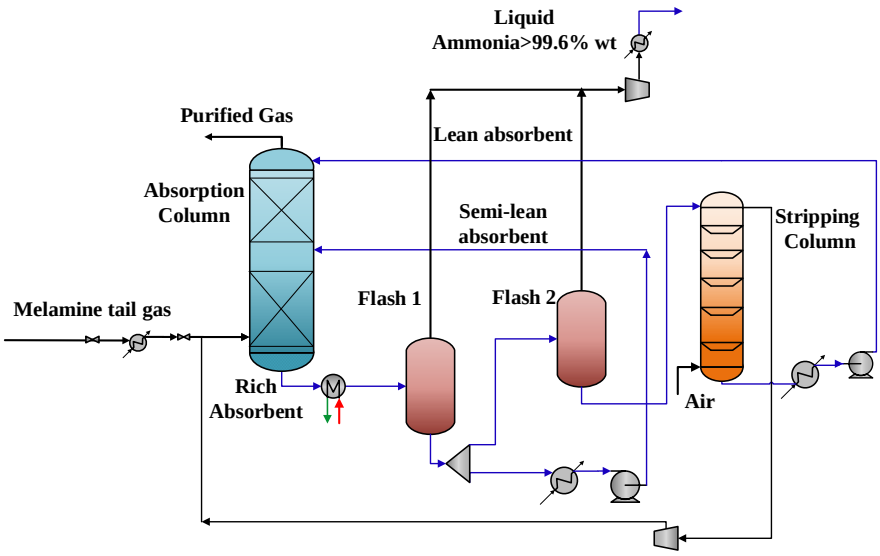

Figure 9 Flow chart of enhanced NH_3/CO_2 separation by [Bim][NTf_2] (IL-En).

3.2.1 Parameter sensitivity analysis using IL

In this part, key parameters of two IL-based NH_3/CO_2 separation process are researched, *e.g.*, the total stage, feed stage of semi-lean, ratio of lean flow and total flow ratio (R_{STL}). Figure 8 and Figure 9 is the flowchart of NH_3/CO_2 separation process from melamine tail gas by IL-0 and IL-En processes.

Absorption pressure

Figure 10 shows the NH_3 purification effect of absorption pressure. From Figure 10, when the adsorption pressure is increased, the trend of decreasing NH_3 concentration in the purified gas follows suit. Considering the operation condition of absorption and NH_3 concentration in purified gas the adsorption pressure is selected as 202.65 kPa for both the IL-0 and IL-En process.

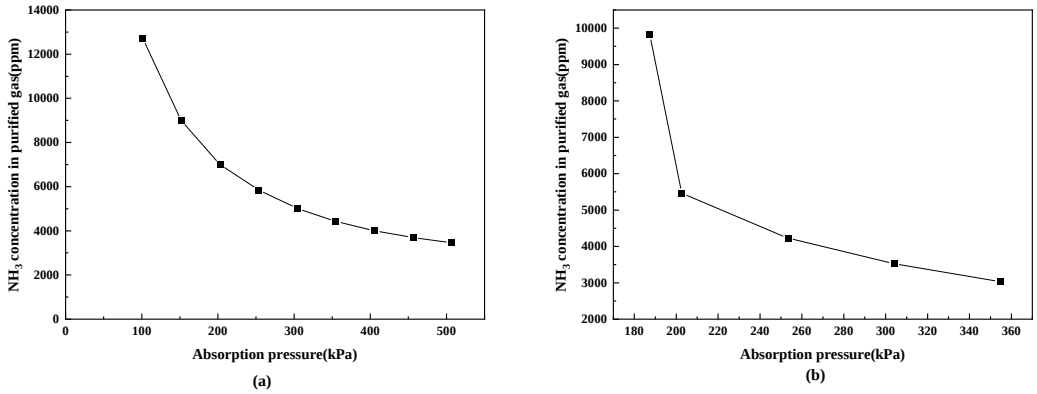

Figure 10 NH_3 mole fraction in purified gas versus absorption pressure of (a) IL-0 and (b) IL-En process.

Stages number of absorption column and IL flow rate

Figure 11 depicts the NH_3 purification effect of IL flow rate and tray number. Previous studies have demonstrated that increasing the number of trays in an absorption column improves its separation efficiency. The tray numbers for the IL-0 process are chosen from Figure 11 (a). Figure 11 (a) shows that with a total tray number of 8 trays, the optimal circulating solvent is 55 $t \cdot h^{-1}$ for the cost of IL and the NH_3 concentration in purified gas. Figure 11(b) depicts the flow rate of IL in the IL-En, with the tray number of absorption set to 7. The concentration of NH_3 in the purified gas decreases as the IL usage increases. The reason for this is that at low IL flow rates, there is insufficient contact between IL and NH_3, leading to poor results in terms of absorption. The absorption performance improves gradually as the IL flow rate increases. When the IL flow rate approaches 40 $t \cdot h^{-1}$, the concentration of NH_3 in purified gas does not change significantly, and this is at a lower flow rate than the IL-0 process.

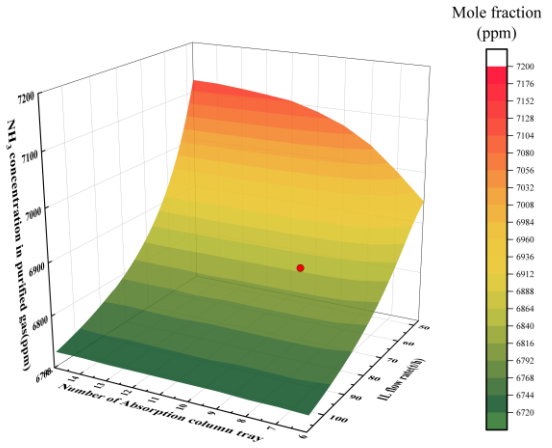

(a)

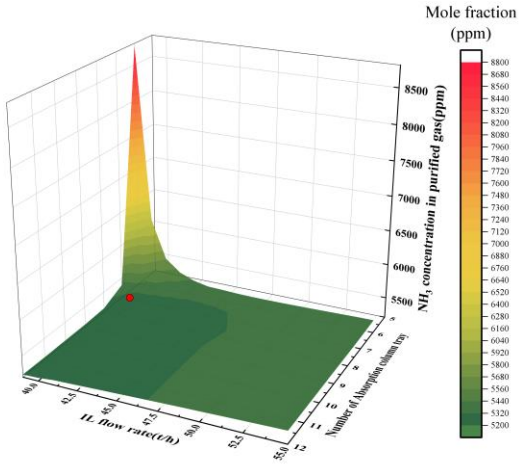

(b)

Figure 11 NH_3 mole fraction in purified gas versus flow rate of IL under different tray numbers (a) IL-0 and (b) IL-En..

Semi-lean liquid feed position

Figure 12 shows the relationship between the purified gas of NH_3 and semi-lean liquid feed position of the two IL-based processes. From Figure 12, the concentration of NH_3 in purified gas decreases as the feed position increases. The semi-lean liquid feed position is selected as 4 for the concentration of NH_3 in purified gas is not increased with the stage position of semi-lean both for the two IL-based processes.

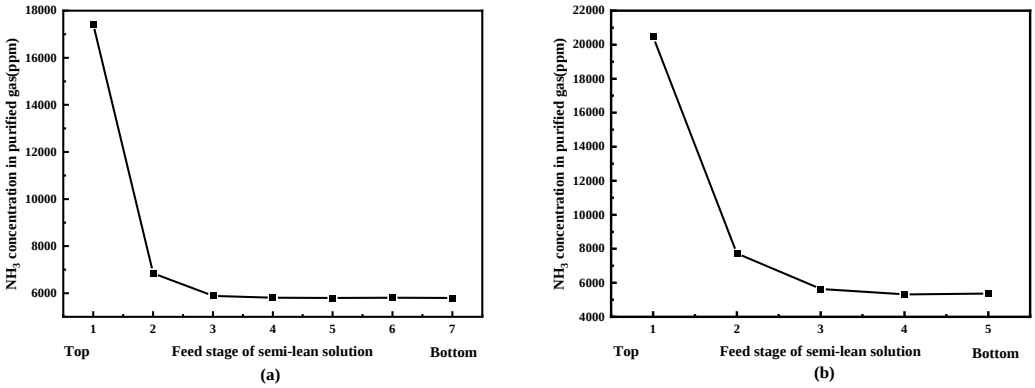

Figure 12 The relationship between the purified gas of NH_3 and the position of the semi-lean liquid at fixed the total trays and total IL flowrate (a) IL-0 and (b) IL-En.

Ratio of lean flow and total flow ratio

R_{SLT} is a critical operational parameter in the absorption process. The effect of R_{SLT} on the concentration of NH_3 in purified gas and the rate of NH_3 recovery is demonstrated in Figure 13. From Figure 13, the NH_3 content in purified gas decreases as R_{SLT} increases, while the NH_3 recovery flow rate increases. When R_{SLT} is high, the NH_3 concentration and recovery flow rate gradually smooth out. Furthermore, the concentration of NH_3 in purified gas is an important indicator for the purification of NH_3-containing gases. Hence, R_{SLT} is selected as 0.4 and 0.48 for IL-0 and IL-En, respectively.

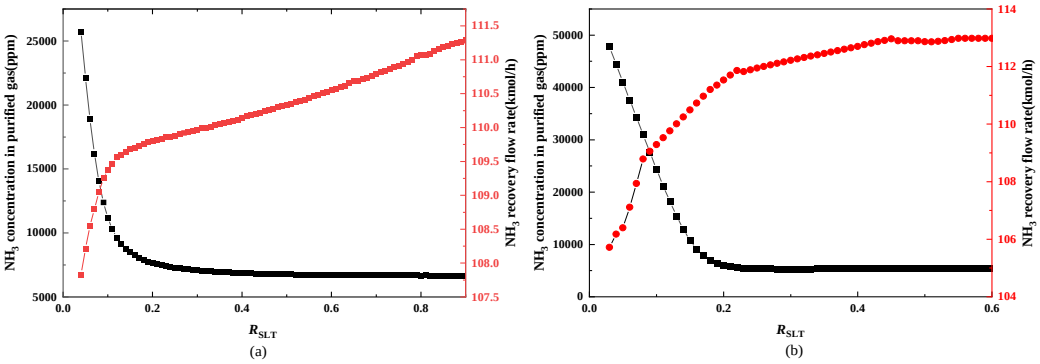

Figure 13 Effect of R_{SLT} on NH_3 concentration in purified gas and recovery flow rate (a) IL-0 and (b) IL-En.

Pressure and temperature of Flash 1 and 2

The temperature and pressure of two flashes are analyzed due to their important role in the regeneration unit. Flash 1 is designed to remove most of the NH_3 in the rich solvent, to attain qualified liquid NH_3

products and purify the solvent back to the absorption column. Thus, the selection of operating parameters in flash 1 depends on the mole fraction of NH_3 in purified gas, as plotted in Figure 14 (a). It can be seen that the NH_3 concentration in purified gas has been decreased by increasing the temperature of flash 1 and decreasing the pressure. Considering the ionic liquid's stability in high temperature and the requirement of purified gas, Flash 1 is operated at 10 kPa and 110 ℃. Figure 15 (a) shows the effects of flash 2 pressure and temperature on the NH_3 concentration in the purified gas. With the same reason, the Flash 2 is operated at 2 kPa and 110 ℃. For the IL-En process, the same sensitivity analysis was shown in Figure 14 and Figure 15 (b).

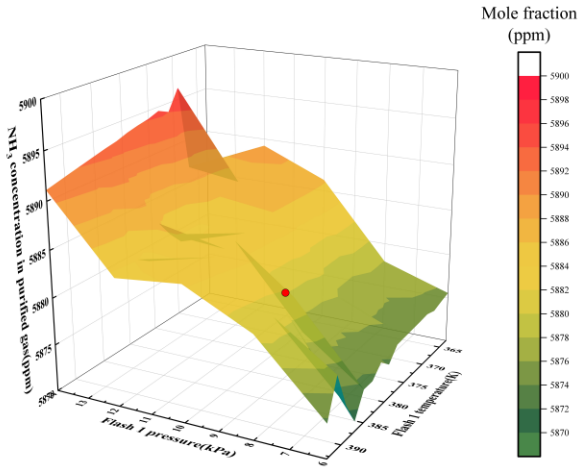

(a)

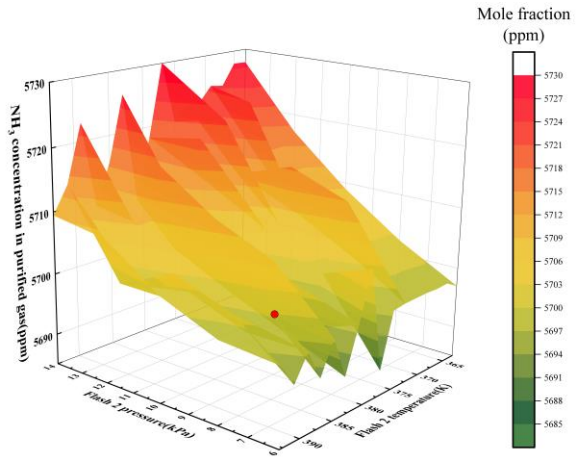

(b)

Figure 14 Effect of temperature and pressure of Flash 1 on NH_3 concentration in purified gas (a) IL-0 and (b) IL-En.

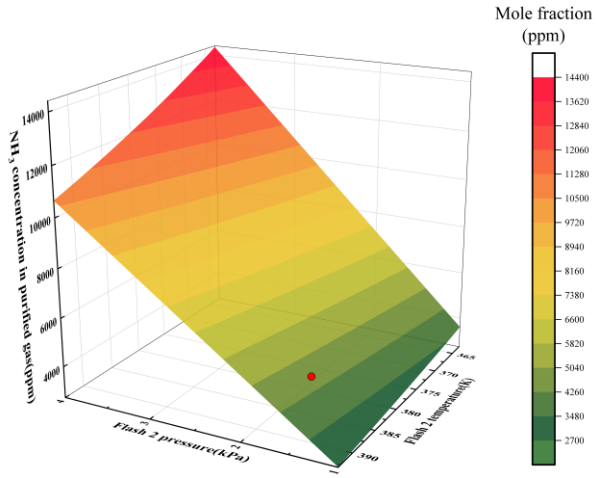

(a)

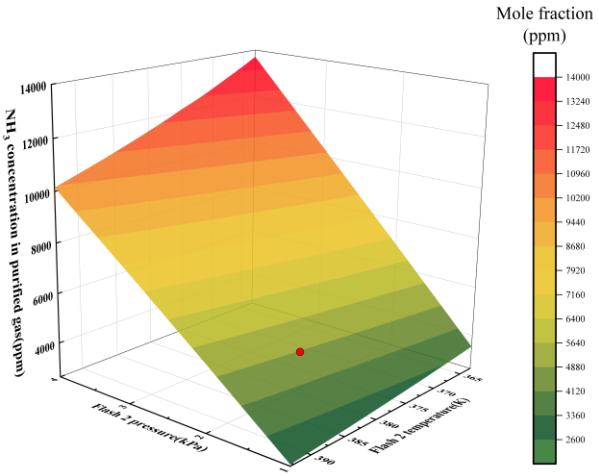

(b)

Figure 15 Effect of temperature and pressure of Flash 2 on NH_3 concentration in purified gas (a) IL-0 and (b) IL-En.

Other sensitivity analysis of IL-En process

Air is introduced in the stripping column to reduce the NH_3 concentration in the semi-lean solvent for the IL-En process, which is responsible for deep cleaning the solvent. Figure 16 depicts the impact of air flow rate on NH_3 in purified gas and NH_3 recovery rate. Air addition will alter the tower's thermodynamic equilibrium and lower the partial pressure of NH_3 in the gas phase, causing more NH_3 to be absorbed during the desorption phase. Figure 16 (a) illustrates how the concentration of NH_3 in purified gas first drops and then quickly rises as the air flow rate increases. The flow rate of NH_3 for

NH_3 recovery reduces as the air flow rate increases. We selected a 220 kg/h^{-1} air flow rate with high NH_3 recovery and nearly the same NH_3 concentration in purified gas as the IL-0 process in order to align the benchmark. Figure 16 (b) shows the stage number of stripping column change with the NH_3 concentration in purified gas. With the increase of stage number of stripping column, the NH_3 concentration decrease, considering the cost of equipment, the number value is fixed as 4. Figure 16(c) depicts the relationship with pressure of stripping column and NH_3 concentration in purified, higher pressure with lead to the decrease of separation performance, considering the equipment cost, the pressure of stripping column is fixed as 100 kPa.

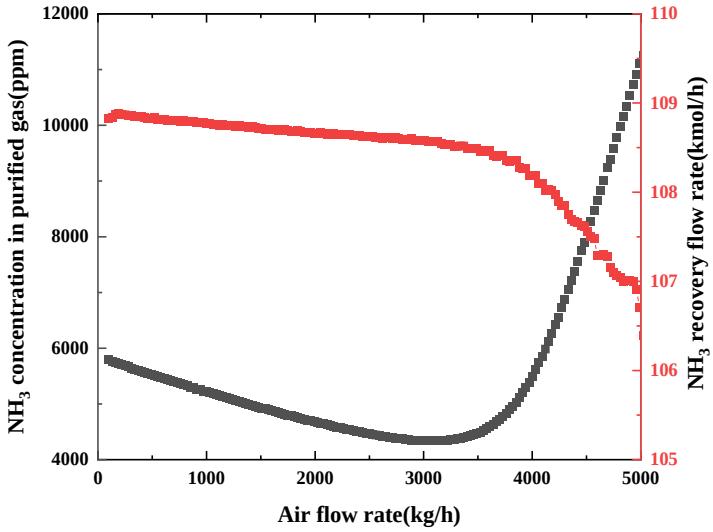

(a)

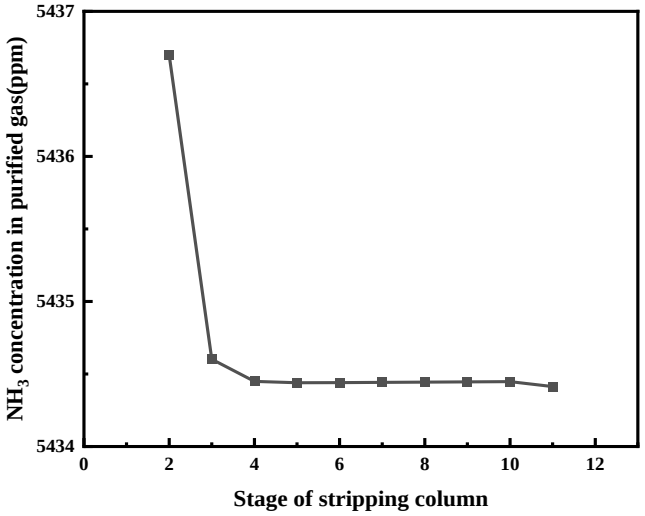

(b)

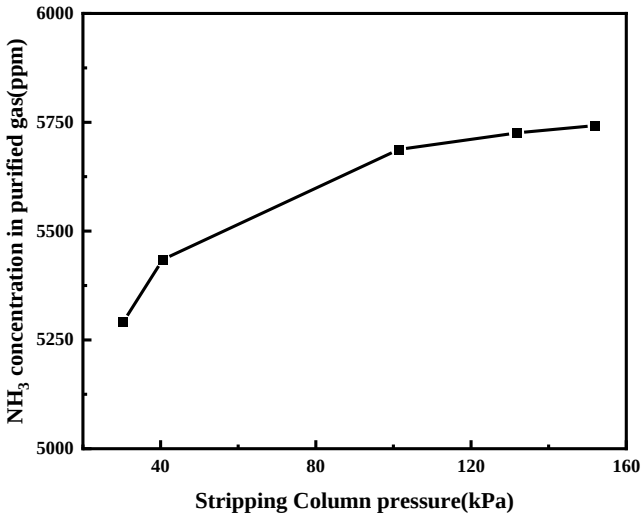

(c)

Figure 16 Sensitivity Analysis of IL-En process (a) The effect of air flow rate on the NH_3 mole percentage in purified gas, as well as the recovery flow rate; (b) NH_3 mole fraction in purified gas versus stripping pressure; (c) The stage of stripping column versus NH_3 mole fraction in purified gas.

3.2.2 Water scrubbing process of separation of NH_3 and CO_2

As the traditional way of NH_3 and CO_2 separation process, water scrubbing are described below, the thermodynamics model for the process simulation was established in Aspen Plus. Because NH_3 and water are polar substances that will interact electrically in this system, we chose the Electrolyte NRTL (ELENRTL) [111]as the basic property method. The most versatile electrolyte property method is the ELENRTL property method. It can handle extremely low and extremely high concentrations. It is compatible with aqueous and mixed solvent systems. The databank can also be used by ELENRTL to find binary chemical interaction parameters for the NRTL property approach.

Water with high availability is used as an absorbent in the water scrubbing process [30]. The conceptual flowsheet employed here is based on a patent for melamine tail treatment gas applying water scrubbing. This invention covers a technique for treating melamine tail gas that includes a NH_3 separation column, a CO_2 separation column, and a water separation column. First, the melamine tail gas flows to the NH_3 separation tower, where it is converted into a CO_2-NH_3-H_2O solution and NH_3. The CO_2-NH_3-H_2O solution received from the NH_3 separation column is treated in the CO_2 separation column to obtain CO_2 and the CO_2-NH_3-H_2O solution; the CO_2-NH_3-H_2O solution acquired from the CO_2 separation tower is delivered to the water separation tower. The CO_2, NH_3, and water vapor are distilled from the water separation tower's top, and the water vapor is condensed into water and returned to the tower, while the uncondensed NH_3 and CO_2 are recycled in the NH_3 separation column. The NH_3 purity in the product is set over 0.996 mass fraction. The conceptual design of the water scrubbing process is shown in Figure 17.

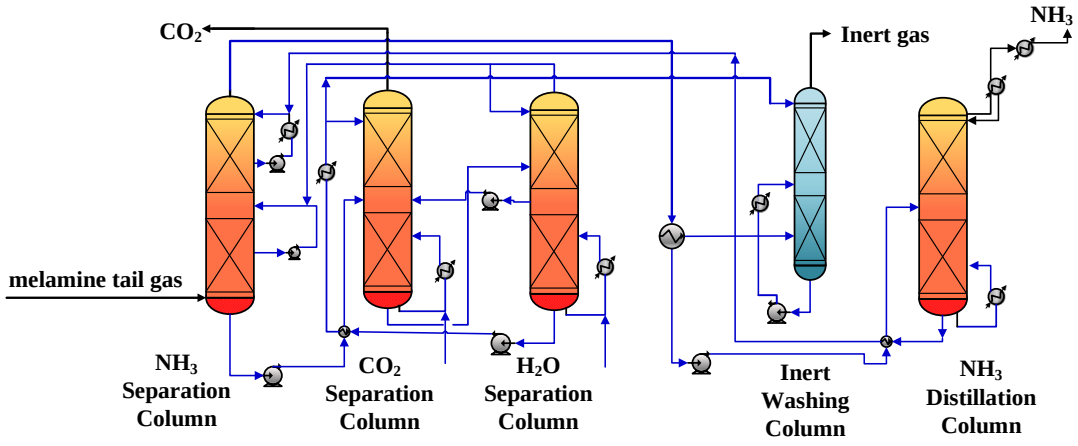

Figure 17 Flow chart of NH_3/CO_2 separation of water scrubbing process.

3.2.3 Operational parameters and mass balance of purification process

The key operational parameters of the absorption process using [Bim][NTf_2] with IL-0 and IL-En processes shows on Table 5 and the main operational parameters by using water scrubbing is shown in Table 6. The mass flow of key streams is shown on Table 7 and Table 8 with two IL-based processes and Table 9 for water scrubbing process.

Table 5 The key operational parameters of the absorption process using [Bim][NTf_2].

Process / Operation parameters	IL-0	IL-En	Unit
Theoretical stage of absorption	8	7	-
Feed stage position of semi-lean	4	4	-
Total IL flow rate	50.00	40.00	$t \cdot h^{-1}$
Absorption pressure	202.65	202.65	kPa
Absorption temperature	332.22	335.11	K
Ratio of gas/liquid in absorption	70	80	-
Pressure of flash 1	10.00	10.00	kPa
Temperature of flash 1	383.15	385.15	K
Pressure of flash 2	2.00	2.00	kPa
Temperature of flash 2	383.15	385.15	K
R_{SLT}	0.40	0.48	-
Stripping column theoretical stage	-	4	-
Stripping column pressure	-	100.00	kPa
Stripping column temperature	-	383.19	K

Table 6 The main operational parameters by using water scrubbing process.

Item	Value	Unit
NH_3 column pressure	400.00	kPa
NH_3 column stage	5	-
CO_2 column pressure	2300	kPa
CO_2 column stage	10	-
H_2O column pressure	300.00	kPa
H_2O column stage	12	-
Inert column pressure	300	kPa
Inert column stage	7	-
NH_3 distillation column pressure	200.00	kPa
NH_3 distillation column stage	10	-
Reflux ratio of H_2O column	1.50	-

Table 7 The mass flow of the key streams using IL-0 process.

Items	Melamine tail gas	Purified gas	Liquid ammonia	Lean solvent	Semi-lean solvent	Rich solvent
NH_3 mass flow (kg/h)	1859.99	9.11	1851.10	548.64	1159.61	3637.75
CO_2 mass flow (kg/h)	3269.15	3258.53	10.61	0.00	0.00	10.65
H_2O mass flow (kg/h)	22.42	20.10	2.37	0.00	0.26	48.57
N_2 mass flow (kg/h)	427.43	427.36	0.07	0.00	0.00	0.07
IL mass flow (kg/h)	0.00	0.00	0.00	20000.00	30000.00	50000.00
Total mass flow (kg/h)	5578.99	3715.10	1864.15	20548.64	31159.87	53697.04
Temperature (K)	393.15	335.10	308.15	333.15	343.15	347.22
Pressure (kPa)	200.00	202.65	1500.00	210.00	210.00	207.47

Table 8 The mass flow of the key streams using IL-En process.

Items	Ammoniac waste gas	Purified gas	Ammonia	Lean solvent	Semi-lean solvent	Rich solvent
NH_3 mass flow (kg/h)	1859.99	9.59	1850.41	524.07	809.26	3243.80
CO_2 mass flow (kg/h)	3269.15	3261.95	7.19	0.00	0.00	7.21
H_2O mass flow (kg/h)	22.42	20.00	2.36	0.00	0.15	36.13
N_2 mass flow (kg/h)	427.43	427.38	0.05	0.00	0.00	0.05
Air mass flow (kg/h)	0.00	220.00	0.00	0.18	0.00	0.00
Ionic liquid mass flow (kg/h)	0.00	0.00	0.00	19200.00	20800.00	40000.00
Total mass flow (kg/h)	5578.99	3938.92	1860.01	19724.3	21609.4	43287.2

Temperature (K)	393.15	334.98	308.15	333.15	343.15	348.89
Pressure (kPa)	200.00	202.65	1500.00	210.00	210.00	206.78

Table 9 The mass flow of the key streams by using water scrubbing process.

Items	Ammonia waste gas	Water	Inert gas	Ammonia	Carbon dioxide
NH_3 mass flow (kg/h)	1859.99	0.00	0.66	1847.86	11.47
CO_2 mass flow (kg/h)	3269.15	0.00	1.18	0.06	3267.91
N_2 mass flow (kg/h)	427.43	0.00	368.42	58.54	0.47
O_2 mass flow (kg/h)	0.00	0.00	0.00	0	0
H_2O mass flow (kg/h)	22.42	270.23	2.85	2.6	287.2
H_3O^+ mass flow (kg/h)	0.00	0.00	0.00	0	0
OH^- mass flow (kg/h)	0.00	0.00	0.00	0	0
Total mass flow (kg/h)	5578.99	270.23	371.11	1909.06	3298.82
Temperature (K)	393.15	283.15	283.26	293.15	329.60
Pressure (kPa)	200.00	300.00	300.00	2000.0	100.00

3.3 Process evaluation

3.3.1 Process evaluation method

The goal of the process's energy and cost evaluation is to determine the total separation cost (TSC), which can be calculated from the annual capital cost (ACC) and total operation cost (TOC). As shown in Equation 8, ACC can be calculated by annualizing the total capital investment (TCI) for the project cycle. Walas' estimation [114] is used to calculate the cost of bought equipment (PEC). Main equipment size data is obtained from Aspen Plus ™.

The ACC can be given as the follow equation:

$$ACC = \frac{TCI}{((1+i_r)^n - 1)/(i_r(1+i_r)^n)} \quad \text{Equation 8}$$

Where i_r denotes the annual interest rate, assuming 7% in this work [89], n denotes project lifetime, assuming 10 years and as the project lifetime is not sensitive to the calculation of TSC with the value large than 5 years, further discussion will be in section 3.3.2.

TOC is formed of variable operating costs (VOC) and fixed operating costs (FOC). VOCs include the costs of electricity, utilities (heating and cooling), and solvent. FOC includes local taxes, maintenance

and supervision costs, and so on. TSC, which contains ACC and TOC, can then be obtained. The input cost of IL is multiplied by the fixed capital investment (FCI) to calculate the TCI and then the ACC. Because of the IL's non-volatile character, it could be almost entirely recovered and recycled during the process, so we assumed no IL loss [115]. Furthermore, in the evaluation, the purification cost of solvents is calculated as the maintenance cost as 3% of FCI. The detailed calculation method of economic is shown in Appendix.

The energy required to process a unit volume of gas is utilized as a process energy consumption evaluation index, which is the ratio of total process energy consumption (TPEC) to the amount of processed gas. Heat and power consumption are typically included in TPEC. Heat consumption is represented by the conversion of thermoelectric conversion efficiency into equivalent electricity consumption. As a result, equations 9-10 are used to calculate the specific process energy consumption (SPEC) per unit volume of gas:

$$TPEC = W_{ele} + Q_{th}\eta \quad \text{Equation 9}$$

$$SPEC = \frac{TPEC}{F_{Volume}} \quad \text{Equation 10}$$

where W_{ele} and Q_{th} are electric energy and heat energy, kW; η is 0.35 shows the conversion efficiency of thermoelectric energy; F_{volume} is the volume flow rate of the purified process gas, Nm^3/h.

NH_3 is a byproduct of the NH_3-CO_2 separation process that has economic importance. The recovery ratio as 11:

$$\eta = \frac{F_{\mathrm{NH_3,\,recovery}}}{F \times x_{NH_3,inlet}} \times 100\% \quad \text{Equation 11}$$

where η is the recovery ratio of NH_3, %; F denotes the mole flow rate of inlet, mol/h; $x_{NH_3,inlet}$ is the NH_3 mole fraction in inlet gas; $F_{\mathrm{NH_3,\,recovery}}$ is the NH_3 recovery mole flow rate.

3.3.2 Process evaluation of IL-0 and IL-En processes

According to the separation performance of [Bim][NTf_2]-based NH_3/CO_2 separation as conducted in section 3.2, this part continues with a detailed process evaluation. The heat exchanger network (HEN) can improve energy utilization efficiency and lower utility consumption of the separation process. At this section, the IL-En separation process is shown as the example and other two process analysis result

is shown in Appendix. The base case of IL-En separation process demands a heating utility of 847 kW and cooling utility of 1692 kW, indicating that the process shows huge potential for energy saving and the design of HEN have been provided in Appendix.

The result of the HEN shows on Table 10. For IL-En process, compared with the base case, HEN can reduce heating utility of 52.92 % and cooling utility of 26.49 % at the price of increasing exchange area to 1.19 times.

Table 10 The result of modifed heating exchanger network for optimization process.

Item		Value	Unit
Base case	Heating	847.24	kW
	Cooling	1692.73	kW
	Heating exchange area	728.65	m^2
HEN	Heating	398.92	kW
	Cooling	1244.41	kW
	Heating exchange area	867	m^2

Because the process can benefit from HEN in general, the assessment in this section compares the base case and HEN for the purification process.

For utilities cost distribution, the result is shown in Figure 18. Electricity cost, as a constant value in the process, accounted for the greatest share of VOC. After HEN design, together with the shrink of cooling water (CW) and low pressure (LP) steam can be reduced from 33 % to 21 % of base case. It caused that the cost of total utilities can reduce 15.13 %. As a result, the HEN design can save the process's heating and cooling utilities. The detailed HEN information of IL-0 and water scrubbing processes is shown in Appendix.

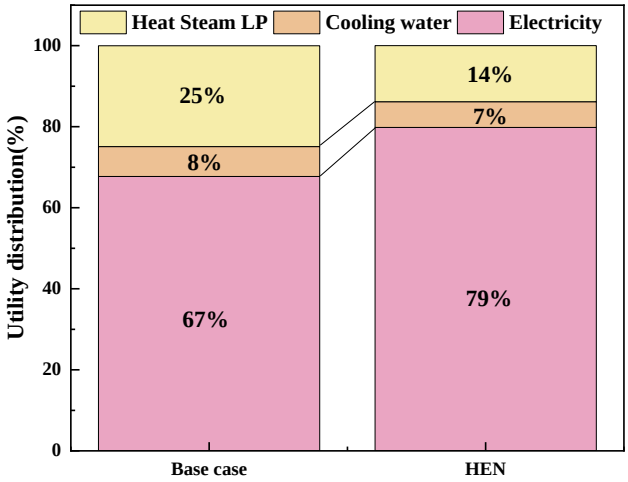

Figure 18 The utilities cost distribution of IL-En process in base case and HEN.

The TSC distribution of the base case and HEN design case of IL-En process are compared in Figure 19, and the equipment cost distribution are compared in Figure 20. For FOC and ACC after HEN, their proportion of TPC changes from 64.17 to 63.99 $/t and 58.79 to 59.54 $/t, respectively. This is because HEN of heating and cooling recovery may raise the cost of equipment. The dramatic drop in VOC-CW and VOC-LP after HEN could be due to lower utility costs. The vacuum pump, compressor, and heat exchanger are the three equipment with the highest cost distribution either in base case (90.59 %) or HEN (90.92 %). For example, the fraction of heat exchanger rises from 43.87% to 46.28%, demonstrating that HEN raises equipment costs.

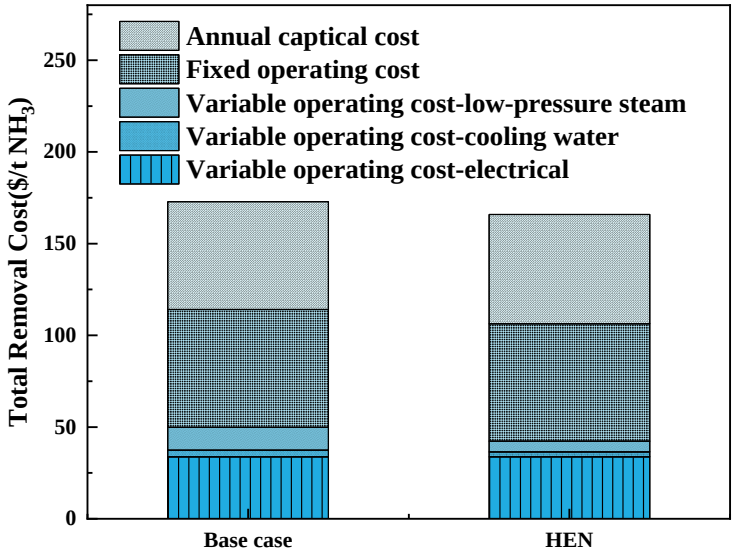

Figure 19 The comparison of total separation cost for NH_3 /CO_2 process at base case and HEN for IL-En process.

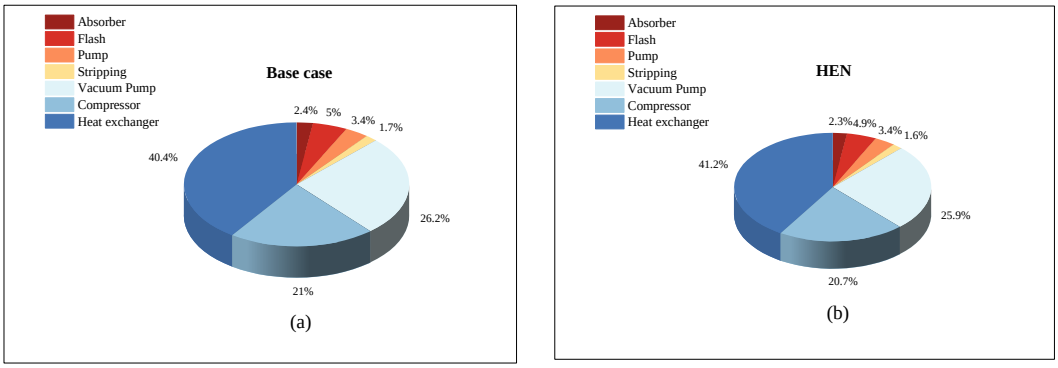

Figure 20 The equipment cost distribution of IL-En process in initial HEN and modified HEN. (a) Base case; (b) HEN.

3.4 Comparation of water scrubbing method and IL-based method

Because the HEN only involves heat exchange between hot and cold streams and does not change the absorption parameter of the separation process, the NH3 recovery remains unchanged. For ionic liquid processes, the influence of heat integration on TSC is observed to be minor. 2.88% reduction for the IL-

0 procedure and 4.21% reduction for the IL-En process. The analysis of the effect of heat integration for water scrubbing process is shown in Table 11, and heat integration can lower the TSC with 1.78%.

Table 11 contains evaluation results from the perspective of process efficiency. Because the HEN solely involves heat exchange between the hot and cold streams and does not modify the absorption parameter of the separation process, the NH_3 recovery remains intact. Heat integration has a minor effect on TSC in ionic liquid processes. A reduction of 2.88% for the IL-0 procedure and 4.21% for the IL-En process. The analysis of the effect of heat integration for water scrubbing process is shown in Table 11, and heat integration can lower the TSC with 1.78%.

Table 11 Efficiency evaluation results of optimization and sensitivity analysis using function IL.

Item	WS		IL-0		IL-En	
	Base case	HEN	Base case	HEN	Base case	HEN
NH_3 recovered in ammonia stream, kg NH_3/h	1847.86	1847.86	1851.22	1851.22	1850.41	1850.41
NH_3 recovery ratio, %	99.35	99.35	99.53	99.53	99.49	99.49
NH_3 purity in ammonia product, %wt.	96.80	96.80	99.30	99.30	99.48	99.48
Total equivalent energy penalty, kJ/Nm^3 tail gas	4024	4004	1033.71	879.16	956.34	830.25
Total cost for NH_3 /CO_2 separation process, \$/t NH_3	435.06	427.32	179.43	174.27	172.85	165.87

The price of liquid NH_3: 471.43 \$/t

Figure 21 and Figure 22 provide information on energy use, equipment costs, and a cost-benefit analysis of separation. For TSC, the IL-0 method has a significant cost advantage of 174.27 \$/t NH_3, which is 60% less than the 427.32 \$/t NH_3 of the water scrubbing process. The primary issue is the high separation costs associated with the energy-intensive distillation method used to collect NH_3 from water. When comparing the IL-0 and IL-En processes, the latter has a somewhat lower TSC than the IL-0 process. This is due to the inclusion of one stripping column, which reduces the concentration of NH_3 in the semi-lean solvent and hence the use of IL in the process. Because IL has a low vapor pressure, it uses less energy than water scrubbing. Furthermore, the IL flowsheets are less complicated than those

for the water scrubbing process. As a result, the IL-0 and IL-En methods clearly beat existing treatment techniques in terms of energy consumption and total separation costs.

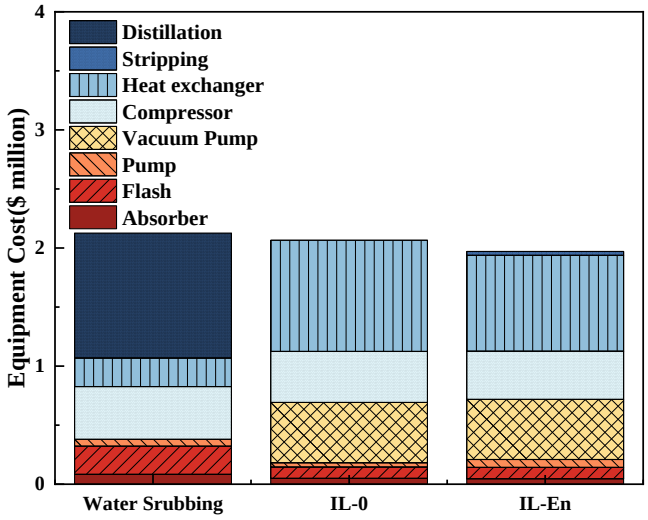

Figure 21 The equipment cost distribution in water scrubbing method and IL-based method.

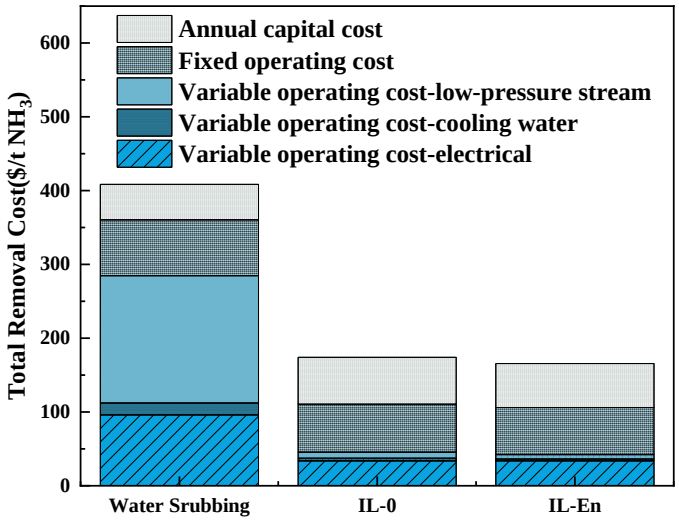

Figure 22 The comparison of total cost for NH_3 /CO_2 separation process at water scrubbing method, IL-0 and IL-En method.

In terms of process selection for NH_3/CO_2 separation, the WS process requires a bigger initial equipment investment than the IL-0 and IL-En processes. The heat exchanger costs 45.60% of the overall cost of the process equipment in the IL-0 process. At the same time, the desorption process is a decompression operation, and the vacuum pump costs 24.67% of the overall cost of the process equipment. Distillation is the most expensive part of the WS process, accounting for 49.75% of the overall equipment cost.

From the point of view of a long-term investment, the operating expenses, which include utilities such as cooling water, low-pressure steam, and energy usage, become the primary contributor to the separation costs. In terms of energy consumption, the WS process has distillation towers, and the reboiler of the distillation tower must be heated to accomplish the separation effect, therefore the WS process consumes 20 times the amount of low-pressure steam as the IL-0 and IL-En processes.

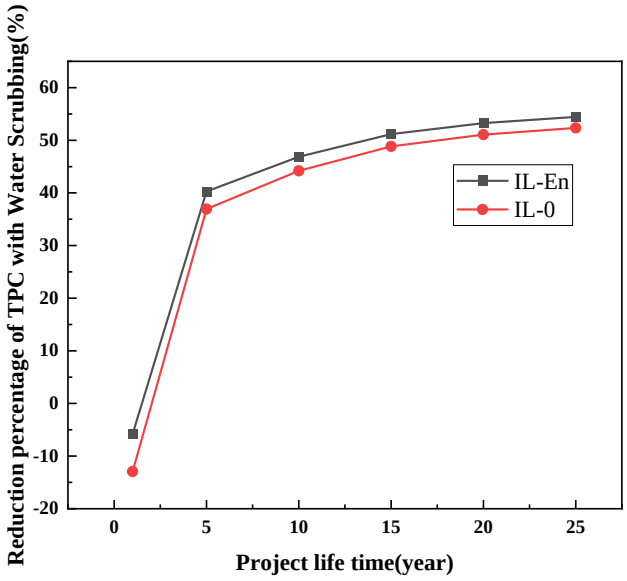

Figure 23 Reduction percentage of TSC with water scrubbing process.

Low-pressure steam is mostly utilized in the ionic liquid method to heat the rich solvent after absorption. Similarly, the application of cooling water differs. The WS method consumes a substantial amount of cooling water for condensation at the top of the distillation tower, whereas the ionic liquid process uses cooling water mainly to cool the semi-lean and lean solvents in the process, with a 79% lower utilization than the WS.

Although the IL-0 and IL-En processes have no significant advantages over the WS process in terms of equipment costs, the WS method has a higher overall separation cost than the IL-0 and IL-En processes due to higher running expenses. This is not appropriate for long-term (5-year) tail gas treatment process operation. As shown in Figure 23, the cost reduction of an IL-based process with water scrubbing is not

visible when the project life time exceeds 5 years. Although the IL-0 and IL-En processes have similar initial equipment costs to the WS process, the operating costs are significantly lower. In the future, the research and development of more energy-efficient processes will be at the heart of energy-saving and consumption-cutting research in the field of gas separation. Furthermore, because of their cheap separation cost, the IL-0 and IL-En procedures will provide a potential method for NH_3 and CO_2 separation.

3.5 Summary

This research investigated two ionic liquid-based NH_3/CO_2 separation procedures (IL-0 and IL-En) as well as a NH_3 recovery process using WS. Thermodynamic models for the NH_3/CO_2 separation processes IL-0 and IL-En were developed. The calculated thermodynamic result agrees well with the experimental data. The various separation methods' energy consumption and economic performance were then analyzed using process simulation and sensitivity analysis utilizing thermodynamic models.

To maximize energy utilization, a whole HEN was developed for all process choices. The HENs helped significantly to substantial energy savings. Furthermore, when compared to the baseline (benchmark) case, the HEN process could reduce the TSC by about 2.88% of the IL-0 process. Finally, an economic comparison of IL-0, IL-En, and WS was performed. The IL-0 process separation cost was reduced by 60% compared to the WS process. The IL-En method may perform even better in terms of energy and separation cost, and it may reduce TSC by 4.82% when compared to the IL-0 process. In conclusion, both of the investigated ionic liquid methods can save energy, providing a potential separation technology for NH_3/CO_2 separation.

4 Case study: Process optimization of IL-based techonology

In this chapter, the optimization of IL-based process of the two new process was given. This chapter was divided into three parts. The first part gives the introduction of the multi-objective optimization in chemical engineering. The second part concentrated on the detailed MOO scheme of the IL- based process with the integration of MATLAB and Aspen Plus. In the last part, the MOO result and analysis was carried out. In conclusion, this chapter was a detailed process multi-objective optimization of the new technology in this PhD project. This chapter is partially based on the published articles: ”Multi-objective optimization of NH_3 and CO_2 separation with ionic liquid process”, 14th International Symposium on Process Systems Engineering, Computer Aided Chemical Engineering, 49, 2022,1147-1152, [2].

4.1 Introduction of multi objective optimization

For the separation of NH_3/CO_2 using ionic liquid as the solvent, it is necessary to achieve energy and cost-effective operation through optimization in order to ensure the long-term development of this new technology. Detailed optimization and analysis based on the different operating parameters and the evaluated performance are required during the development of new technologies. In the chemical engineering process, MOO is widely used to balance the trade-off between process performance and energy-economic cost. The Multi Objective Genetic Algorithm (MOGA) [116] is employed to solve MOO to avoid falling into a locally optimal solution when sequential iteration is used in the iterative process. To integrate the simulation software of Aspen Plus and MATLAB, ActiveX [73] is used in the MOO process. The objective function, decision variable, and constraint conditions are three critical factors in the MOO process. In chemical process engineering, MOO problems are ones that demonstrate a trade-off at least two different aspects of objectives or performance criteria [117].

The most commonly used optimization algorithms for MOO are the weighted sum technique [75] [76], ε-constraint technique [77], and some genetic algorithms (such as NSGA-II [78]). Among them, the metaheuristics (or stochastic algorithms) that are mostly population-based and include evolutionary algorithms. In general, evolutionary algorithms have been widely used in chemical engineering for MOO applications [118]. For this work, we adopted the NSGA-II technology [78]. The variation method is Gaussian variation, with a variation probability of 0.1, a population size of 100, and a generation count of 15. The crossover probability is 0.8 [118].

4.2 MOO scheme of two IL-based process

4.2.1 MOO scheme of IL-0 process

The base case has already been constructed, and a flow chart of the NH_3/CO_2 separation process with ionic liquids is displayed in Figure 8 [1]. And the detailed flow chart description has been introduced in the previous section.

MOO was employed to study the internal relationship between different variables and the TSC of the ionic liquid-based process. The NSGA-II is used in the MOO of the NH_3 and CO_2 separation process in this work. For the IL-0 process, six design parameters are simultaneously optimized, including pressure of absorption, ratio of lean solvent to total solvent, total usage of solvent, temperature of Flash1, pressure of Flash1 and 2 (P, R_{LT}, F, T, P_{F1}, P_{F2}), the value range of each parameter is shown in The tray number of absorption is fixed at 8 in this study and is not employed as a decision variable.

Table 12. The tray number of absorption is fixed at 8 in this study and is not employed as a decision variable.

Table 12 Range of parameters of NH_3/CO_2 separation with ionic liquid.

Operation parameters	P (kPa)	R_{LT}	F (t/h)	T (K)	P_{F1} (kPa)	P_{F2} (kPa)
Lower bound	101	0.2	10	363.15	10	1
Higher bound	405	0.8	100	383.15	50	10

The objective functions in process optimization are to minimize TSC (Total Separation Cost) and TPCOE (Total Process Emission of CO_2). The constraints are that $y_{NH3\ purified} \leq 6000$ ppm, $x_{NH3,\ wt} \geq 0.996$, TSC ≥ 0, TPCOE ≥ 0, the ratio of gas and liquid 1 (GL1) ≤ 1000, and the ratio of gas and liquid 2 (GL2) ≤ 500. Figure 24 depicts the MOO technique for an ionic liquid-based process. The type of selection is binary tournament selection. The likelihood of crossing is 0.8. The variation method is Gaussian variation, and the variation probability is 0.1, the population size is set as 100, and the number of generations is set as 15. The crossover probability is 0.8.

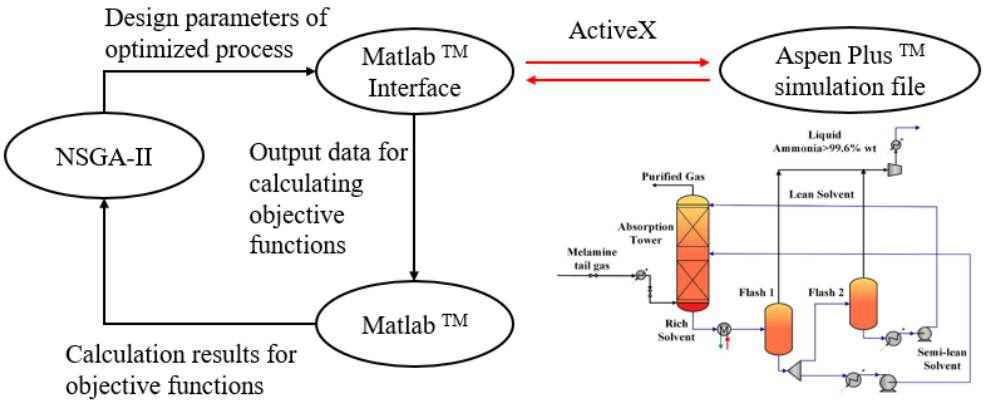

Figure 24 The MOO procedure of ionic liquid-based process.

4.2.2 MOO scheme of IL-En process

In this process, NH_3 concentration in purifies gas stream (y_{NH3}), specific process energy consumption (SPEC), and total separation cost (TSC) are set as the three objective functions based on the aspect of technical-energy-economic analysis. The objective functions were minimized by changing the decision variables. Detailed information about the decision variable and the boundary is given in Table 13. In this study, the tray number of absorption and stripping column is not used as a decision variable and it

is fixed at 8 and 4, respectively. The constraints are that $y_{NH3} \leq 6000$ ppm, $x_{NH3,\,wt} \geq 0.99$, SPEC ≥ 0, TSC ≥ 0, the ratio of gas and liquid 1 (GL_1) ≤ 1000, the ratio of gas and liquid 1(GL_2) ≤ 500. The MOO procedure of enhanced ionic liquid-based NH_3/CO_2 process is shown in Figure 25. For this work, we adopted the NSGA-II technology. The variation method is Gaussian variation, and the variation probability is 0.1, the population size is set as 100, and the number of generations is set as 15. The crossover probability is 0.8.

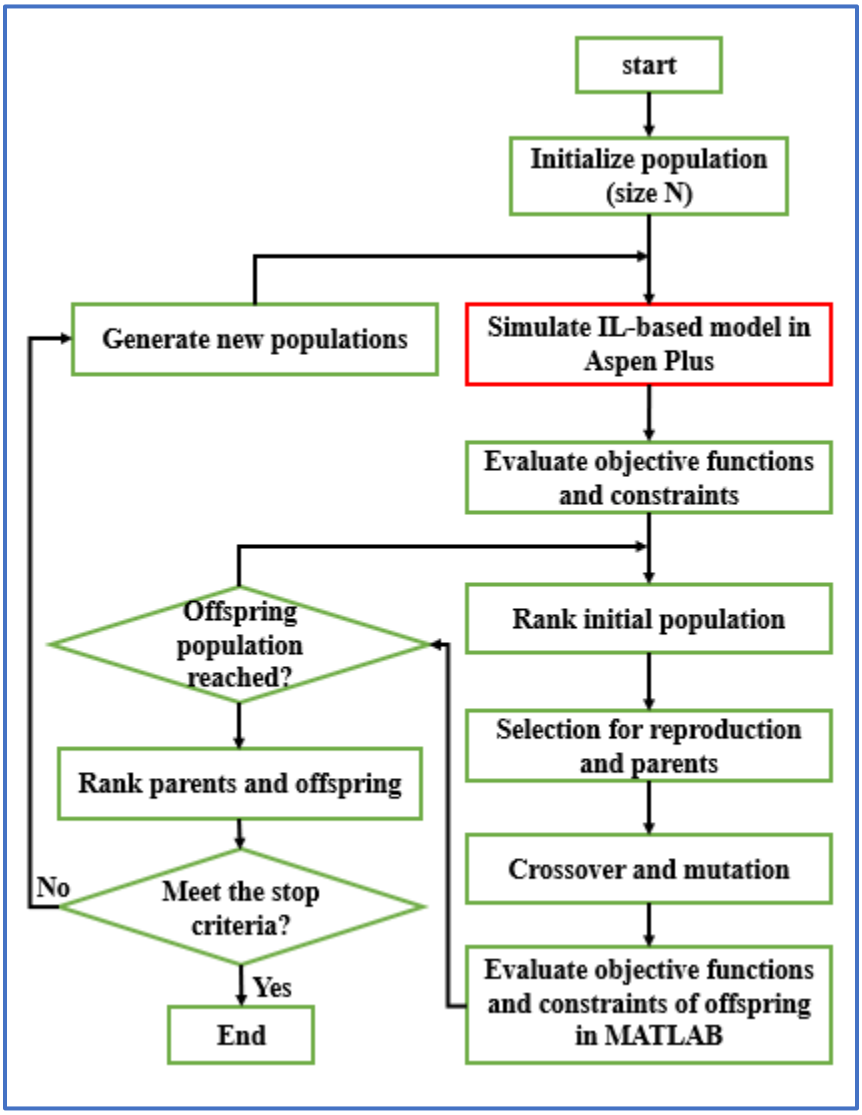

Figure 25 The MOO flowchart for the IL-En NH_3/CO_2 separation process.

Table 13 The value range of operational parameter for optimization.

Decision parameters		unit	Lower Boundary	Higher Boundary
Pressure of absorption column	P_{ab}	kPa	101.33	405.30
Ratio of lean to total solvent	R_{LT}	-	0.2	0.8
Flow rate of total solvents	F_{total}	t/h	10	100
Temperature of Flash 1 and 2	T_{F12}	K	363.15	383.15
Pressure of Flash 1	P_{F1}	kPa	10.13	50.66
Pressure of Flash 2	P_{F2}	kPa	1.01	10.13
Flow rate of air	F_{air}	t/h	0.01	0.25
Pressure of stripping column	P_{st}	kPa	101.325	405.30

4.3 MOO result and analysis of two IL-based process

4.3.1 Result and analysis of IL-0 process

The MOO is performed based on the sensitivity analysis of the ionic liquid-based process to obtain the solution for this chemical process that can realize the two optimal objective functions: TSC and TPCOE. Figure 26 (a) shows the relationship between TSC and TPCOE. The Pareto optimal solution of the NH3 and CO2 separation process shows that TSC increases as TPCOE increases. Reduced TSC in the separation process means reduced energy consumption, which leads to a lower TPCOE.

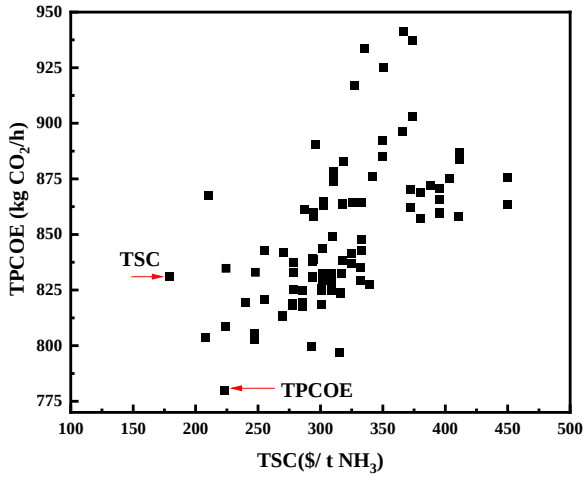

Figure 26 The MOO results. (a) The Pareto optimal result of NH_3 and CO_2 separation of TSC and TPCOE.

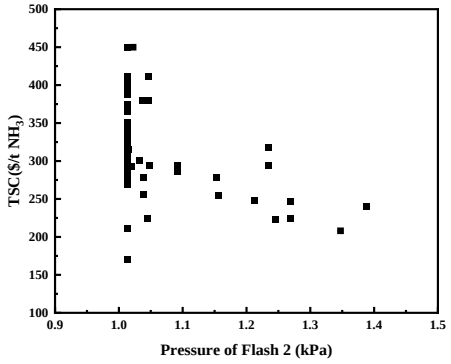

(a)

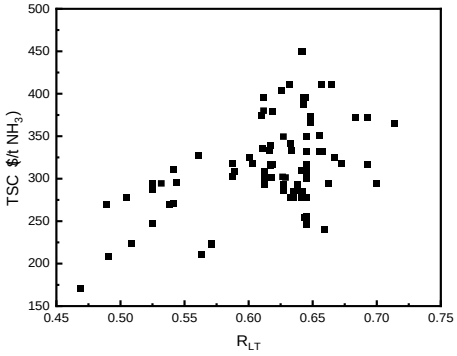

(b)

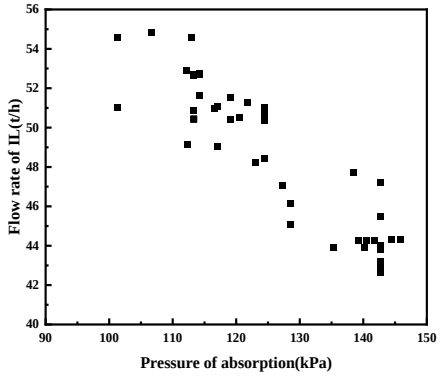

(c)

Figure 27 (a) Effects of key variable ratio of lean solvent to total solvent (R_{LT}). (b) Effects of key variable pressure of Flash 2(P_{F2}). (c) Relationship between Pressure of absorption (P) and Flow rate of ionic liquids (F).

Figure 27(a) and (b) show the effects of crucial input variables (P_{F2}, R_{LT}) on TSC. From Figure 27(a), the pressure change of Flash 2 will lead to the diversification of objective function TSC. From Figure 27(b), TSC varies with R_{LT} because a greater R_{LT} means more lean solvent will flow into the Flash 2 and provide the Flash 2 more burden at a lower pressure.

For effect among the input parameters, Figure 27(c) demonstrates the relationship between ionic liquid absorption pressure and flow rate. As pressure rises, more NH_3 is absorbed by ionic liquids, requiring fewer ionic liquids to be used in this process. Although increasing the flow rate of ionic liquid can lower the solvent cost, the operation can also lower the absorption pressure. These two parameters balance each other in terms of their effect on TSC.

Because there are two objective functions, we select the designs in the Pareto optimal solution named case 1 and 2 with the lowest TSC and TPCOE. case 1 has the lowest TSC of 170.87 $/t NH3, which is

5% lower than the base case, while case 2 has the lowest TPCOE of 779.85 kg/h, which is 12% lower than the base case. In conclusion, the optimized results might provide more detailed information on the ionic liquid-based NH3/CO2 separation method, which presents a future perspective for separation technology.

Table 14 offers TSC and TPCOE of all configurations of the ionic liquid process. As the calculation, case 1 has the lowest TSC of 170.87 \$/t NH_3, which is 5% lower than the base case, while case 2 has the lowest TPCOE of 779.85 kg/h, which is 12% lower than the base case. In conclusion, the optimized results might provide more detailed information on the ionic liquid-based NH_3/CO_2 separation method, which presents a future perspective for separation technology.

Table 14 Optimization results of NH_3/CO_2 separation with ionic liquid.

Operation parameters	Case 1	Case 2	Unit
Theoretical stage of absorption	8	8	-
Feed stage position of semi-lean	4	4	-
Total ionic liquid flow rate	47.09	43.90	$t \cdot h^{-1}$
Absorption pressure	128	142	kPa
Pressure of Flash 1	10	10	kPa
Temperature of Flash 1	366.10	363.98	K
Pressure of Flash 2	1	2	kPa
Temperature of Flash 2	366.10	363.98	K
R_{LT}	0.47	0.57	-
TSC	170.87	222.91	\$/t NH_3
TPCOE	831.29	779.85	kg/h

4.3.2 Result and analysis of IL-En process

The operating parameters of absorption and desorption-stripping section which effect the performance of NH_3/CO_2 separation process, are important to be analyzed. First, the effect of the operating variables on the y_{NH3}, SPEC and TSC are analyzed. In this part, key parameters of ionic liquid-based NH_3/CO_2 separation process (e.g. P_{ab}, R_{LT}, F_{ab}, $T_{F12,}$ P_{F1}, $P_{F2,}$ $F_{air,}$ P_{st}) are investigated.

Technical analysis

The technical analysis is based on the sensitivity of each decision variable versus $y_{NH3.}$ From Figure 28 and Figure 29, there are eight decision variables. Among all these, P_{ab}, R_{LT}, F_{ab}, T_{F12} and F_{air} all have negative relationship with y_{NH3}. For example, a higher temperature of the desorption section will lead to more NH_3 emissions, thus lowering the NH_3 concentration in the purified gas stream. Among all the eight variables, with a reasonable range of lower and higher bounds, the change of P_{F2} has the most

effect on the y_{NH3}. When the P_{F2} increases from 1 to 5 kPa, the y_{NH3} increase from 3000 ppm to 14000 ppm. However, from Figure 29, the change of F_{air} and P_{st} have litter effect on $y_{NH3.}$ The y_{NH3} only changes from 5500 ppm to 5675 ppm within the reasonable range of the two stripping relevant variables. From the aspect of the linear relationship, the P_{F2}, F_{air} and T_{F12} have linear relationship with $y_{NH3,}$ other five variable shows a non-linear relationship with this technical evaluation. In summary, all the eight are set as the decision variables in the process and to separate the two gases effectively, the P_{F2} is set at 1-5 kPa. The change of P_{F2} is the most sensitive variable among all the eight decision variables. If decision-makers want to gain better performance of NH_3/CO_2 separation, the P_{F2} should be given more attention in the design process.

Energy analysis

The energy analysis is based on the sensitivity of each decision variable versus SPEC. From Figure 28 and Figure 29, there are eight decision variables. Among all these, P_{ab}, R_{LT}, F_{total}, T_{F12}, and F_{air} all have a positive relationship with SPEC. For example, the higher pressure of the absorption section will lead to more NH_3 emission; thus, the utility consumption of the two equipment: 1) compressor which transports the recycled gas from stripping column back to the absorption column 2) tail gas feed compressor will increase. Among all the eight variables, with a reasonable range of lower and higher bound, the change of P_{ab}, F_{total}, and T_{F12} have the most effect on the SPEC. For example, when the IL flow rate increase from 34 to 60 t/h, the SPEC increase from 900 to 1200 kJ/Nm^3 tail gas. The same phenomenon for the P_{ab} and T_{F12}. However, from Figure 29, the change of F_{air} and P_{st} has little effect on SPEC. The SPEC only changes from 958 to 964 kJ/Nm^3 tail gas within the reasonable range of the two stripping relevant variables. From the aspect of the linear relationship, the T_{F12} have a linear relationship with SPEC. The other seven variables show a non-linear relationship with this technical evaluation. The reason is mainly that the change of T_{F12} have a direct impact on heat exchange's utility consumption. In summary, the change of P_{ab}, F_{total}, and T_{F12} are more sensitive than other decision variables. If decision-makers want to gain the better energy consumption of NH_3/CO_2 separation, the T_{F12} could provide lower SPEC for the new technology.

Economic analysis

The economic analysis is based on the sensitivity of each decision variable versus TSC. From Figure 28 and Figure 29, among all these, the P_{ab}, R_{LT}, F_{total}, T_{F12}, and F_{air} all have a positive relationship with SPEC. Among all the eight variables, with a reasonable range of lower and higher bounds, the change in F_{total} has the most effect on the TSC. For example, when the IL flow rate increase from 34 to 60 t/h, the TSC increase from 0.058 to 0.068 \$/Nm^3 tail gas. However, from Figure 29, the change of F_{air} and

P_{st} has litter effect on TSC. The TSC only changes from 0.0591 to 0.0592 \$/Nm^3 tail gas within the reasonable range of the two stripping relevant variables.

The analysis of TSC has a similar relationship with SPEC for some of the decision variables. The P_{ab}, R_{LT}, F_{total}, T_{F12} and the P_{F1} all have the parallel tendency as SPEC. However, the TSC of the P_{F2} did not have the same change tendency with SPEC. The reason is that within the range of P_{F2} lower than 5 kPa, the calculation of vacuum is almost the same; However, the energy consumption is verified. From the aspect of the linear relationship, the T_{F12} and F_{total} have a linear relationship with TSC, the other six variables show a non-linear relationship with this technical evaluation. The reason is mainly that the change of T_{F12} have a direct impact with heat exchange equipment cost. In addition, the F_{total} change is calculated in the solvent cost in VOC. In summary, the change in F_{total} is the most sensitive than other decision variables. From the aspect of economic analysis, if decision-makers want to gain a better economic evaluation of NH_3/CO_2 separation, the F_{total} is important, and the different kinds of IL have different prices, which is most valid in the strategy decision. The stripping column's decision variables have less impact on the evaluation compared with other variables in this new technology.

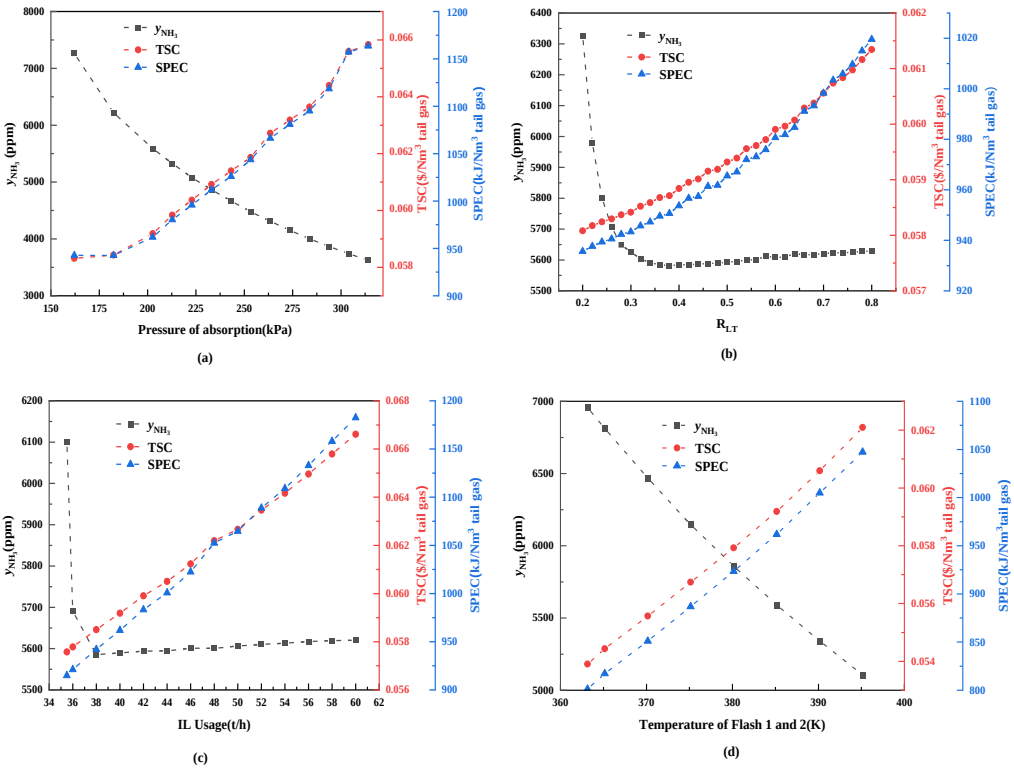

Figure 28 Influence of decision variables on y_{NH3}, SPEC and TSC.

(a) P_{ab} (b) R_{LT} (c) F_{total} (d) T_{F12}

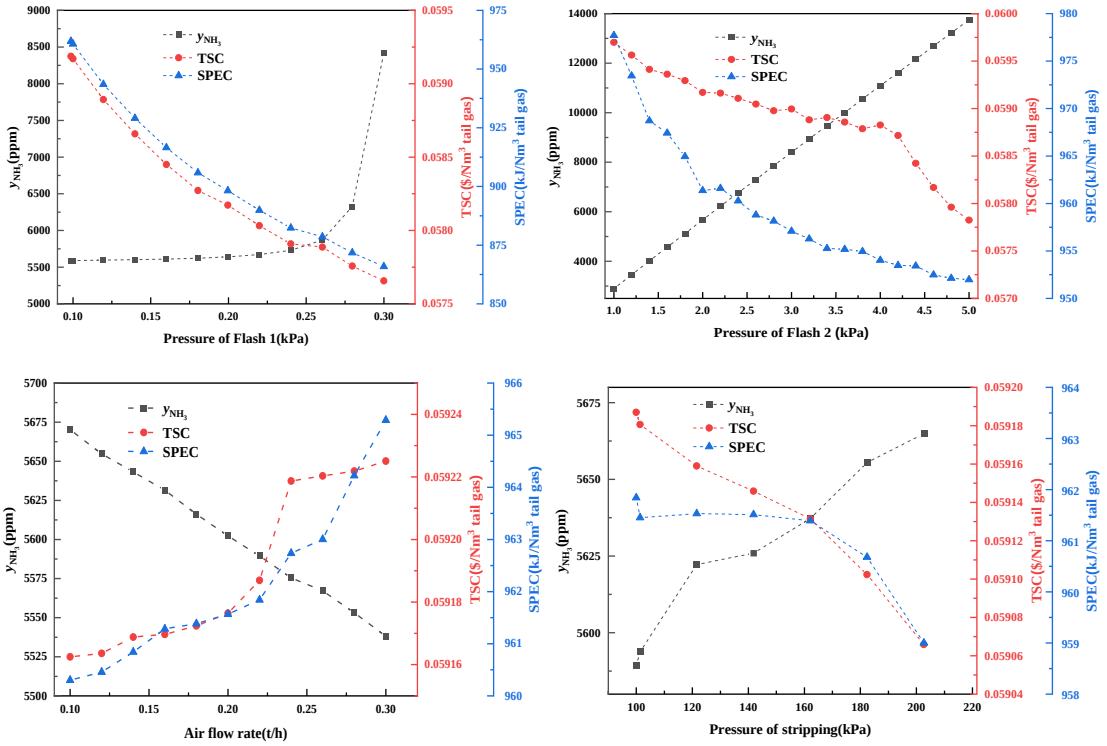

Figure 29 Influence of decision variables on y_{NH3}, SPEC and TSC.

(a) P_{F1} (b) P_{F2} (c) F_{air} (d) P_{st}

After the decision variable's sensitivity analysis, the process optimization is carried out to obtain the different scenarios. Those scenarios can achieve the optimal objective functions (i.e., y_{NH3}, SPEC, and TSC). Figure 30 shows the process of MOO with the increase of generations. In the first generation, most of the solutions are without constraints, and in the 4th generation, all the solutions realize the constrained setting but cannot give a clear relationship with all the objective functions. With the increase of the generation numbers, the 200th generation results give a clear relationship with each objective function. From Figure 31, with decreasing of y_{NH3}, SPEC and TSC increase. This is because reducing y_{NH3} means the high operation cost and utility consumption, increasing SPEC and TSC. In addition, SPEC increases with increasing TSC. This is because the calculation of TSC consists of the utility cost

and equipment price increase along with the higher utilities. The detailed relationship among the three objective functions is provided in Appendix.

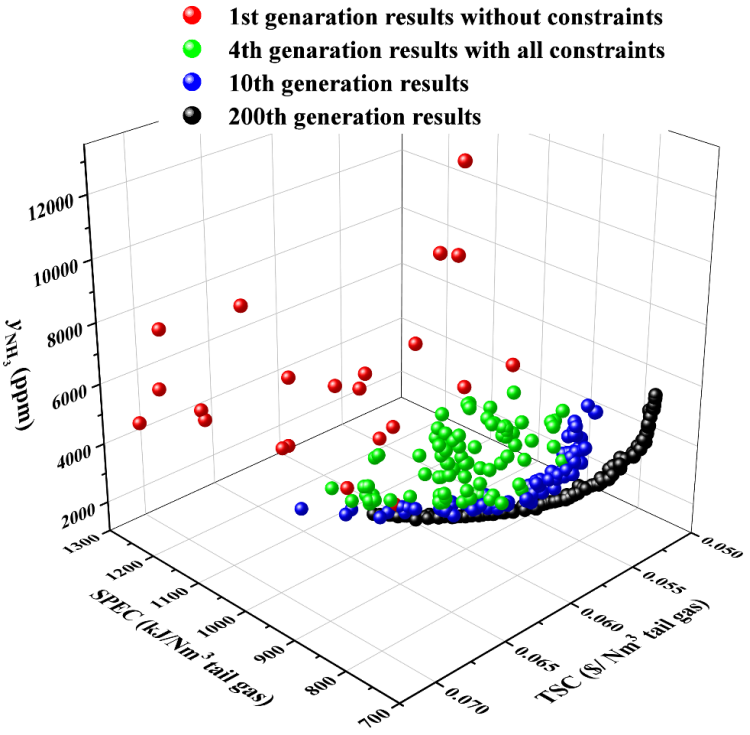

Figure 30 Pareto front with NH_3/CO_2 separation MOO process.

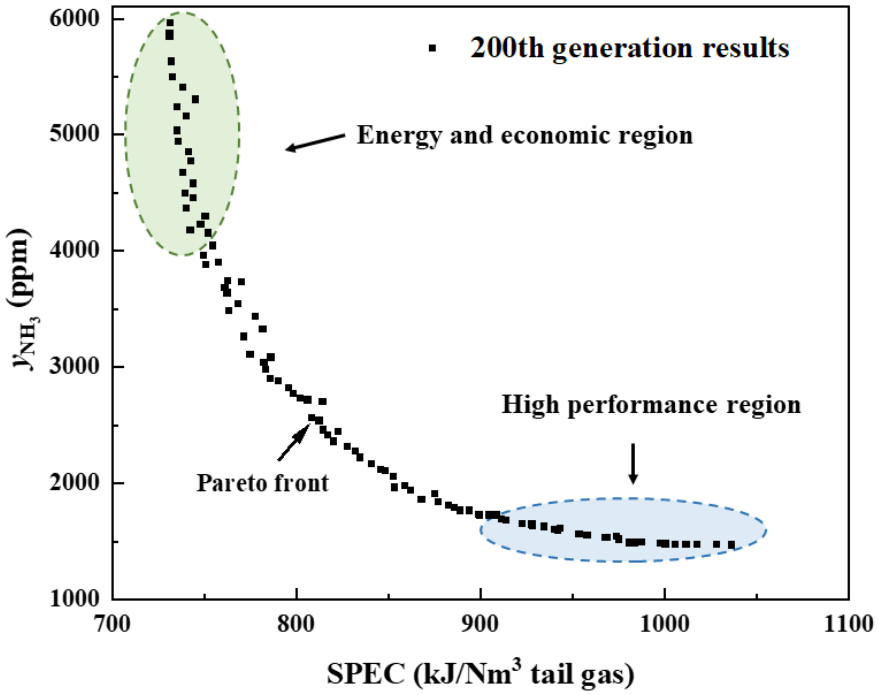

Figure 31 Pareto front of y_{NH3} and SPEC.

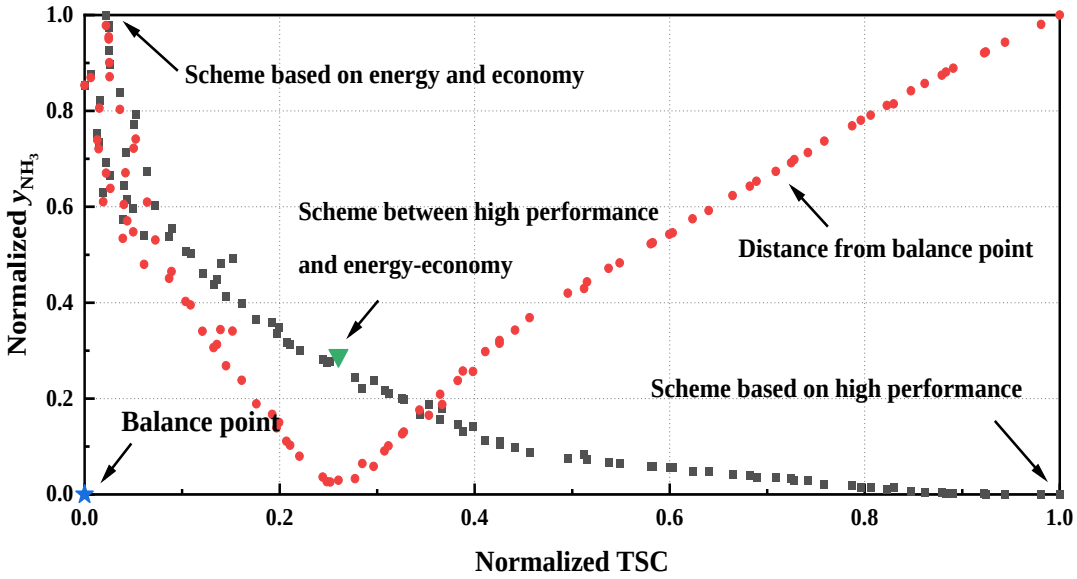

Figure 32 Distance between the ideal point and Pareto front.

To give more detailed support to the new technology industrial application, we analyze the relationship of SPEC and y_{NH3} in the generation of the 200th as example. From Figure 30, in the energy and economic region, when the y_{NH3} is in the range of 4000 to 6000 ppm, the value of SPEC is in the 700 to 750 kJ/Nm^3 tail gas which shows low improvement of energy consumption with significant decrease of separation performance. It means that energy and economic cost represents low sensitivity with the decrease of separation performance in this region. At the same time, separation performance is very sensitive with a little change of energy cost. The same trend is observe for TSC. Regarding on the y_{NH3} value of this region, if the new ionic liquid-based technology is designed as one part of the whole fertilizers production process, the decision-maker could pay less cost and integrate the new technology with other purified gas treatment technology to have better process sustainability, for example the production of ammonia bicarbonate of this purified gas stream with water thus saves the carbon source. However, if this new technology needs to have lower y_{NH3} less than 4000 ppm, the decision-maker should afford more consumption in energy and economic cost. In the high performance region, the separation process has the best technology separation performance, which could achieve a low as 1500 ppm in the purified gas. In this region, when the y_{NH3} is in the range of 1500 to 2000 ppm, the value of SPEC is in the 900 to 1050 kJ/Nm^3 tail gas which shows low improvement of separation performance with significant increase of energy and economic consumption. It means that separation performance represents low sensitivity with the increase of energy and economic in this region. In contrast, the consumption of energy in this region is 1.4 times than that in the energy and economic region. The reason is mainly for that deeper separation performances require more strict operating conditions. In this situation, the decision-maker could get high clear purified gas and pay more for the utility and relevant equipment cost. The two different regions based on technical-energy-economic evaluation represents the conflict between technology with energy and the economic aspect.

Based on the pareto front of the MOO, it is obvious that the separation performance and energy-economic evaluation change in opposite directions. For the MOO technology, it is important to choose different suitable schemes from the pareto front, Sayyaadi et al [84] proposed the normalized forms to replace the actual values in order to avoid the influences of the different units of the objective functions. The equations of the normalized forms of objective functions as y_{NH3} and TSC as below,

$$y_{NH3,no} = \frac{y_{NH3} - y_{NH3,min}}{y_{NH3,max} - y_{NH3,min}} \quad \text{Equation 12}$$

$$TSC_{no} = \frac{TSC - TSC_{,min}}{TSC_{,max} - TSC_{,min}} \quad \text{Equation 13}$$

Where $y_{NH3,min}$ and $y_{NH3,max}$ are minimum and maximum NH_3 concentration in purified gas; $y_{NH3,no}$ is the normalized NH_3 concentration in purified gas; $TSC_{,min}$ and $TSC_{,max}$ are minimum and maximum TSC; $TSC_{,no}$ is the normalized TSC.

The Pareto front by normalized is shown in Figure 32. From Figure 32, the front is divided into two parts, at the left part is the energy and economic friendly area and at the right part is the high-performance friendly area. Two objective functions y_{NH3} and TSC, have the minimum value at the balanced point with blue star in Figure 32. However, the balanced point is a virtual point thus, the nearest point to the balanced point to the Pareto front is chosen as one of the solutions. The red line represents the distance from the front point to the balanced point. The point showed with green as the balanced scheme with y_{NH3} and TSC (case 1), with the y_{NH3} as 4627 ppm and TSC as 0.055 \$/Nm^3 tail gas. The minimum of y_{NH3} case was found in point y_{NH3} as 1468 ppm with the TSC as 0.072 \$/Nm^3 tail gas (case 2). The minimum TSC point was found in the point with y_{NH3} as 5962 ppm with the TSC as 0.052 \$/Nm^3 tail gas (case 3).

Parameter influence analysis with objective functions

Effect of main operational parameters on y_{NH3} SPEC and TSC has been shown on Figure 33. From Figure 33, the y_{NH3} is decreased with the increase of P_{ab}. It is due to that the higher pressure will absorb more NH_3 in the absorption column. For F_{ab}, more IL will lead to less NH_3 in the purified gas. From Figure 33, the SPEC are positive correlated with P_{ab} and F_{Total}. For P_{ab}, it is due to that the high absorption pressure is necessary to increase the pressure of NH_3/CO_2 tail gas into the absorption tower, which will cause much energy consumption, resulting in the increase of SPEC. In contrast, SPEC are negative correlated with F_{total}. Increasing F_{total} can reduce the value of SPEC. From Figure 33, the TSC are positive correlated with P_{ab} and F_{IL}. For F_{ab}, high absorption pressure will cause much energy consumption, resulting in the increase of TSC. In contrast, TSC are negative correlated with F_{total}. Increasing F_{total} can reduce the value of TSC.

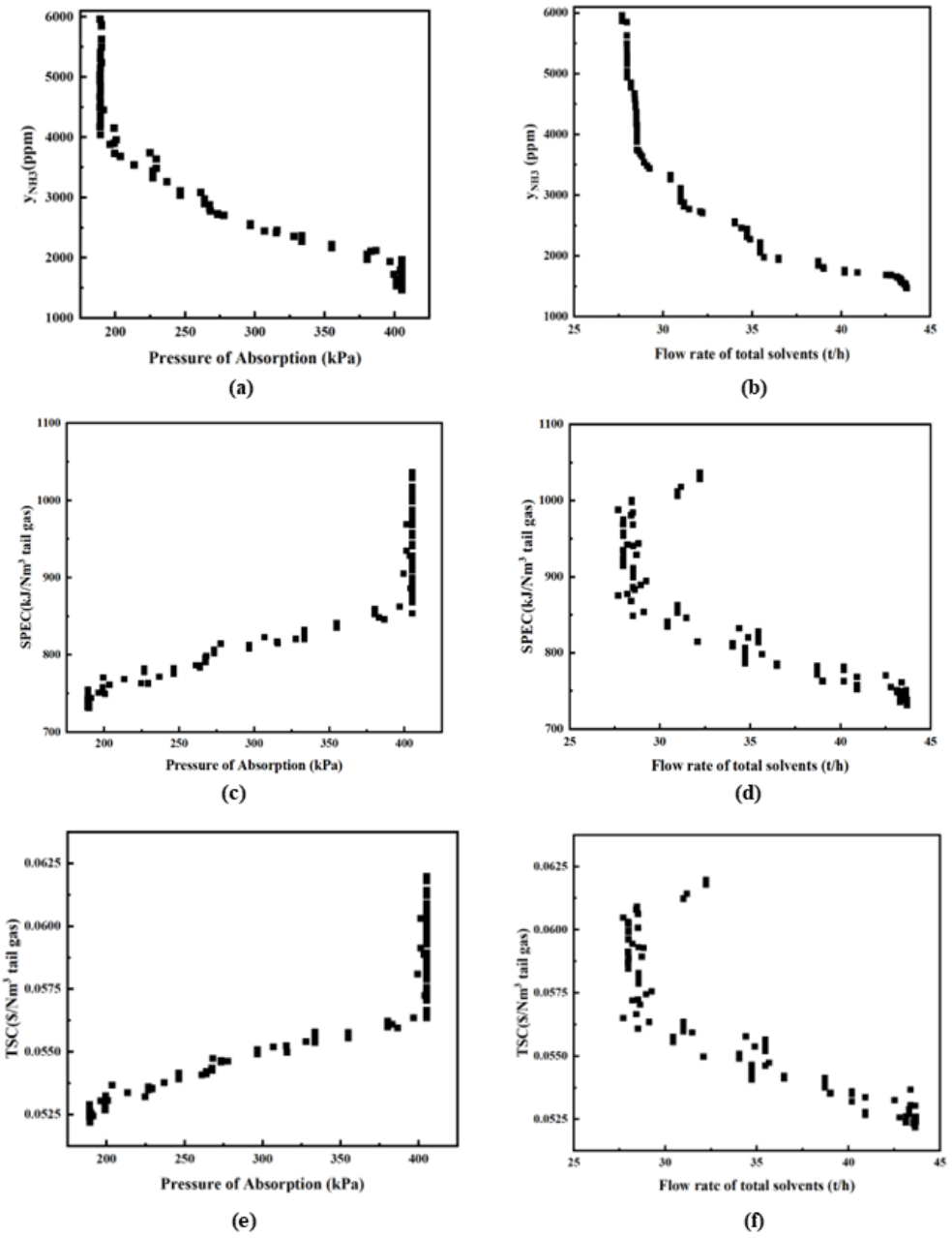

Figure 33 Main operational parameters versus y_{NH3}, SPEC and TSC. (a) P_{ab} vs. y_{NH3}; (b) F_{Total} vs y_{NH3}, (c) P_{ab} vs. SPEC; (d) F_{Total} vs SPEC, (e) P_{ab} vs. TSC; (f) F_{Total} vs TSC

Process parameter internal coupling relationship discussion

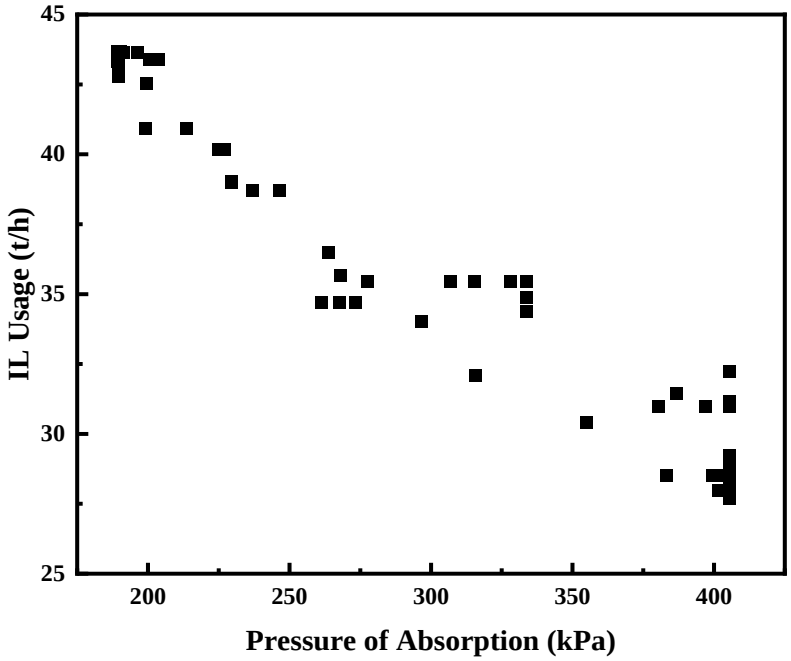

Figure 34 The relationship of operational parameters. P_{ab} vs $F_{ab.}$

Figure 34 shows the relationship of operational parameters. Additionally, from Figure 34, P_{ab} is negative correlated with IL Usage. The two decision variable of pressure of absorption and IL usage both is sensitive to the three evaluation index, higher pressure of absorption will need less IL in the process. Although increasing F_{total} can gain the solvent cost and high operational cost in gas stripping section, it is observed that the operations can reduce P_{ab} from Figure 34. The detail analysis of the internal parameter relationship will give more support in the technology design in the industrial application.

Process evaluation

The different scenarios' operational parameters have been shown in Table 15. Since there are three objective functions and the selection based on energy and economic evaluation have almost the same choice, we select the designs in Pareto front named cases 1, 2, and 3 with the objective functions, lowest y_{NH3} (1468 ppm), the lowest TSC (0.052 \$/Nm^3 tail gas), respectively. From Figure 35, compared with the base case, case 2 is over 24.6% of that of base case TSC and 23.5% in SPEC. In y_{NH3}, case 2 is 1468 ppm than the base case of 6000 ppm. Compared with case 2, case 3 has lower P_{ab} and higher P_{F1} and P_{F1}, which cause the lowest TSC. Furthermore, the process economy still plays an essential and prior

role in transforming and constructing separation technology. Hence, the best economic scenario (case 3) is selected for the separation process.

The comparison of cases 1, 2, and 3 in the economic analysis is shown in Figure 35. From Figure 35, in TSC, case 3 has the lowest TSC as 0.052 \$/Nm^3 tail gas, which decreased by 5.45% with the balanced case and 27.78% with case 2(high-performance case). Case 3 has the lowest P_{ab} and F_{total}, and the corresponding equipment cost is lower than in other cases. From Table 15, regarding the separation performance of this process, case 2 has the lowest y_{NH3} at 1468 ppm, which is half of the balanced case and decreased 75% of the economic friendly case. In summary, it is more important for the decision-makers to evaluate the operation parameters and objective functions based on existing melamine production plants and the corresponding matching factory equipment.

Table 15 Optimization Results of the NH_3/CO_2 Separation Process by ionic liquids.

Operation parameters	Base case	Case 1 (balanced)	Case 2 (high performance)	Case 3 (lowest TSC)	Unit
Theoretical stage of absorption	7	7	7	7	-
Feed stage position of semi-lean	4	4	4	4	-
Total IL flow rate	40.00	35.70	43.69	32.22	t/h
Absorption pressure	202.65	200.00	405.30	189.48	kPa
Pressure of flash 1	10.00	9.86	16.21	21.28	kPa
Temperature of flash 1	385.15	363.28	383.15	385.15	K
Pressure of flash 2	2.00	1.94	1.01	1.32	kPa
Temperature of flash 2	385.15	363.28	383.15	385.15	K
R_{LT}	0.48	0.5	0.26	0.37	-
Stripping column theoretical stage	4	4	4	4	-
Stripping column pressure	100.00	100.00	101.33	208.73	kPa
y_{NH3}	6000	4627	1468	5962	ppm
TSC	0.069	0.055	0.072	0.052	\$/Nm^3 tail gas
SPEC	956.34	798.19	1036.37	731.52	kJ/Nm^3 tail gas

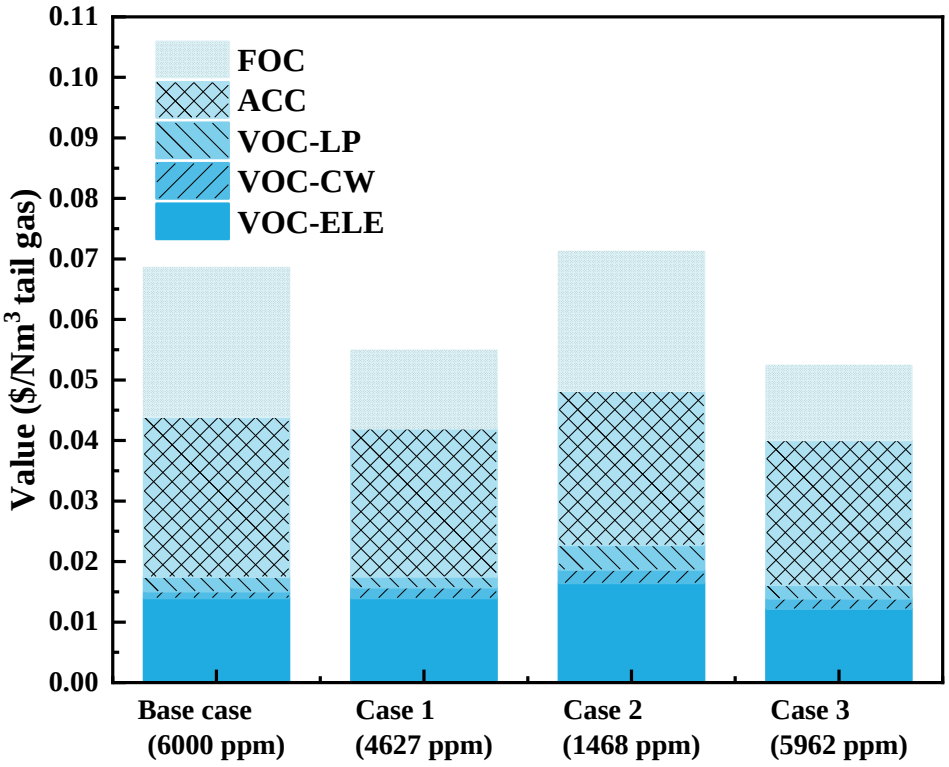

Figure 35 The comparison of the base case with the case 1, 2 and 3.

4.4 Summary

MOO was carried out to separate NH_3 and CO_2 using the IL in this work. After the sensitivity analysis based on technical-energy-economic, the change of pressure of absorption, IL flow rate, and pressure of Flash 2 are the three key sensitive decision variables with the objective functions. After the MOO, the result demonstrated that absorption pressure and the total usage of solvent affect TSC. In addition, the pressure of absorption and flow rate of IL are two operation parameters that conflict and balance with each other. In terms of technical-energy-economic evaluation, three different solutions were discovered. It was investigated that each case could provide decision-makers with helpful guidance. For the operation parameters, the results showed that the effect of absorption pressure, IL flow rate, and desorption pressure is critical for SPEC and TSC. The optimization results provide detailed and rigorous case design from the Pareto front with different objective functions, represents energy and economic improvement, and support the process design and operation of the CO_2 and NH_3 separation process with ionic liquids in regard to technology, energy, and economic objectives.

5 Case study: Dynamic evaluation and regulatory control of IL-based technology

This chapter gives a case study of the IL-based gas separation process dynamic behavior and regulatory control design. This chapter was divided into four parts. The first part gives the basic definition of the control problem of this process. The second part mainly concentrated on the necessary conversion from steady-state to dynamic mode with detailed equipment sizing, necessary inlet flow rate controller specification and inventory control for stable dynamic running without product quality control. The third part is the dynamic open loop simulation with tail gas fluctuation step test on the flash liquid volume control. The last part is the proposing and testing of the basic PID control layer with dynamic closed loop about the product quality control. In conclusion, this chapter was a detailed investigation about the process dynamic behavior and regulatory control design.

5.1 Definition of the control problem

5.1.1 Steady-state simulation in HYSYS

Once a steady-state design and the energy-economics evaluation have been analyzed, the next step is to perform dynamic analysis to gain insight on the transient behavior of the process in the presence of common disturbances and set-point changes.

The IL-based NH_3/CO_2 separation process dynamic control strategy is designed in Aspen HYSYS. The steady-state simulation was first carried out in HYSYS, and the simulation result is the same as our previous result in Aspen Plus for the two software used the same property package. The detailed key stream information and operation conditions were shown in Table 16.

Table 16 The key operational parameters of the balanced case in Aspen Plus and Aspen HYSYS.

Process / Operation parameters	Aspen Plus	Aspen HYSYS	Unit
Theoretical stage of absorption	7	7	-
Feed stage position of semi-lean	4	4	-
Total IL flow rate	35.07	35.07	$t \cdot h^{-1}$
Absorption pressure	200.00	200.00	kPa
Pressure of flash 1	9.86	9.86	kPa
Temperature of flash 1	363.28	363.28	K
Pressure of flash 2	1.94	1.94	kPa
Temperature of flash 2	363.28	363.28	K
R_{LT}	0.5	0.5	-
Stripping column theoretical stage	4	4	-
Stripping column pressure	100.00	100.00	kPa
NH_3 concentration in purified gas	4627	4627	ppm
NH_3 recovery	99.49	99.49	%

From Table 16, the key operation parameter and process objectives, such as NH_3 concentration and recovery is the same. In order to avoid the differences caused by the various software version HYSYS Dynamic function was employed in the simulation of the dynamic control strategy. Based on the steady-state simulation, the conversion to dynamic mode can be carried out. Section 5.2 gives the detailed conversion procedure with this IL-based process.

5.1.2 Definition of dynamic problem

It is essential to know the definition of the control problems before the designing of plant wide control strategy. Figure 36 showed the running data of the melamine tail gas fluctuation in the cooperated Chinese factory in 700 hours. From Figure 36, the main composition change is the increase both of NH_3 and CO_2 and corresponding decrease of air in the tail gas. For the IL-based process, the definition of the fluctuation of feed tail gas is set as the tail gas flow rate and composition fluctuation. Tail gas composition change is increase of NH_3 and decrease of air at the same time. Based on the running history, the step test scenario of fluctuation range for composition and flow rate of tail gas is defined as ±5%.

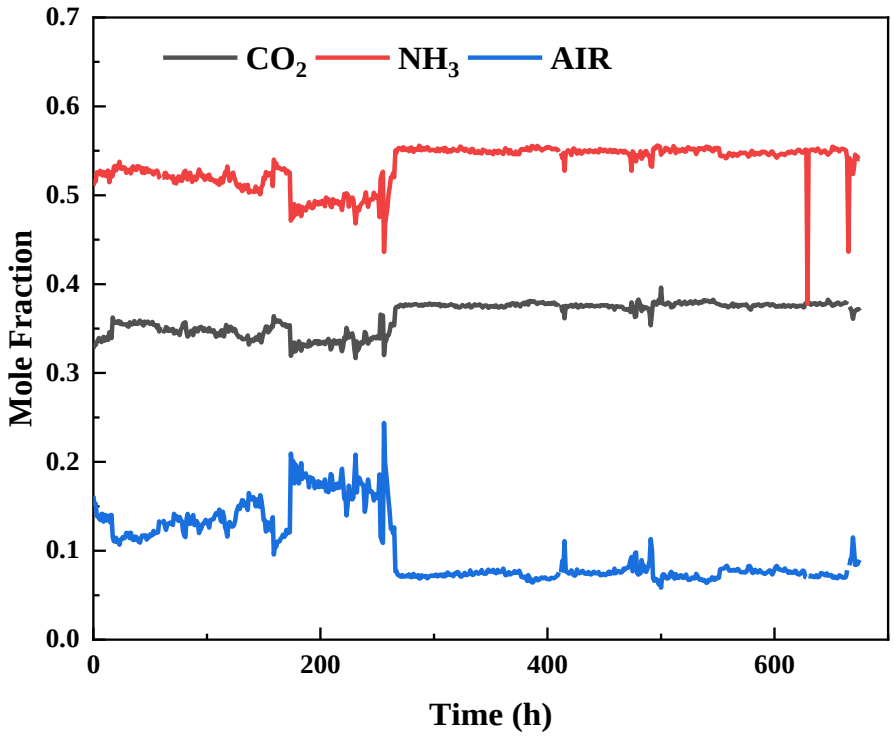

Figure 36 Fluctuation of tail gas composition in melamine factory.

5.2 Conversion from a steady state to a dynamic simulation

5.2.1 Conversion from steady state to dynamic mode

The difference between steady-state and dynamic mode is that there is no accumulation in the equipment, all the streams enter and exit from the process at the same time. In addition, most steady-state models did not consider the pressure-flow hydraulic relationships. Dynamic models account for material and energy accumulation and hold up. In Aspen HYSYS, the pressure–flow hydraulic behavior will be employed. It is obvious that dynamic model requires more information as compared with the steady-state model especially the setting of all the equipment. As a new technology with dynamic simulation, the safety and operation feasibility can be confirmed with desired process performance. By defining the detailed specifications of equipment in the dynamic simulation, the equipment functions as expected can be verified in an actual plant situation. The inherent complexity of the gas separation process means that a base layer of PID controllers needs to be implemented such that the dynamic process simulation can operate without diverging significantly from steady state. Inventory control was a primary objective for the design of a regulatory control strategy for chemical engineering process. Effective inventory control in chemical engineering can help improve the stability of the process and ensure process safety.

For the conversion of the process from steady-state to dynamic mode, the simulation flowsheet should be set up so that a realistic pressure difference is accounted for across all the plants. The detailed steps are shown below: 1) Adding unit operations: two units operations with no pressure flow must be specified in Dynamic mode, for example, valves, pumps and heat exchangers should define a pressure flow change. 2) Equipment sizing: Vessels (separators, condensers, reboilers) should be sized for about 5-15 minutes of liquid holdup time. All the valves should be sized with a 50% valve opening and a pressure drop between 15 and 30 kPa. For the absorption and stripping column sizing, the crucial variables of the internal column setting are Tray diameter, tray spacing, weir length, and height. In this step, the adjustments should be carried out for the column pressure. In HYSYS, the column pressure profiles can also be calculated by the Nozzle Pressure Flow K-factors to better model the pressure drop across the column. 4) Adding control operations: Identify key control loops that exist within the process. Some disturbances can be modeled using the transfer function operation. After all the above steps checked, the steady-state can be transferred to Dynamic environment. In the setting of the desorption section, the volume of the two flashes are calculated as 20.00 m^3 and 10.00 m^3 with resident time as 10 mins and with 50% liquid volume, respectively.

The detailed calculation of the size of the flash are showed below as example. As key equipment in this process, flash is responsible for desorbing the NH_3-rich solvents and emitting NH_3 as the products. The residence time for the two flashes is set as 10 mins in this process as recommended residence time when the fluid occupies 50% of the equipment volume. At previous steady-state design, the volume of flash 1 and 2 are 6.46 m^3 and 2.94 m^3. There are two main indicators for setting the size of the tank. One is that the velocity of the steam must be low enough to facilitate gas-liquid separation, which means that the cross-sectional area must be large enough. Second, the holdup of liquid in the tank must be sufficient for the required surge capacity. Take the volume calculation of flash 1 as an example. The steam flow rate is 1606 kg/h, and the density is 0.054 kg/m^3, and then the velocity of the steam should be 8.26 m^3/s. Usually the maximum allowable vapor velocity can be estimated by a simple empirical formula, which is related to the density. The greater the density, the smaller the maximum allowable velocity, and the F factor is used below:

$$F\ factor = V_{max}\sqrt{\rho v} \qquad \text{Equation 14}$$

For separation flash, the F=0.61, so the maximum allowable vapor velocity is:

$$V_{max} = \frac{0.61}{\sqrt{0.054}} = 2.625\ m/s \qquad \text{Equation 15}$$

The calculated cross section based on the vapor load is: 3.15 m^2 and the diameter related to the flash is 2 m.

Then calculate the size based on the holdup requirement. The liquid flow rate is 41680 kg/h, the gas density is 1372 kg/m^3, and the volume flow rate can be calculated as: 0.506 m^3/min. For a holdup of 10 mins, the liquid volume should be 5.06 m^3. Since liquid accounts for 50%, the total volume should be 10.12 m^3. Assuming L/D ratio is 2, then the diameter can be calculated as 1.86 m. Since this value is smaller than the diameter calculated from the vapor load (2 m), the larger of the two is chosen. Finally, in order to ensure the safety operation of the flash, the total volume should be round up to 20 m^3.

The internal type of absorber and stripping column is chosen as Sieve and the weir height is 50 mm and length as 1.6 m and 1.2 m, respectively. The hydraulics data of the two column are show in Appendix. The overall k value of rich solvent, semi lean and lean are 460.1, 219.1 and 38.5 kPa kg/m^3, respectively. The compressor with connection between recycle gas from stripping column to absorber column has the duty of 28970 kJ/h, adiabatic efficiency with 75% and polytropic efficiency as 78%. All the valve's dynamic specification are shown in Table 17 with the total delta pressure and calculated conductance by Aspen HYSYS. In addition, in order to avoid the backflow of valve, all the valve are set as check valve. Table 17 shows the size of key equipment for converting from steady-state to dynamic mode.

Table 17 Size of equipment of the IL-based process.

Equipment	Diameter (m)	Length (m)
Absorption column	2.014	7
Stripping column	1.5	4
Flash 1	2	4
Flash 2	1	2
Equipment	Total Delta P (kPa)	Conductance (Cv) (USGPM(60F,1psi))
VLV-AB-L	3.389	236.9
VLV-AIR	11.21	44.11
VLV-F1-L	0.01	7075
VLV-F1TOF2	7.91	132.6
VLV-F1-P	0.82	5411
VLV-F2-L	0.001	34650
VLV-F2-P	0.91	1824
VLV-FEED	20.3	690.8
VLV-IL-M	27.91	0.1531
VLV-LEAN	5.01	152.9
VLV-RICH	179.5	72.95
VLV-SEMI	11.13	106.7
VLV-ST-L	12.07	99.97
VLV-ST-P	21.33	55.21
VLV-AB-P	107.1	226.7

With all the equipment operation parameters finished, Aspen HYSYS needs the integrator of the execution of dynamic simulations. With other calculation execution as default, the Composition and Flash Calculations is changed from the default 10 to 1 as the two reasons. First the two flash are the key equipment in this process. Second, lower of the value, the flash calculation will be performed more frequently. This can slow down the calculation speed of Aspen HYSYS, but it may result in more accurate compositions and results in this case. This number can be reduced in cases where the phase change in an individual vessel is being studied and a high degree of accuracy is required with regard to the phase composition. Figure 37 shows the integrator setting of this process.

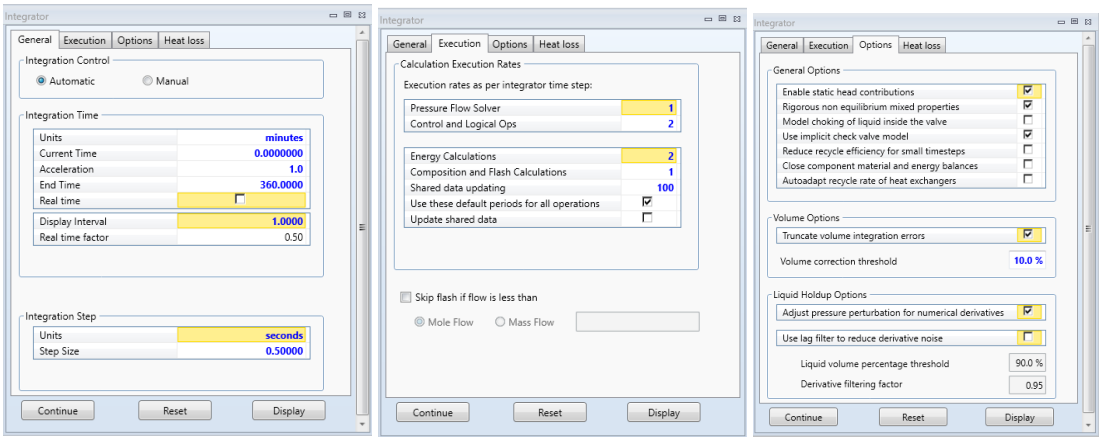

Figure 37 Integrator setting of the process in Aspen HYSYS.

5.2.2 Inlet flow rate controller specification

Dynamic simulations in Aspen HYSYS require flow specifications to be set by control valves with a pressure specification after the control valve. All inlet and outlet material streams of the process within the limit must have either pressure or flow specification fixed. Pressure specifications are used in Aspen HYSYS dynamic mode typically. The fluid flow is based on a pressure gradient.

For all the control loops, the process gain is defined as the ratio of the change/deviation in the process output to the change/deviation in the process input. The time constant defines the speed of the response. All the control loops in this process are set as feedback control, the simplest and most widely used control structure in chemical process systems. The input to the feedback controller is called the error or the difference between the output process variable and the set point, and the error is defined differently depending on whether the process has a positive or negative steady-state gain. Two key input streams in this process are the tail gas feed stream and the IL-makeup stream. Both controllers have a reverse control action, and the valve is chosen as the stream outlet valve correspondingly. The gain K_C and integral time are 0.5 and 0.3 mins as recommended in HYSYS help document with flow rate controller, respectively. Necessary parameter tuning is vital to all the controllers. In simulation software, there are some default values for the gain and integral time. However, user can also choose to let the software to self-calculate the gain and integral time of each controller. From Figure 38 (a) and (b), both feed gas controllers show better control performance with the autotuner showed with red thicker solid line. Figure 38 (c) and (d) showed the corresponding valve position, higher gain cause quick to the set point but with less stability. Considering the stable time and process robustness, both the two input flow rate controllers choose the autotuner value of gain.

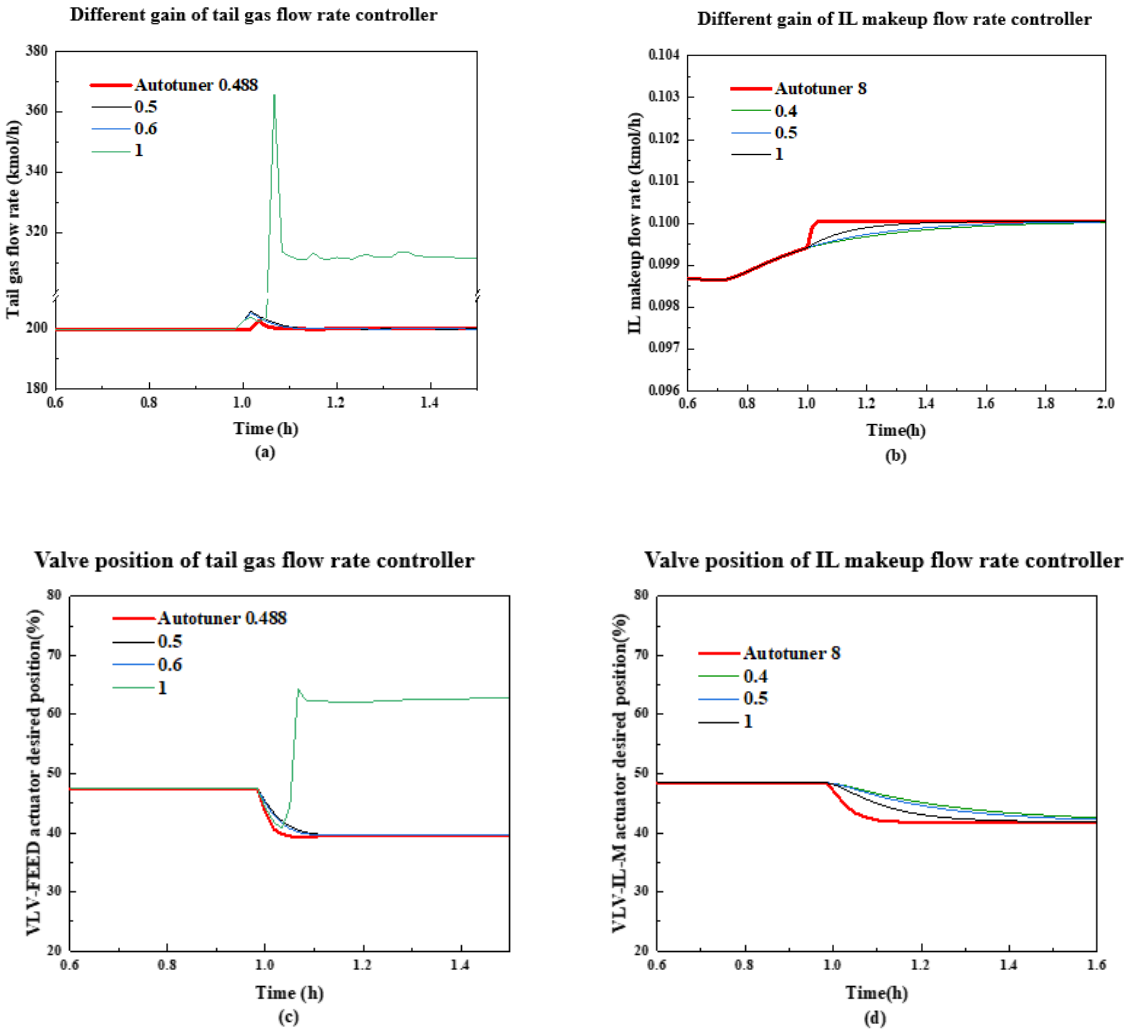

Figure 38 Comparison of different gain of the(a) tail gas, (b) IL-makeup controllers and (c-d) corresponding valve position.

Table 18 Controller parameter of tail gas and IL-makeup controllers.

	Gain (%/%)	Integral time (mins)	Design type
Tail gas flow rate controller	0.488	0.0733	PI
IL makeup flow rate controller	8.00	0.0733	PI

After the specification of process pressure flow, sizing of all the equipment and tuning of the necessary inlet flow rate controller, the process now is ready for dynamic analysis. There are two signal for successful conversion from steady-state to dynamic mode. 1) If the dynamic simulation can be ran without any system and singular error like: Pressure flow solver failed to converge; Negative pressure detected and so on. 2) If the key separation index as NH_3 concentration in purification can be stable after run for a while. If not, check all the pressure specification and equipment sizing and operation parameter setting are reasonable. The next step is the realization of inventory control.

5.2.3 Inventory control

Inventory control was a primary objective for the design of a regulatory control strategy for this IL-based technology. To finish the step test of the whole process, first, the stable running of the process without any controller is carried out. Figure 39 shows the steady running of the process only with two necessary input controllers. From Figure 39, both the NH_3 concentration in purified gas and NH_3 recovery go stable after 1 h, and this process can facilitate stable running within 6 hours. Based on the stable running data results, the step test can be carried out with fluctuation. It can be seen from Figure 39 that there is some fluctuation at the beginning of the dynamic simulation. The reason is the initialization of the dynamic system by software and only happened at a few seconds.

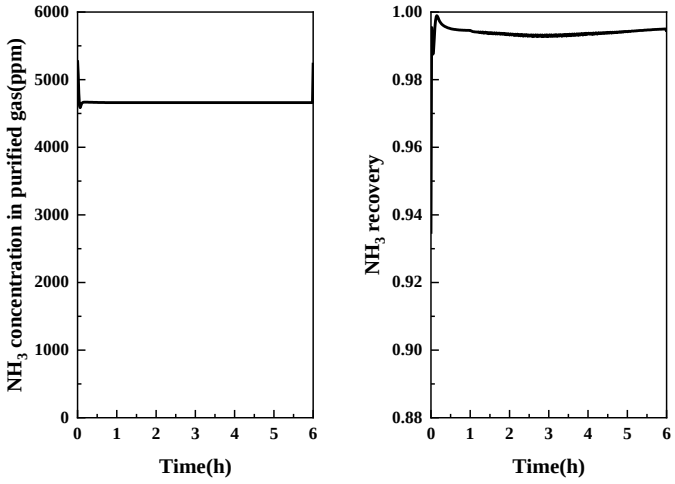

Figure 39 Dynamic performance with inventory control.

5.3 Dynamic open loop simulation result

In order to evaluate the dynamic performance of the process, the step test will be carried out with the fluctuation of tail gas flow rate and NH_3 concentration. Open loop control refers to the control process in which there is only forward action between the control objective and the manipulated variable, and there is no reverse connection. First, the open loop simulation dynamic simulation was carried out. As the key units of the desorption section, the liquid level of the two flashes must be controlled. The valve downstream of the controlled inventory serves as the manipulated variables for these liquid level controlled variables. The setting of two liquid level control of the Flash 1 and 2. All the control have a direct control action, and the valve position at the liquid outlet stream of each flash were set as the outlet target variables. The gain K_C and integral time are 2 and 10 mins as recommended in the HYSYS help document with liquid level controller. Figure 40 showed the IL-based NH_3/CO_2 separation process dynamic open loop control simulation with two flash liquids level control. According to the melamine factory running data in Figure 36, the flow rate and NH_3 concentration step change are set as ± 5.

5.3.1 Simulation result with tail gas flow rate +5%

Figure 40 showed the dynamic performance with tail gas flow rate +5%. With introducing the fluctuation after 1 hour, more of the tail gas flow into the absorber column, the NH_3 concentration in purified first decrease a little and then increases above 5000 ppm and after 4 hours the value stable at 5240 ppm. For the NH_3 recovery, with more of the NH_3 in the system, the NH_3 recovery increase with the increase of tail gas flow into the process.

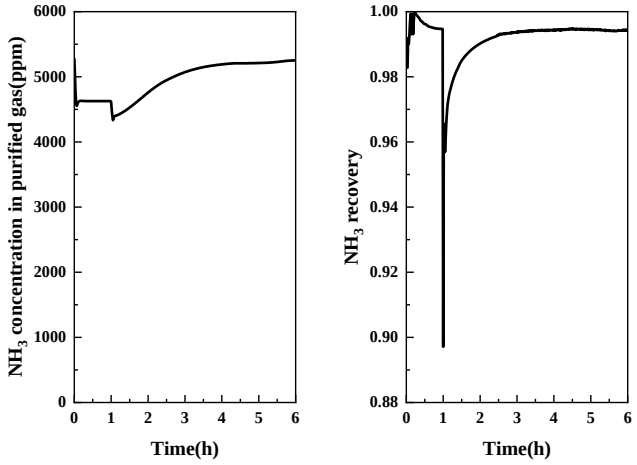

Figure 40 Dynamic performance with tail gas flow rate +5%.

As the key solvent in the NH_3/CO_2 separation process, IL plays an essential role in the dynamic control of the system. With the increase of the tail gas flow rate, first the flow rate of IL in rich solvent suddenly goes down to about 83.25 kmol/h and then goes stable after 6 hours to 84 kmol/h. The relationship between IL flow rate in rich solvent and NH_3 concentration in purified shows as less IL will lead to more NH_3 in the purified gas and decrease the separation performance.

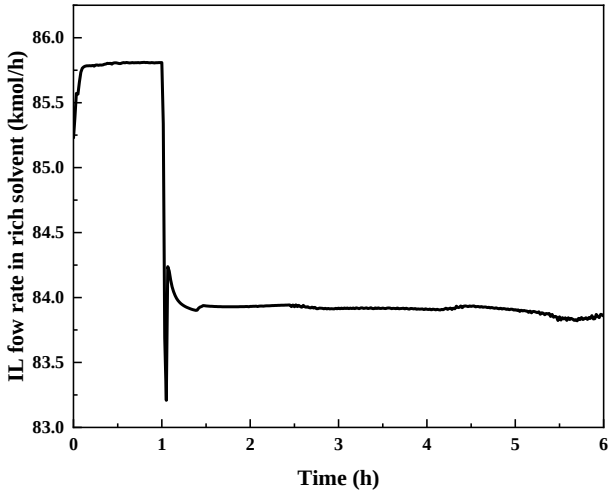

Figure 41 IL flow rate in rich solvent with tail gas flow rate +5%.

Figure 42 (a) shows the liquid volume percent of flash 1 and 2 with these two controllers. It can be seen that the liquid volume percent, both goes stable and maintain the set point. Figure 42 (b) shows the corresponding valve position change. In order to keep the liquid volume in flash 1, the valve increase and then go stable. For other manipulated variables and controlled variables in the process, Figure 44 showed the change of pressure of flash 1 and 2 and the corresponding gas flow rate out from flash 1 and 2. The result showed the potential of employing the gas outlet valve of flash to control the pressure of the two flashes.

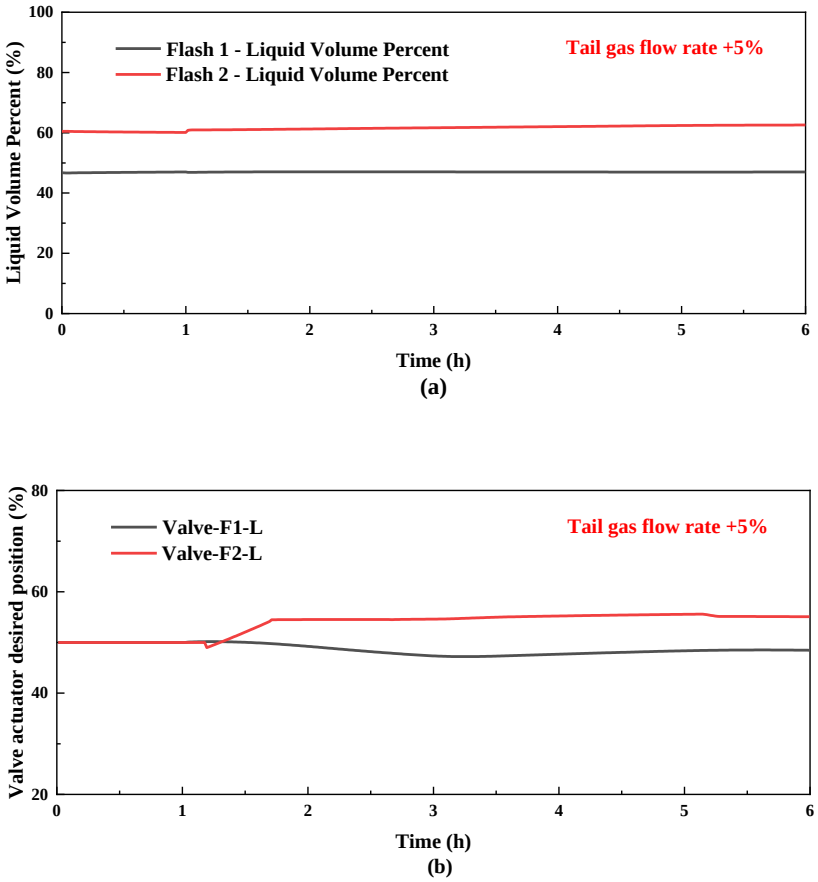

Figure 42 (a) Liquid volume percent of flash 1 and 2 with tail gas flow rate +5% (b) corresponding valve position.

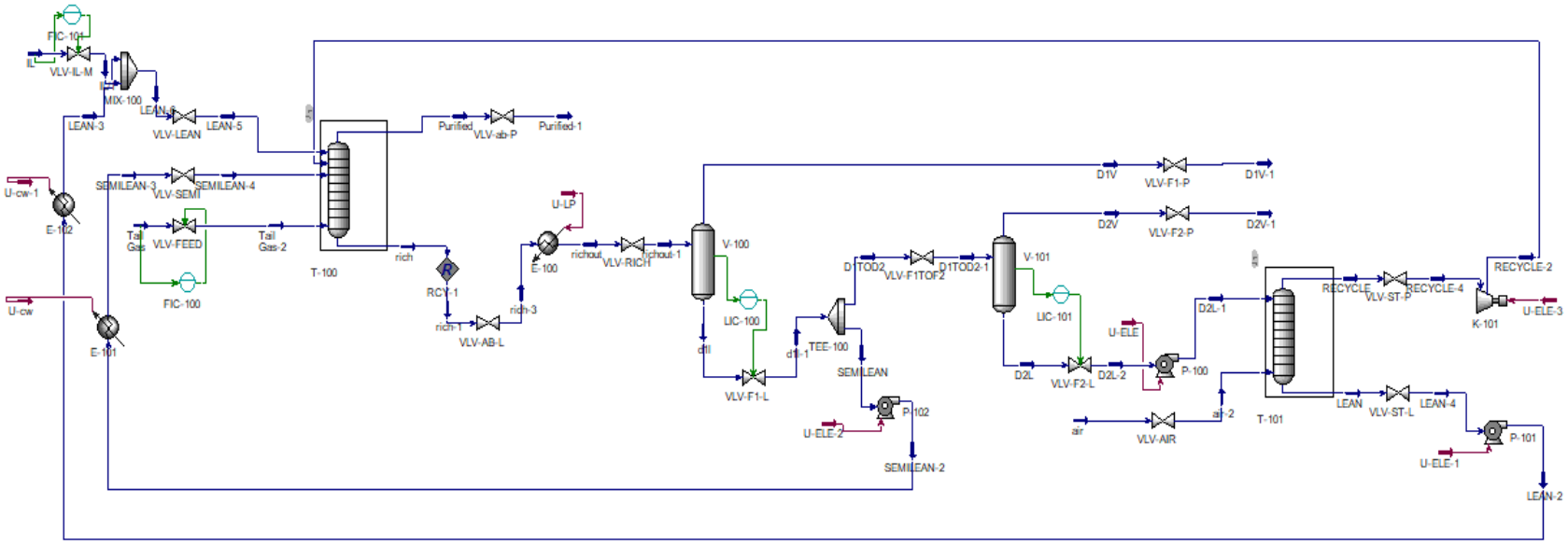

Figure 43 IL-based NH_3/CO_2 separation process dynamic open loop control simulation with two flash liquids level control.

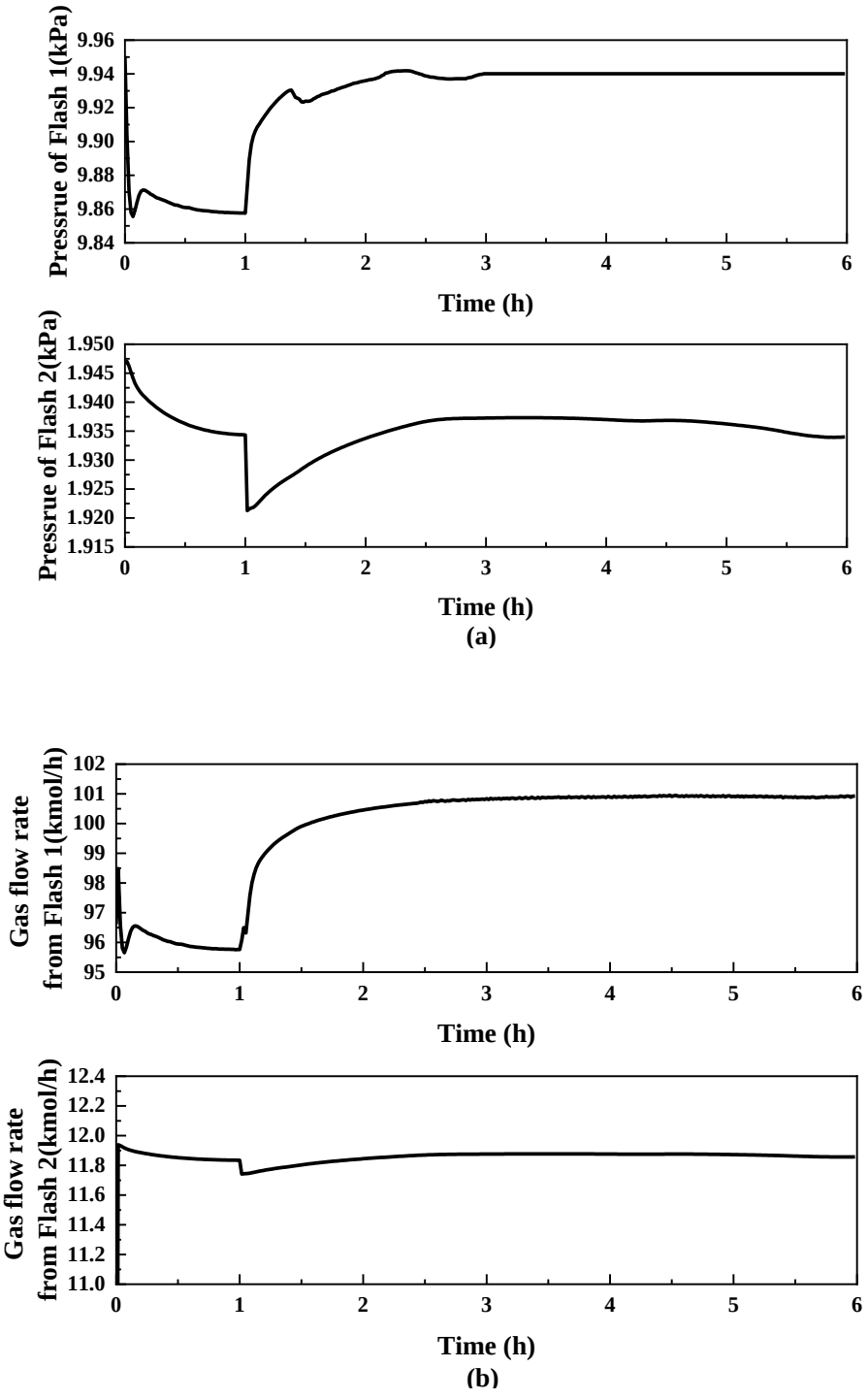

Figure 44 (a) Pressure change of flash 1 and 2 (b) Gas flow rate from flash 1 and 2 with tail gas flow rate +5%.

From Figure 45, the temperature of lean, semi lean and rich solvents all decrease after the tail gas flow rate increase, this may be caused by the change of the NH_3 and IL flow rate in this system and

related utilities used in these three streams should be the controlled variable with the manipulated variable of the three stream temperature. As shown in Figure 45, before introducing the tail gas fluctuation, the change of semi lean temperature is not completely stable, but as analyzed in steady-state, the temperature of semi lean didn't affect too much to the separation performance compared with the pressure of two flashes.

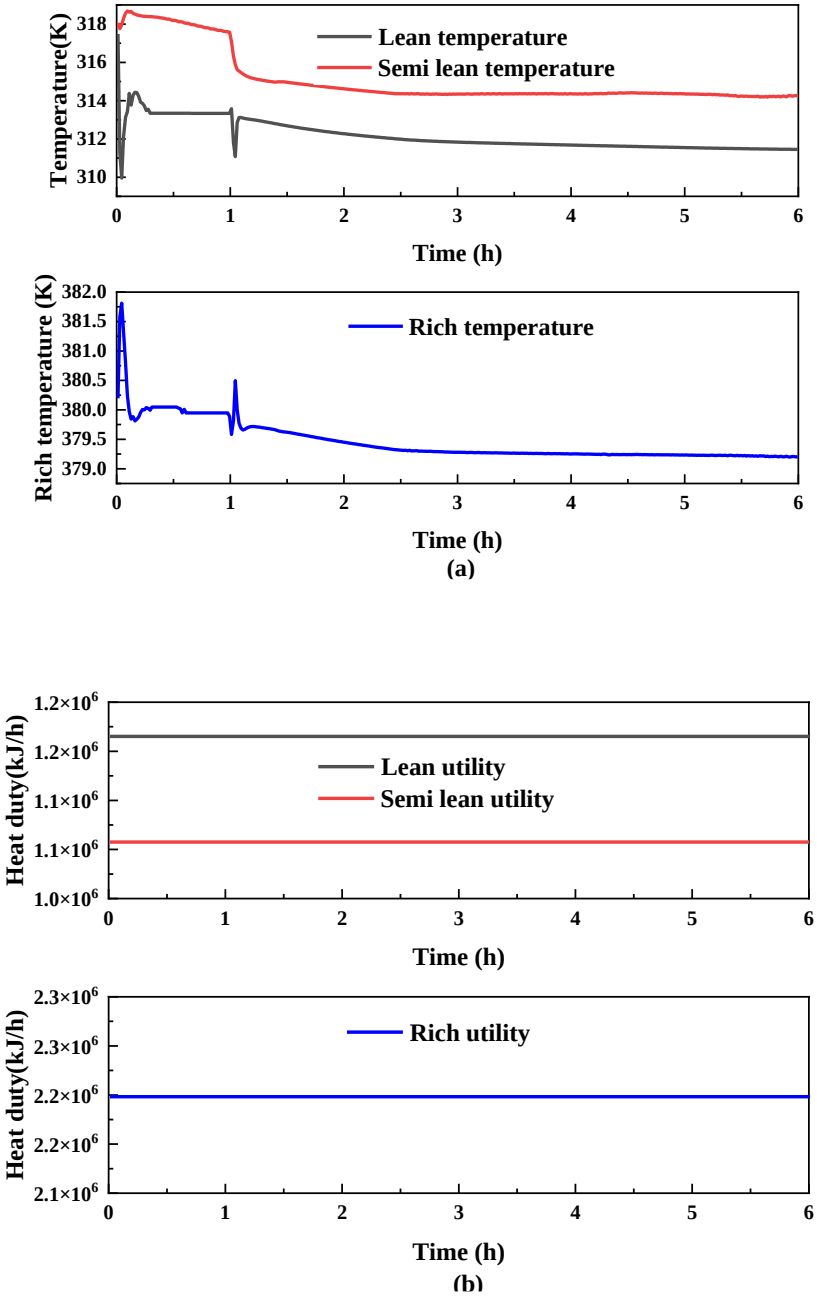

Figure 45 (a) Temperature of rich semi lean and lean stream with tail gas flow rate +5%, (b) corresponding heat duty.

5.3.2 Simulation result with tail gas NH_3/AIR concentration +5%

Figure 46 showed the dynamic performance with tail gas NH_3 concentration +5%. With introducing the fluctuation after 1 hour, more of the NH_3 flow into the absorber column, the NH_3 concentration in purified increase above 5000 ppm and after 4 hours the value stable to 5870 ppm which is higher than when the fluctuation is tail gas flow rate +5%. For the NH_3 recovery, with more of the NH_3 into the system, the NH_3 recovery first decrease and then increase stable with the increase of tail gas into the process. Regarding on the difference between the tail gas flow rate and NH_3 concentration fluctuation, the stabilization time of concentration change was longer than the flow rate change for the NH_3 recovery, the reason is caused by the unstable change of pressure of flash 2.

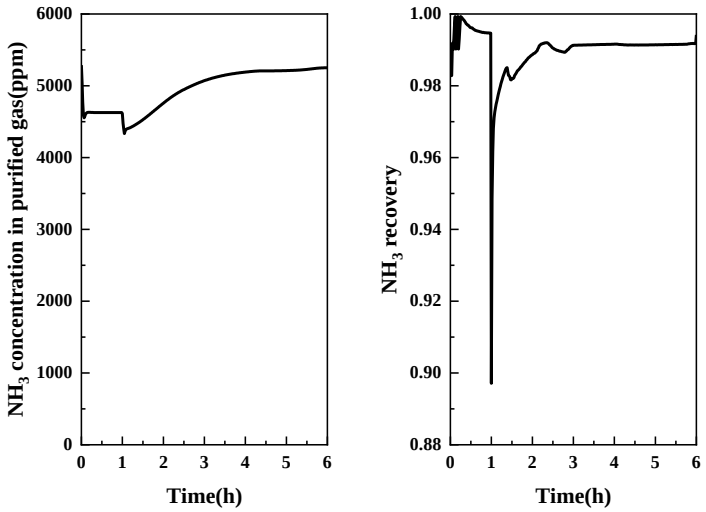

Figure 46 Dynamic performance with tail gas NH_3 concentration +5%.

For the behavior of the IL flow rate in rich solvent, with the increase of the tail gas NH_3 concentration, first the flow rate of IL in rich solvent suddenly goes up to about 87 kmol/h and then goes down to 85.5 kmol/h after 4 hours. The relationship between IL usage and NH_3 concentration in purified gas is also reasonable: less IL will lead to more NH_3 in the purified gas and decrease the separation performance. Figure 48 shows the liquid volume percent of flash 1 and 2 with these two controllers, and it can be seen that the liquid volume percent all goes stable and maintain the set point. For other couplings with manipulated and controlled variables, Figure 49 shows the change of pressure of flash 1 and 2 and the corresponding gas flow rate out from flash 1 and 2. The result showed the potential of employing the gas outlet valve to control the pressure of the two flashes.

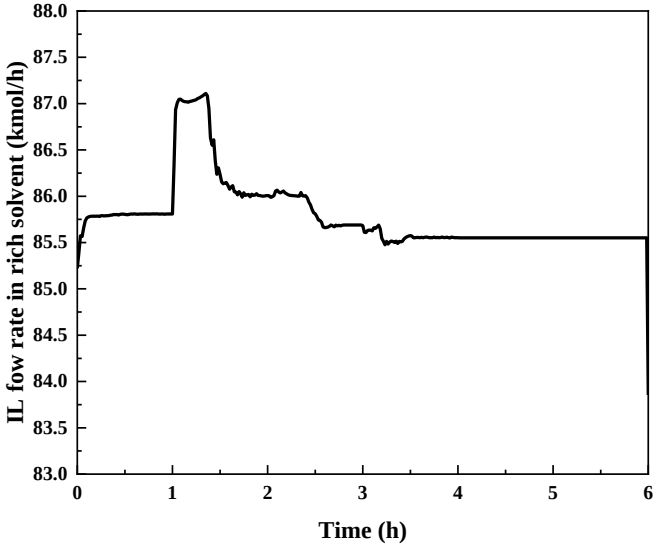

Figure 47 IL flow rate in rich solvent with tail gas NH_3 concentration +5%.

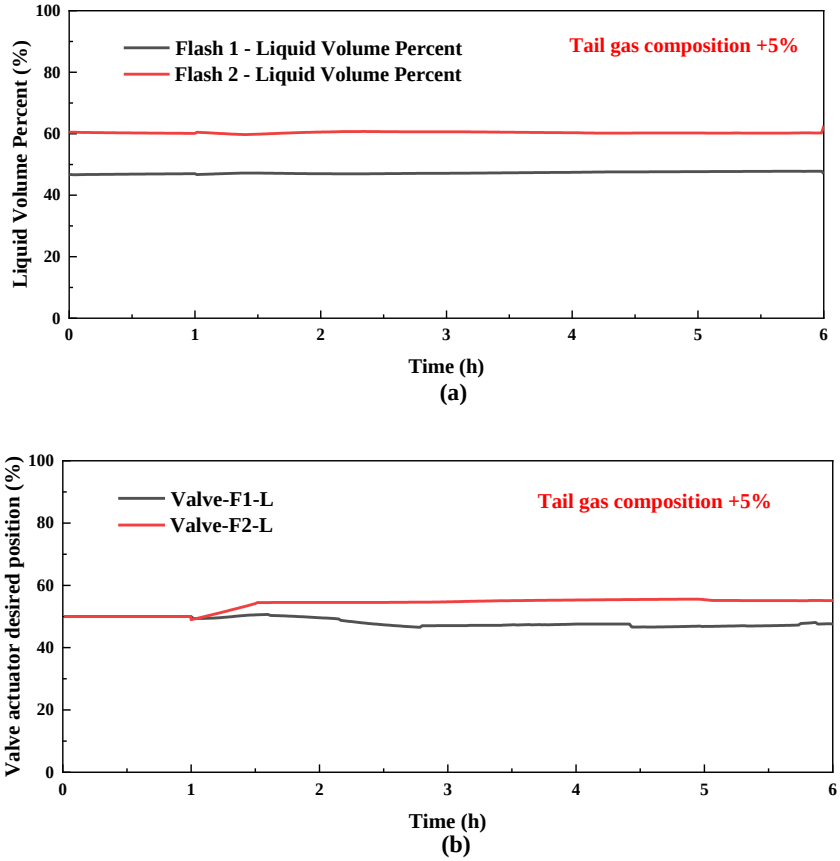

Figure 48 Liquid volume percent of flash 1 and 2 with tail gas NH_3 concentration +5% (a) and corresponding valve position (b).

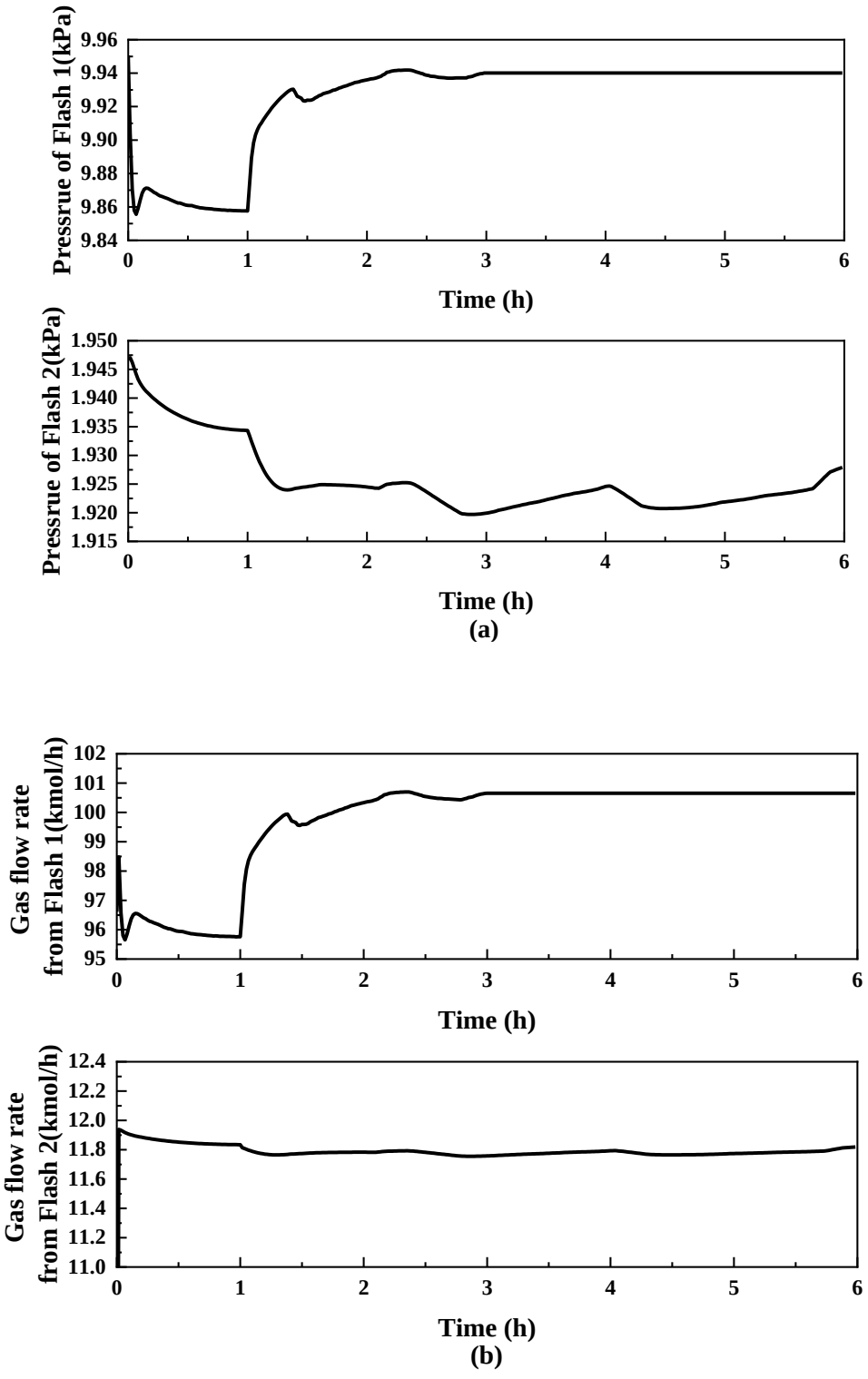

Figure 49 (a) Pressure change of flash 1 and 2 (b) Gas flow rate from flash 1 and 2 with tail gas NH_3 concentration +5%.

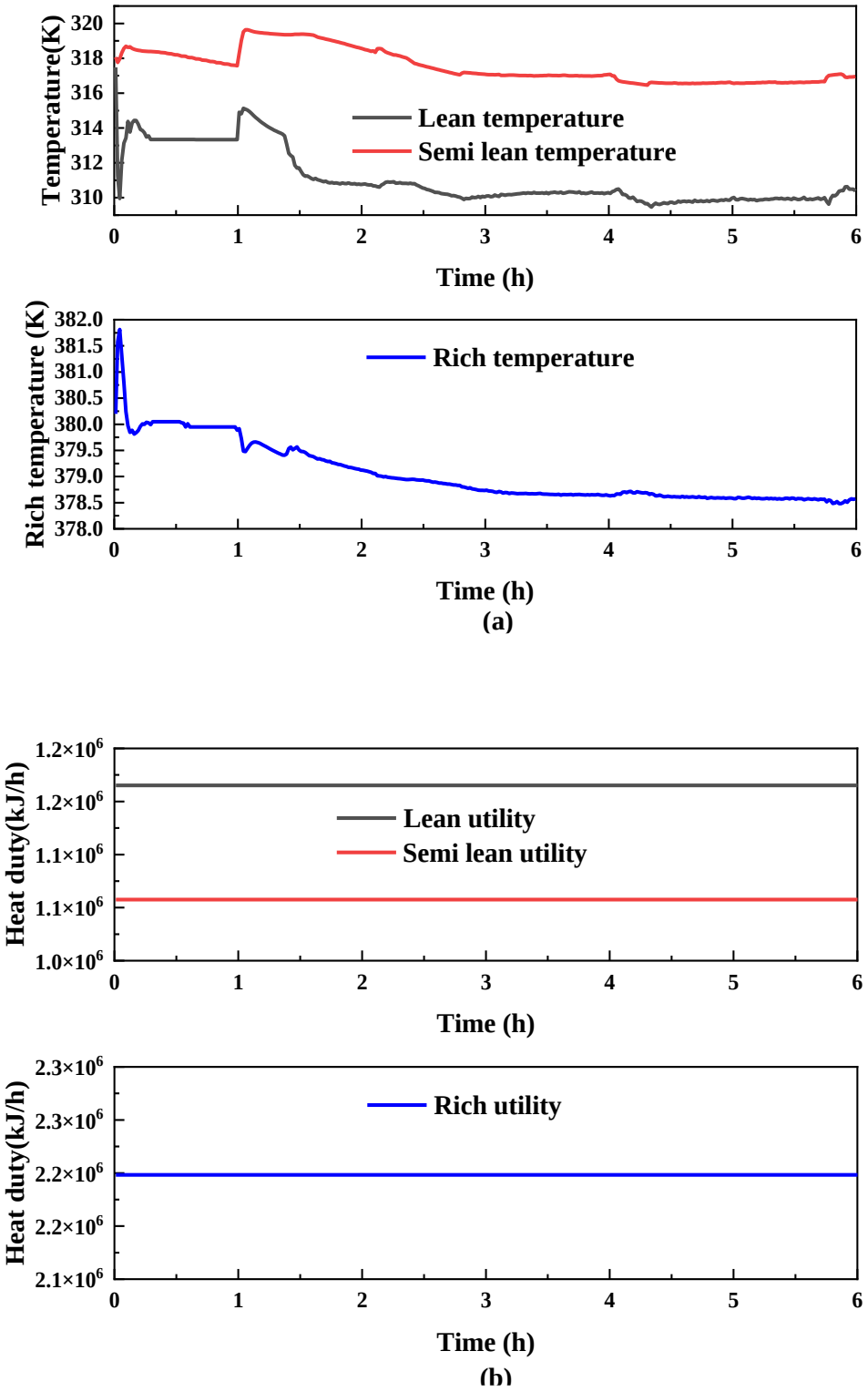

Figure 50 (a) Temperature of rich semi lean and lean stream with tail gas NH_3 concentration +5%, (b) corresponding heat duty.

From Figure 50, the temperature of lean, semi lean and rich solvents all have decreased after the tail gas flow rate increase. This may be caused by the change of NH_3 and IL flow rate in this system, and related utilities used in these three streams should be the controlled variable with the manipulated variable of the three stream temperatures.

Based on the above open loop control analysis, the simulation showed that the process can achieve the stable running and reject the fluctuation of tail gas flow rate and NH_3 concentration. However, the NH_3 concentration in purified gas and NH_3 recovery can not back to the set point. In the next step work, the depth design of the closed loop dynamic simulation regard on the product quality dynamic control should be carried out.

5.4 Dynamic closed loop design

In order to have suitable dynamic control of the IL-based process, the choice of manipulated and controlled variables is important. In this part, we can design the scenario that we want to test and targets. The output of the system are measured, and the measured result could be fed back to the input terminal to subtract the input to obtain the deviation, and then the deviation generates direct control to eliminate the deviation. The whole system forms a closed loop. Solving the process dynamic problem can have stable running of the new technology and save cost from design through operation and maintenance by removing the consequences of inefficient decisions and maintaining a safe environment. Based on the coupled manipulated variables and corresponding variables. Table 19 shows this process's potential coupling of manipulated and controlled variables. To control the process regarding on tail gas fluctuation, 5 control loops will be added to test the control performance. The product quality are defined as the NH_3 concentration in purified and NH_3 recovery.

The control scheme will be designed as follows: 1) the pressure of flash 1 and 2 are controlled by the outlet gas from the two flashes; 2) there are three temperature controller for the semi-lean and lean solvents back the absorption column, rich solvent to the Flash 1, the output temperature of the three solvent heat exchanger were controlled by the utility consumption. The two flashes pressure controller gain K_C and integral time are 2 and 10 mins as recommendation in HYSYS help document with pressure controller and with direct action. For the three temperature controllers, the control action are all reverse. The controller gain K_C and integral time are 0.1 and 0.2 mins as recommended in HYSYS help document with temperature controller. In addition, the dead time are set as 10 mins. Table 19 showed the controlled variables and manipulated variables information of the detailed proposing dynamic closed loop design strategy.

Table 19 Setting information of controller

Controlled variables and set point	Manipulated variables	Process variable min	Process variable max	Action	K_C	T_i
Flash 1 liquid volume percent (46.66%)	VLV-F1-L position	0	100	Direct	1.8	102
Flash 2 liquid volume percent (63.20%)	VLV-F2-L position	0	100	Direct	1.8	106
Flash 1 pressure (9.86 kPa)	VLV-F1-P position	5	15	Direct	2	10
Flash 2 pressure (1.92 kPa)	VLV-F2-P position	1	2.5	Direct	2	10
Rich temperature (379.5 K)	U-LP control valve	60	160	Reverse	0.1	0.2
Lean temperature (313 K)	U-CW control valve	0	100	Reverse	0.1	0.2
Semi-lean temperature (317 K)	U-CW control valve	0	100	Reverse	0.1	0.2

Figure 51 showed the dynamic simulation result of the proposed dynamic strategy with feed tail gas flow rate and NH_3 concentration fluctuation on +5%. The result showed that the both the fluctuation of tail gas flow rate and concentration can be controlled regard on the NH_3 concentration in purified gas and NH_3 recovery. After 4 hours, the NH_3 concentration in purified gas back to 5000 ppm with tail gas flow rate increase to 210 kmol/h. For the tail gas concentration, the NH_3 concentration in purified gas can back to 5000 ppm more quickly. In addition, the value the NH_3 concentration in purified gas is 4811 ppm and the flow rate +5% is 4954 ppm. The NH_3 recovery both back to 0.99 after 4 hours. The result showed the better control performance compared with the dynamic open control results. In order to have better dynamic control performance, the cascade control of feed tail gas and ionic liquids make-up solvent and advanced dynamic control strategy could be carried out.

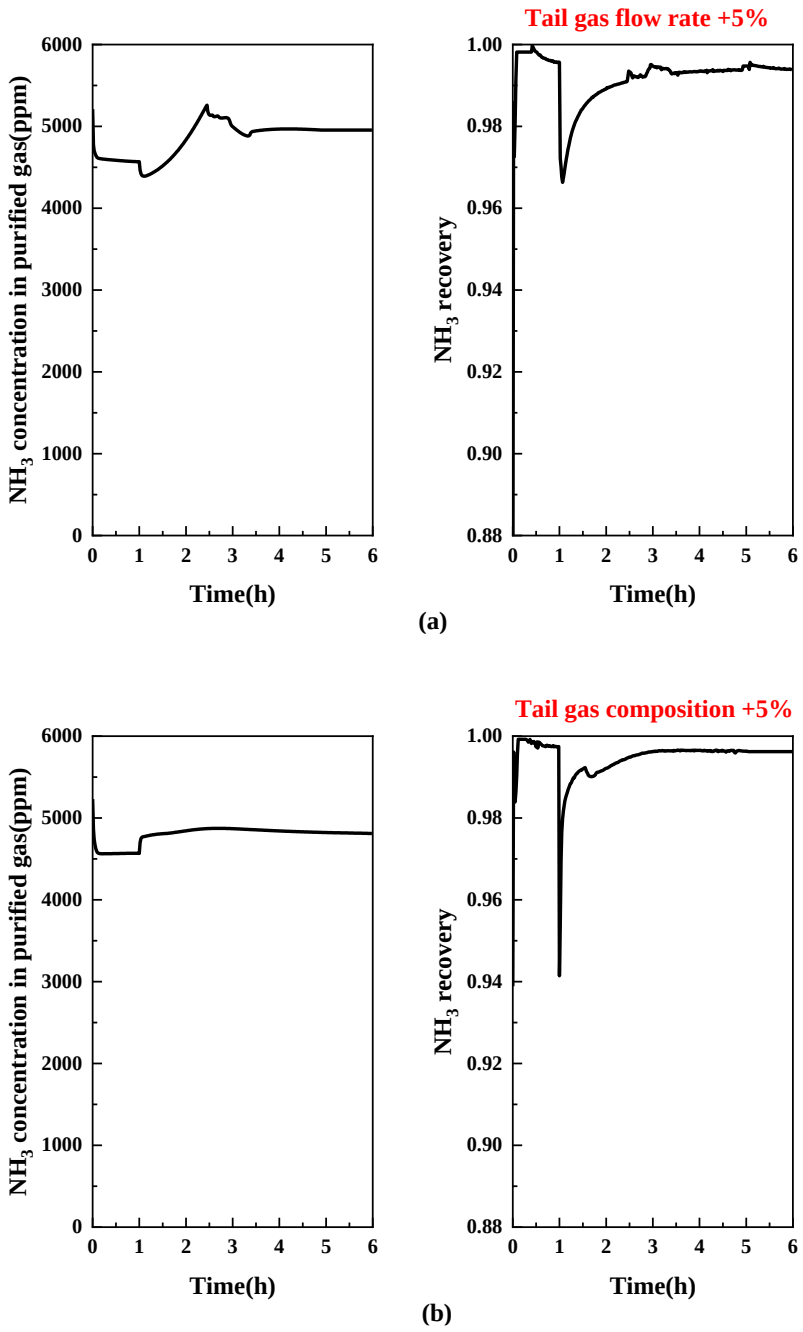

Figure 51 Dynamic performance with tail gas NH_3 concentration +5% of proposed dynamic control strategy.

Figure 52-56 showed all the seven controlled variables and relevant manipulated variables change with the tail gas fluctuation of flow rate and NH_3 concentration +5% with the dynamic closed control strategy. The result showed that all the controlled variables can be controlled to the set point and thus ensure the product quality.

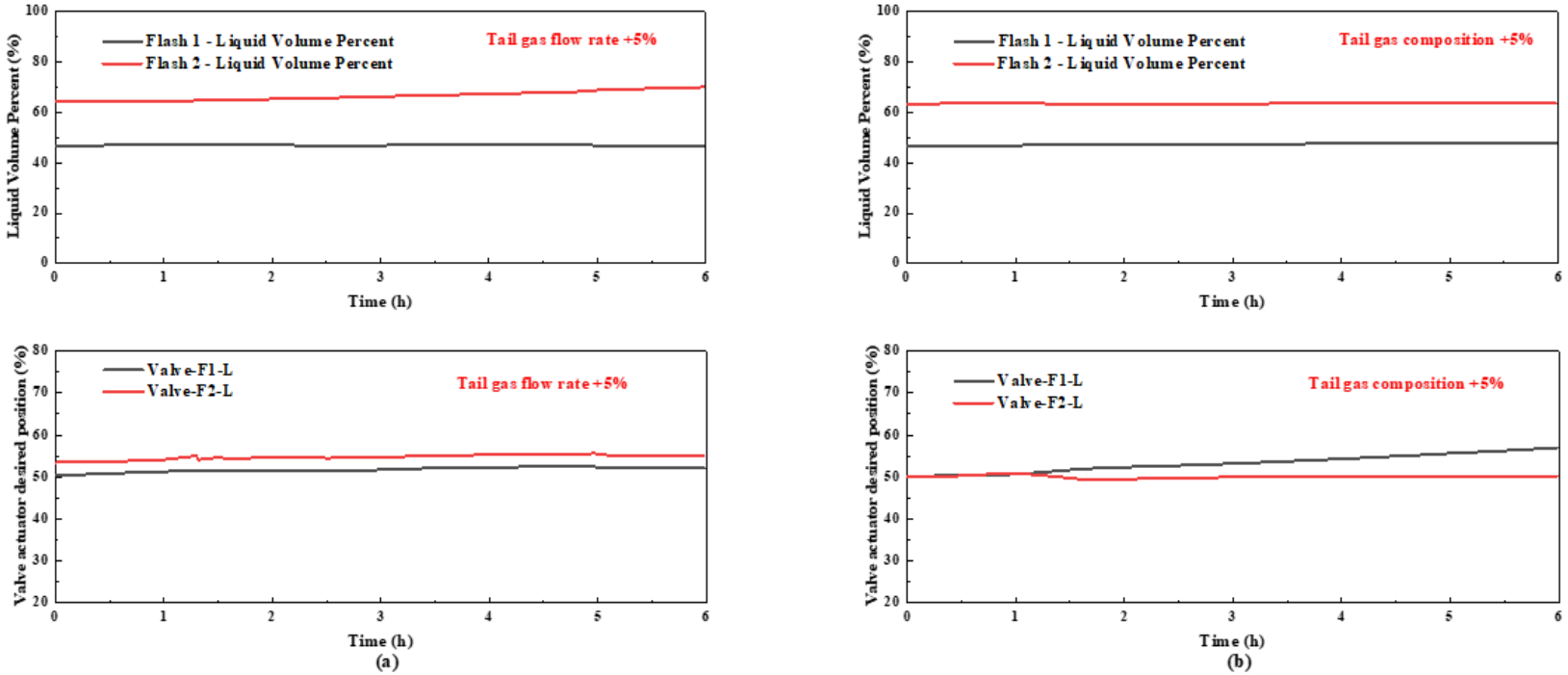

Figure 52 (a) Liquid volume percent of flash 1 and 2 with tail gas flow rate +5% and corresponding valve position. (b) Liquid volume percent of flash 1 and 2 with tail gas NH_3 concentration +5% and corresponding valve position.

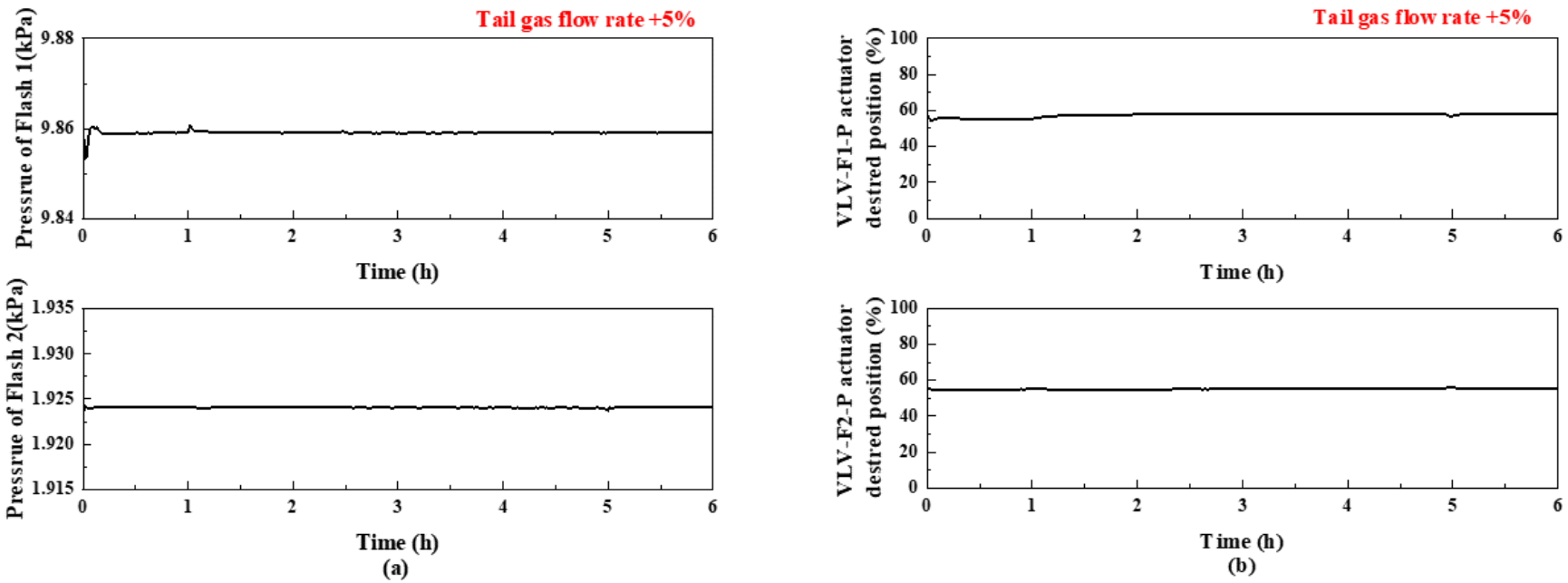

Figure 53 (a) Pressure change of flash 1 and 2 and valve actuator desired position change with tail gas flow +5%.

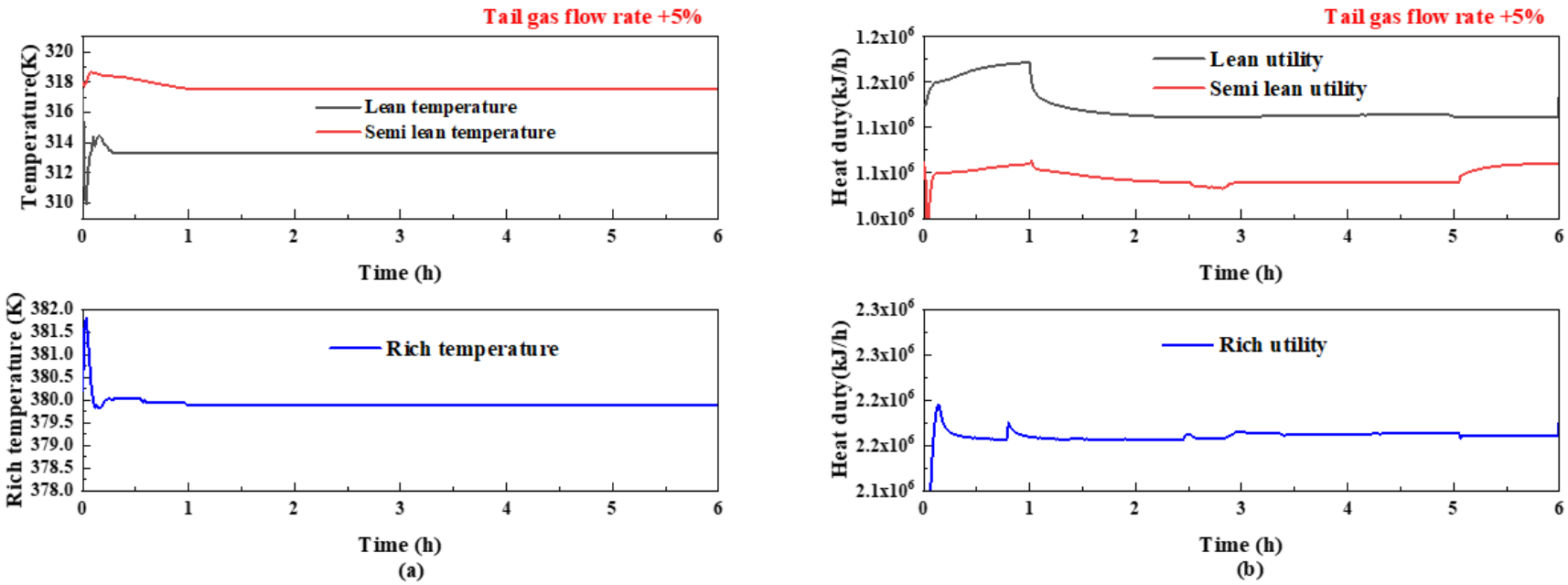

Figure 54 (a) Temperature of rich, semi lean and lean solvent with tail gas NH_3 flow rate +5% and (b) corresponding heat duty.

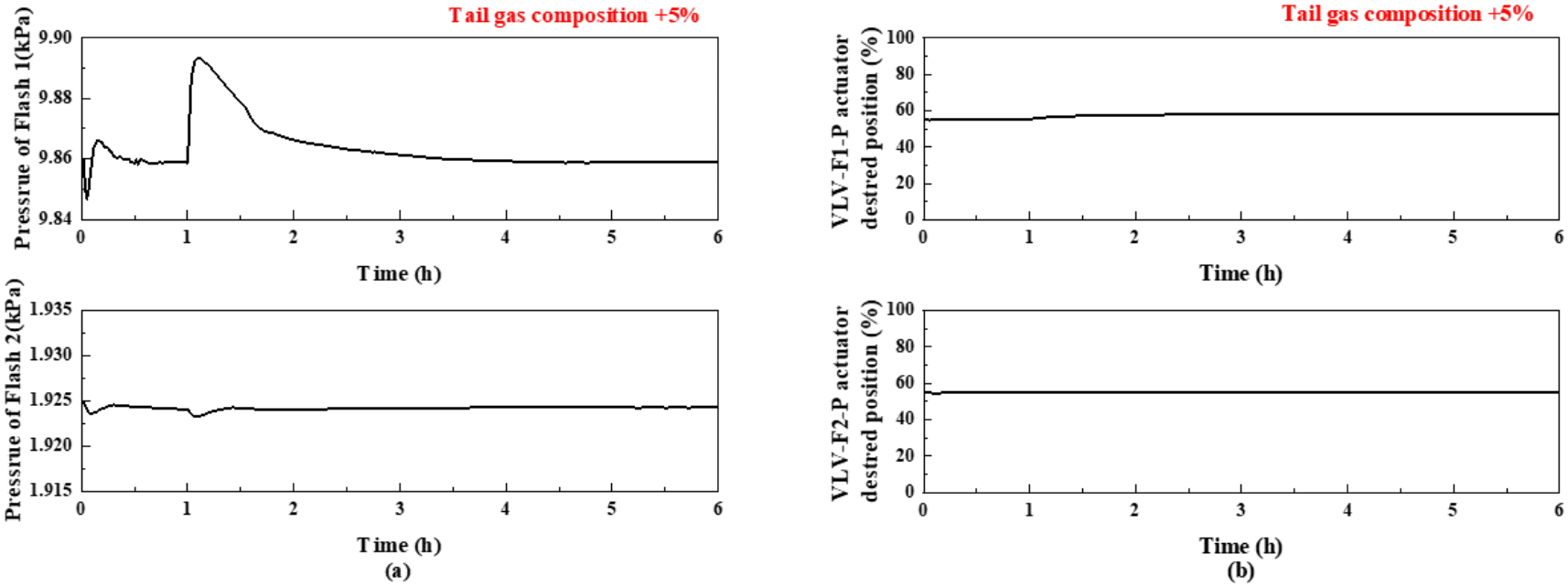

Figure 55 (a) Pressure change of flash 1 and 2 (b) valve actuator desired position change with tail gas NH_3 concentration +5%.

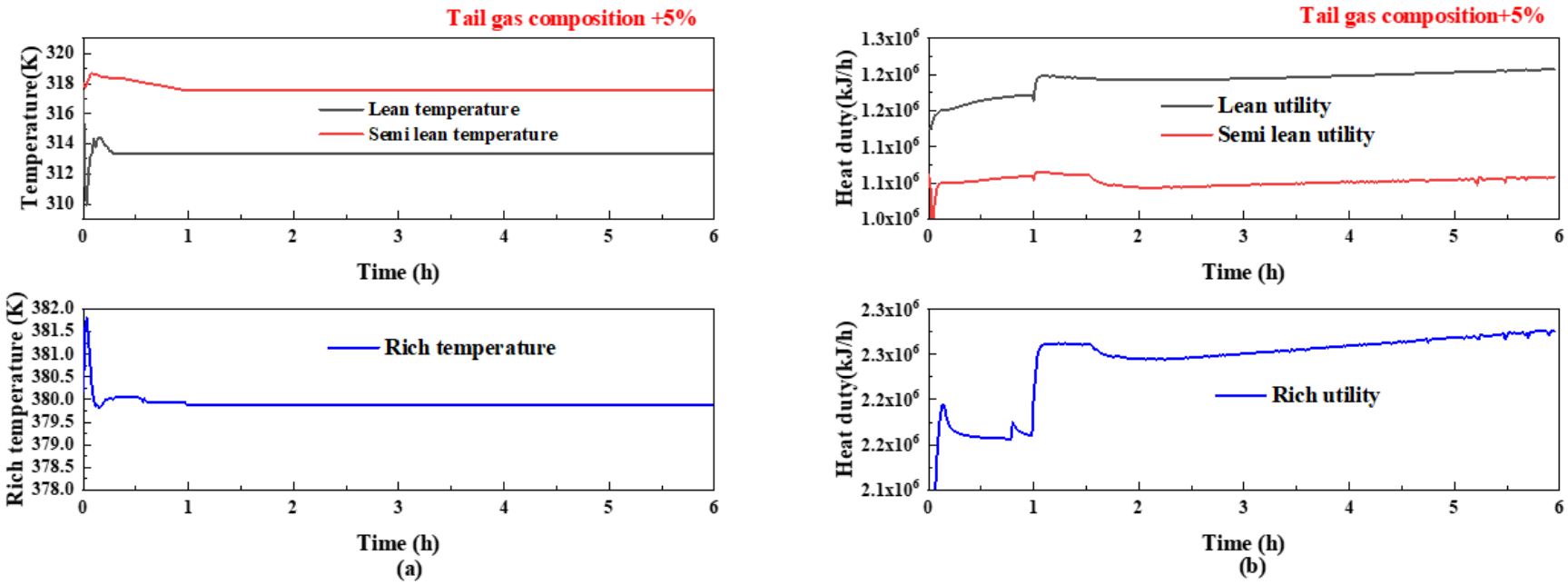

Figure 56 (a) Temperature of rich, semi lean and lean solvents with tail gas NH_3 concentration +5%, (b) corresponding heat duty.

5.5 Summary

The IL-based NH_3/CO_2 separation process dynamic control behavior evaluation was carried out:

1) The dynamic fluctuation was defined based on the melamine factory running history.
2) The conversion from steady-state to dynamic mode was simulated in Aspen HYSYS, and detailed equipment sizes were calculated for dynamic running. Necessary input stream controller setting parameters were chosen to guarantee the inventory stabilization of the process without a specific control scheme.
3) The step test was carried out with tail gas fluctuation of flow rate and NH_3 concentration at ±5% about the dynamic open loop simulation.
4) The potential dynamic control strategy was proposed and test with effective product quality control performance and advanced control strategy is expected to be employed for future dynamic control investigation.

The simulation results showed that NH_3 concentration and NH_3 recovery have a positive response with more tail gas and NH_3 in the system. With the analysis of the parameter behavior on the different tail gas fluctuations, basic dynamic control could be built to guarantee stabilization with different fluctuations. Based on the detailed investigation about this process's dynamic behavior, this new technology is fairly easy and simple to operate.

The different magnitudes of fluctuation will be needed to test the basic control scheme's performance. After the base layer PID control design and analysis, an advanced control scheme needs to be designed and analyzed for the IL-based NH_3/CO_2 separation process and provide support to the new technology industrial application.

6 Discussion

In this chapter, overall summarizing and discussion are presented of the main challenge output and limitation of this new IL-based technology in this thesis. This chapter is partially based on the published articles: ” Process simulation and evaluation for NH_3/CO_2 separation from melamine tail gas with protic ionic liquids”, Separation and purification Technology, 288 (2022) 120680 [1]. ”Multi-objective optimization of NH_3 and CO_2 separation with ionic liquid process”, 14th International Symposium on Process Systems Engineering, Computer Aided Chemical Engineering, 49, 2022,1147-1152, [2] and the manuscript “Technical-energy-economic multi-objective optimization of ionic liquid-based CO_2 /NH_3 separation from melamine tail gas”.

6.1 Summarizing of the thesis

The working structure of this thesis can be found in Figure 57. First, the process simulation and evaluation were designed and carried out based on the thermodynamic model of IL and binary regression of IL-NH_3 and IL-CO_2. In order to make comparison of the IL-based technology with traditional water scrubbing technology, the energy- economic process evaluation was employed to the research (Chapter 3). Second, as a novel and new technology, the process parameter and detailed energy-economic performance should be further investigated. The multi-objective optimization method was introduced to the system and different operation scenario were gotten based on technology-energy-economic evaluation index (Chapter 4). As the full simulation package, the dynamic control is necessary for the new technology. To investigate the dynamic behavior of the IL-based technology, the step test with tail gas flow rate and composition fluctuation were carried out to analyze and explore the need for stabilizing and regulatory control (Chapter 5). Finally, all the research work above will provide a full simulation package of IL-based NH_3/CO_2 separation process and give detailed data support to the new technology industrial application.

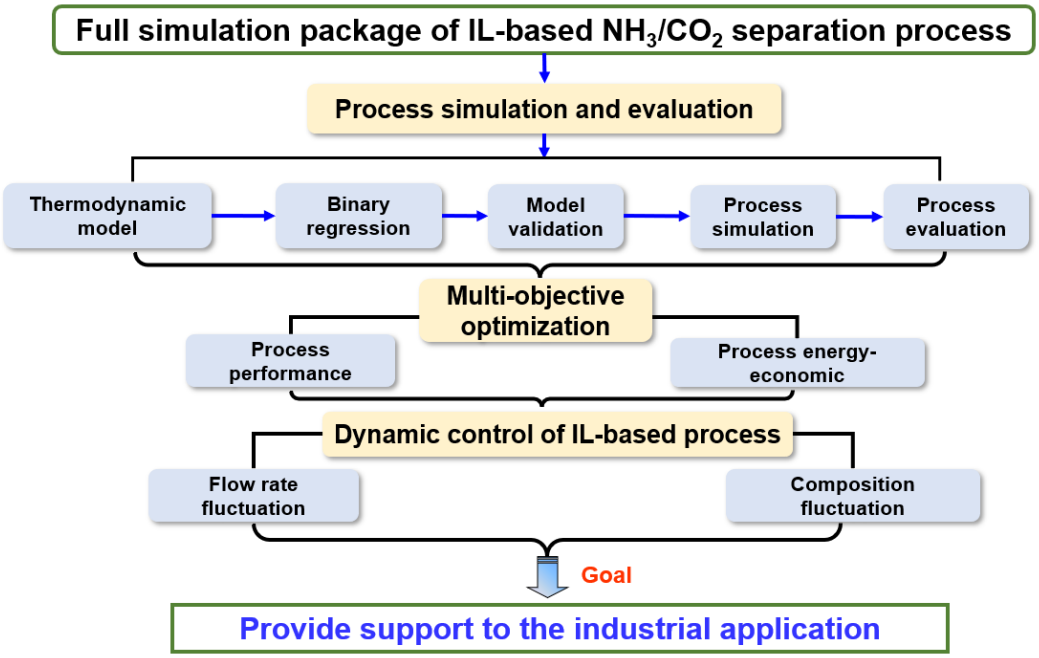

Figure 57 Working structure of the thesis.

6.2 Discussion and limitation of the thesis

6.2.1 Discussion of the main research output of the IL-based technology

As an important industrial raw material, melamine can be condensed and polymerized with formaldehyde to produce melamine resin, widely used in tableware, heat insulation materials, coatings, adhesives, etc. However, the content of NH_3 in melamine tail gas is high, NH_3 and CO_2 are easy to react directly, and separation is relatively difficult. The separation of NH_3 and CO_2 in melamine tail gas is of great significance for resource utilization, reduction of triamine cost, and expansion of production capacity. The traditional melamine separation technology, such as water scrubbing, solvent absorption technology has high energy consumption, high investment cost, and low ammonia recovery rate, and it is difficult to popularize and apply to the industry. It is urgent to develop a green and energy-saving NH_3 and CO_2 separation technology.

Ionic liquids are a new class of solvents composed of positive and negative ions, which have a structure similar to NaCl and are non-volatile. Ionic liquids have hydrogen bond-electrostatic-cluster interaction, resulting in high NH_3 solubility; designable structure and adjustable polarity lead to good NH_3 selectivity; extremely low vapor pressure and small specific heat capacity lead to low energy consumption and no pollution; Therefore, ionic liquids separate and recover NH_3 is expected to become a new transformative technology.

The main difficulty of NH_3/CO_2 separation is that the NH_3 and CO_2 concentrations are high and easy to crystallize. The traditional water scrubbing in which NH_3 and CO_2 are easily absorbed by water simultaneously, and the recovery rate of pure NH_3 is low. To solve these problems, high NH_3 absorption and high selectivity ionic liquids are selected for absorption, and the multi-stage absorption-desorption-stripping process is enhanced further to reduce the process energy consumption and economic costs. The new ionic liquids process has simple flowsheet, consumes less energy and enables direct obtention of pure NH_3 products.

The main innovations of this research work are: 1) The new green technology of NH_3/CO_2 separation and NH_3 recovery of ionic liquid from melamine tail gas was developed for the first time, which broke through the problem of crystallization and difficult separation of NH_3/CO_2 and realized the high-purity and efficient green separation and recovery of NH_3 in melamine tail gas. 2) Through the multi-objective optimization method, the separation process based on different operating parameters of separation performance, energy consumption and economic cost was screened out, and the parameter analysis and energy cost optimization of the ionic liquid process were further discussed. 3) Explore the potential of the process for plantwide dynamic control through step test with tail gas flow rate and concentration fluctuation. The new technology solves the common

technical problems faced by the melamine industry, has obvious economic, environmental and social benefits, will promote technological change in the melamine industry, and lead the transformation and upgrading of the melamine industry.

Based on the full simulation process package of this new ionic liquid technology, the new technology can also be extended to industrial ammonia-containing gas industries, such as synthetic ammonia emission gas, low-concentration NH_3-containing tail gas in molybdenum metallurgy, organic chemical industry, etc. This new technology has broad market demand and application prospects.

6.2.2 Industrial application of the new IL-based technology

Based on the strong research background and technology transformation of the ionic liquids research department in IPE. During the period of external study at IPE, this project also includes the in-depth participation in the industrialization of ionic liquids-based process design. In the industrialization of ionic liquids-based process design, the research group in IPE is mainly responsible for the design and synthesis of the specified ionic liquids and providing the initial design data package to the factory. My role in this project is: 1) thermodynamic properties regression of the ionic liquids, 2) detailed process design and simulation of the proposed ionic liquids-based technology. Finally, giving a detailed simulation package of this new technology to the cooperated factory, now the simulation package had been evaluated and provided to the factory. The large scale of 1.5 billion Nm^3/year melamine tail gas cleaning process by ionic liquids is now under construction. For the industrial application of NH_3/CO_2 separation, the first industrial test pilot plant (Figure 58) with 50 $Nm^3 \cdot h^{-1}$ of IL-based NH_3 recovery from melamine tail gas worldwide was built by the Institute of Process Engineering, Chinese Academy of Sciences, with 3500 h stable running[69]. Based on the industrial test pilot of the IL-based NH_3 recovery from melamine tail gas. The cooperated industrialization project between IPE and data provided company: Shandong Shuntian Chemical Company is currently under construction with the scale of 1.5 billion Nm^3/year melamine tail gas cleaning process by ionic liquids. During the promotion of the industrialization project, mainly responsible for the regression of the physical properties of commercial ionic liquids and process design, including process optimization, equipment calculation and selection, etc., and completed the preliminary process simulation data package of this industrial project. This new industrial application also passed the achievement identification by Petroleum and Chemical Industry Federation of China and the appraisal committee unanimously agreed that the technology has independent intellectual property rights, is highly innovative, ranks at the international leading level, and has broad market demand and application prospects[119].

Figure 58 The first industrial test pilot plant with 50 Nm^3/h of IL-based NH_3 recovery from melamine tail gas.

6.2.3 Limitation of the IL-based technology

As a new and innovative technology, IL-based technology has some limitations. The discussion will be shown from high-efficient solvent, hybrid and integrated process technology design, kinetic model development, intelligent process design, and optimization method.

As a novel green solvent, more NH_3-efficient functional ionic liquids should be paid much more attention. With the high price of ionic liquids solvents, the economic performance could be cheaper with less solvents used in the system. The stability of the ionic liquids could also extend the life of the solvent and lower the loss rate, thus decreasing the economic cost. The key of the high NH_3 absorption solvents relies on the hydrogen bond functional group. Introducing functional groups of weak hydrogen bond donors and strong hydrogen bond acceptors to improve NH_3 absorption capacity and selectivity is one possible way to enhance the separation performance with less solvent usage. Yuan et al. [66] designed and synthesized a variety of bifunctional protic ionic liquids which have weakly acidic and hydroxyl to enhance the NH_3 absorption performance of ionic liquids. It is found that [EtOHim][NTf_2] has the highest NH_3 solubility, which is 3.11 mol $NH_3 \cdot mol^{-1}$ IL, and the highest NH_3 mass solubility is [EtOHim][SCN] with a value of 0.221 g $NH_3 \cdot g^{-1}$ IL. At the same time, these ionic liquids can select NH_3/CO_2 and NH_3/N_2 up to 65 and 104 respectively. Sun et al. [120] designed and synthesized the triazole cation-functionalized ionic liquids (TCFILs) by introducing multiple protic H sites into N-heterocyclic cations for enhancing NH_3 absorption. These TCFILs showed superhigh NH_3 mass capacity up to 0.365 g NH_3/g IL at 30 °C and 1 bar, which is the maximum among the reported absorbents. the TCFILs also exhibited excellent selectivity of NH_3/CO_2 up to 182 and recycling stability.

Process intensification methods are mainly divided into process synthesis of the unit and mixed operation integration, enhanced equipment design, and improved process mass transfer. In the gas-liquid absorption process, deep purification of absorbent is an effective method to reduce energy consumption. In recent years, more high-efficiency absorption and desorption equipment and technology have been designed to enhance the gas-liquid relationship. Zhan et al. [121] designed the stripping-enhancement process to purify the NH_3-containing industrial gas and this research provide a novel strategy and guidance for deep purification of NH_3 capture.

During the scale-up process of ammonia-carbon separation of ionic liquids, it is necessary to study the liquid flow rules inside the participating equipment, such as absorption columns and desorption columns. Using the mass-momentum conservation equation, the macroscopic bubble behavior and transfer laws in ionic liquids based on the molecular level could be obtained. So as to guide the optimal design of the internal components of the absorption column. Palomar et al. [122] made evaluation of over 50 ionic liquids from molecular simulation, gravimetric experiments and process analysis to analysis the thermodynamics and kinetics on the physical absorption of CO_2.

With the rapid development of the intelligent algorithms and widely application in chemical engineering, more research are concentrated on the machine learning-based ionic liquids solvent screen and design [123]. Song et al. [124] predicted the CO_2 solubility in ionic liquids using machine learning methods and the result showed reliable prediction on the CO_2 solubilities in ILs with the artificial neural network using group contribution methods. Wang et al. [125] employed the machine learning methods to screen the suitable solvents with support vector machine model for the ionic liquid-based CO2 capture from fuel gas. The result showed screening IL [EMIM][TCM] is the most suitable solvent for CO_2 separation from flue gas and having 12.9% economic cost saving compared to the common solvent [EMIM][Tf_2N]. As future trends of the machine learning in chemical engineering, mixed intelligence models and algorithms to obtain better prediction results with complex process and industrial problems [126].

7 Conclusion and future work

7.1 Conclusions

This work studied the full simulation package of the IL-based NH_3/CO_2 separation processes, two ionic liquid-based NH_3/CO_2 separation processes (IL-0 process and IL-En process) as well as NH_3 recovery process by water scrubbing process. Thermodynamic models related to IL-0 and IL-En NH_3/CO_2 separation processes were developed. The estimated thermodynamic result shows a good accordance with experimental data. Then with the thermodynamic models, the energy consumption and economic performance of the different separation processes were evaluated using process simulation and sensitivity analysis.

A complete HEN was designed for all process options to optimize energy usage. The HENs contributed to significant energy savings. In addition, compared to the base case (benchmark) case, the HEN process could reduce the TSC about 2.88 % of IL-0 process. Finally, an economic comparison between IL-0, IL-En and WS was conducted. The IL-0 process separation cost was decreased 60% of that of WS process. The IL-En process could have even better performance in aspect of energy and separation cost and can decrease the TSC of 4.82 % compared to that of IL-0 process. Both of the studied ionic liquid processes can realize energy saving, which provides a perspective separation technology NH_3/CO_2 separation in the future.

Next step, the MOO was carried out to separate NH_3 and CO_2 using the ionic liquid in this work. After the sensitivity analysis based on ethnic-energy-economic, the change of pressure of absorption, ionic liquid flow rate, and pressure of Flash 2 are three key sensitive decision variables with the objective functions. After the MOO, the result showed that absorption pressure and the total usage of solvent affect TSC. In addition, the pressure of absorption and flow rate of ionic liquid have conflict and balance with each other. The optimal case has the NH_3 mole concentration as 4627 ppm and TSC as 0.055 \$/Nm^3 tail gas. The lowest NH_3 mole concentration can be 1468 ppm. The lowest TSC case has a TSC of 0.052 \$/Nm^3 tail gas, which can decrease 5.45% of optimal case and 27.78% of case 2(high-performance case). The results showed that the effect of absorption pressure, IL flow rate, and desorption pressure is critical for SPEC and TSC. The optimization results support the optimal design and operation of the NH_3 and CO_2 separation process with ionic liquids considering technology, energy, and economic objectives.

The IL-based NH_3/CO_2 separation process dynamic control behavior evaluation was carried out. First, the dynamic fluctuation was defined based on the pilot-plant running history as the tail gas fluctuation of flow rate and NH_3 concentration at ±5%. Second, the conversion from steady-state to

dynamic mode was simulated in Aspen HYSYS, and detailed equipment sizes were calculated for dynamic running. Inlet stream controller setting parameters were chosen to guarantee the inventory stabilization of the process without a specific control scheme. Third, the step test was carried out with tail gas fluctuation of flow rate and NH_3 concentration about the dynamic open loop simulation with flash liquid level control. Last, the potential dynamic control strategy was proposed for future dynamic control investigation.

The simulation results showed that NH_3 concentration and NH_3 recovery have a positive response with more tail gas and NH_3 in the system. With the analysis of the parameter behavior on the different tail gas fluctuations, basic dynamic control could be built to guarantee stabilization with different fluctuations and provide support to the new technology industrial application.

7.2 Future work

Considering the increasingly stringent emission standards of tail gas containing NH_3, in order to further promote the industrial application of IL-based technologies, the following suggestions are put forward:

(1) Combined with molecular simulation methods, speed up the research and development of absorbents/catalysts/adsorbents containing NH_3 gas, obtain media with good separation effect on NH_3, and promote the development of low-energy and high-efficiency purification processes.
(2) Combining process simulation and optimization methods, comprehensively analyze and evaluate the purification process system, realize the comprehensive utilization of energy and materials in the system, obtain a process operation plan with low energy consumption, good economy, and low CO_2 emissions, and form a low-cost, green, and energy-saving new NH_3-containing tail gas purification technology.
(3) As a green medium, ionic liquid needs to evaluate the environmental impact of the solvent itself, and incorporate the environmental impact of the process into the evaluation scope of multi-objective optimization to gain a more detailed understanding of the new process.
(4) In terms of process simulation optimization evaluation, at the beginning of process evaluation modeling, artificial intelligence methods such as machine learning can be combined to carry out fitting analysis on relevant experimental data to construct an accurate physical property prediction model, which can be coupled with the evaluation process to provide environmental evaluation Provide basic data to improve the efficiency of process evaluation.
(5) For the dynamic control of this new process, based on the stable running of the regulatory control, the closed dynamic control loop will be designed and made the PID layer control regard on product quality control. The advanced dynamic control scheme can also be designed

and researched in order to give full support to this new IL-based technology.

Taking into account the increasingly stringent emission standards of NH_3-containing tail gas and the needs of domestic enterprises, it is necessary to speed up the research on the purification process of NH_3-containing tail gas, improve different purification processes, and develop a high-efficiency purification and recovery process of NH_3-containing tail gas. In addition, the cooperation between enterprises and scientific research units should be actively promoted to promote the development of new NH_3-containing tail gas purification technology, so as to realize the industrialization, scale, low cost and green application of my country's tail gas purification technology.

References

[1] Y. Duan, G. Zhan, F. Chang, S. Shi, S. Zeng, H. Dong, J. Abildskov, J. Kjøbsted Huusom, X. Zhang, Process simulation and evaluation for NH_3/CO_2 separation from melamine tail gas with protic ionic liquids, Sep. Purif. Technol., 288 (2022) 120680.
[2] Y. Duan, G. Zhan, F. Chang, S. Shi, J. Abildskov, J.K. Huusom, X. Zhang, Multi-objective optimization of NH3 and CO2 separation with ionic liquid process, in: Y. Yamashita, M. Kano (Eds.) Computer Aided Chemical Engineering, Elsevier, 2022, pp. 1147-1152.
[3] L. Kang, L. Shi, Q. Zeng, B. Liao, B. Wang, X. Guo, Melamine resin-coated lignocellulose fibers with robust superhydrophobicity for highly effective oil/water separation, Sep. Purif. Technol., 279 (2021) 119737.
[4] X. Zhang, Y. Wu, X. Liu, S. Reis, J. Jin, U. Dragosits, M. Van Damme, L. Clarisse, S. Whitburn, P.F. Coheur, B. Gu, Ammonia Emissions May Be Substantially Underestimated in China, Environmental science & technology, 51 (2017) 12089-12096.
[5] W. Zhou, J. Wang, P. Chen, C. Ji, Q. Kang, B. Lu, K. Li, J. Liu, R. Ruan, Bio-mitigation of carbon dioxide using microalgal systems: Advances and perspectives, Renewable and Sustainable Energy Reviews, 76 (2017) 1163-1175.
[6] E.E. Agency(EEA), Ammonia (NH3) emissions, in: E.E. Agency(EEA) (Ed.), 2015, 2015.
[7] U.S.E.P. Agency, 2017 National Emissions Inventory (NEI) Technical Support Document (TSD), in: U.S.E.P. Agency (Ed.), 2017.
[8] M.o.E.a.E.o.t.P.s.R.o. China, 2020 China Ecological Environment Statistical Annual Report, in: M.o.E.a.E.o.t.P.s.R.o. China (Ed.), 202.
[9] L. Kong, X. Tang, J. Zhu, Z. Wang, Y. Pan, H. Wu, L. Wu, Q. Wu, Y. He, S. Tian, Y. Xie, Z. Liu, W. Sui, L. Han, G. Carmichael, Improved Inversion of Monthly Ammonia Emissions in China Based on the Chinese Ammonia Monitoring Network and Ensemble Kalman Filter, Environmental science & technology, 53 (2019) 12529-12538.
[10] X. Zhang, Y. Wu, X. Liu, S. Reis, J. Jin, U. Dragosits, M. Van Damme, L. Clarisse, S. Whitburn, P.-F. Coheur, B. Gu, Ammonia Emissions May Be Substantially Underestimated in China, Environmental science & technology, 51 (2017) 12089-12096.
[11] M. Crippa, E. Solazzo, G. Huang, D. Guizzardi, E. Koffi, M. Muntean, C. Schieberle, R. Friedrich, G. Janssens-Maenhout, High resolution temporal profiles in the Emissions Database for Global Atmospheric Research, Scientific Data, 7 (2020) 121.
[12] J. Lelieveld, J.S. Evans, M. Fnais, D. Giannadaki, A. Pozzer, The contribution of outdoor air pollution sources to premature mortality on a global scale, Nature, 525 (2015) 367-371.
[13] M. Sillanpää, R. Hillamo, S. Saarikoski, A. Frey, A. Pennanen, U. Makkonen, Z. Spolnik, R. Van Grieken, M. Braniš, B. Brunekreef, M.-C. Chalbot, T. Kuhlbusch, J. Sunyer, V.-M. Kerminen, M. Kulmala, R.O. Salonen, Chemical composition and mass closure of particulate matter at six urban sites in Europe, Atmospheric Environment, 40 (2006) 212-223.
[14] T. Selleri, A. Melas, P. Bonnel, R. Suarez-Bertoa, NH3 and CO Emissions from Fifteen Euro 6d and Euro 6d-TEMP Gasoline-Fuelled Vehicles, 12 (2022) 245.
[15] M.o.E.a.E.o.t.P.s.R.o. China, Letter on Soliciting Opinions on the National Environmental Protection Standard "Emission Standard of Odor Pollutants (Draft for Comment)", in: M.o.E.a.E.o.t.P.s.R.o. China (Ed.), 2018.

[16] D.o.E.a.E.o.S. Province, Shandong: Emission Standards of Air Pollutants for Thermal Power Plants (DB37/664—2019)-Industry News-News-Shandong Thermal Power Design Institute, in: D.o.E.a.E.o.S. Province (Ed.), 2019.
[17] M. intelligence, MELAMINE MARKET - GROWTH, TRENDS, COVID-19 IMPACT, AND FORECASTS (2023 - 2028), in, Mordor intelligence, 2022.
[18] M.R. Consulting, Melamine: 2022 World Market Outlook and Forecast up to 2031, in, 2022.
[19] S.P.G.C. Insights, Melamine Chemical Economics Handbook, in, 2020.
[20] I.a. info, 2020 China Melamine Market Research Report - Research on Market Operation Status and Development Prospects, in, 2022.
[21] V. Danielik, J. Jurišová, P. Fellner, R. Štefancová, M. Kučera, Absorption of ammonia in the melt of ammonium nitrate, Chemical Papers, 72 (2018) 3119-3128.
[22] R. Sander, Compilation of Henry's law constants (version 4.0) for water as solvent, Atmos. Chem. Phys., 15 (2015) 4399-4981.
[23] M. Higa, E.Y. Yamamoto, J.C.D.d. Oliveira, W.A.S. Conceição, Evaluation of the integration of an ammonia-water power cycle in an absorption refrigeration system of an industrial plant, Energy Conversion and Management, 178 (2018) 265-276.
[24] J.A. Joshi, J.A. Hogan, R.M. Cowan, P.F. Strom, M.S. Finstein, Biological removal of gaseous ammonia in biofilters: space travel and earth-based applications, Journal of the Air & Waste Management Association (1995), 50 (2000) 1647-1654.
[25] Y.-C. Chung, C. Huang, C.-P. Tseng, Biological elimination of H2S and NH3 from wastegases by biofilter packed with immobilized heterotrophic bacteria, Chemosphere, 43 (2001) 1043-1050.
[26] T. Lan, Y. Zhao, J. Deng, J. Zhang, L. Shi, D. Zhang, Selective catalytic oxidation of NH3 over noble metal-based catalysts: state of the art and future prospects, Catalysis Science & Technology, 10 (2020) 5792-5810.
[27] C. Yeom, Y. Kim, Adsorption of ammonia using mesoporous alumina prepared by a templating method, Environmental Engineering Research, 22 (2017) 401-406.
[28] B. Yang, L. Bai, S. Zeng, S. Luo, L. Liu, J. Han, Y. Nie, X. Zhang, S. Zhang, NH3 separation membranes with self-assembled gas highways induced by protic ionic liquids, Chemical Engineering Journal, 421 (2021) 127876.
[29] F. Li, Q. Zhang, P. Chen, Y. Wang, C. Wei, W. Zhang, Melamine exhaust treatment process and equipment in, China, 2009.
[30] Y. Tang, Y. Gong, D. Kun, Y. Mo, D. Rao, X. Kuang, A melamine tail gas treatment system, in, China, 2013.
[31] P. Walden, Molecular weights and electrical conductivity of several fused salts, Bull. Russian Acad. Sci., (1914) 405–422.
[32] H.L. Chum, V.R. Koch, L.L. Miller, R.A.J.J.o.t.A.C.S. Osteryoung, Electrochemical scrutiny of organometallic iron complexes and hexamethylbenzene in a room temperature molten salt, 97 (1975) 3264-3265.
[33] J.S. Wilkes, J.A. Levisky, R.A. Wilson, C.L. Hussey, Dialkylimidazolium chloroaluminate melts: a new class of room-temperature ionic liquids for electrochemistry, spectroscopy and synthesis, Inorganic Chemistry, 21 (1982) 1263-1264.
[34] J.S. Wilkes, M.J. Zaworotko, Air and water stable 1-ethyl-3-methylimidazolium based ionic liquids, Journal of the Chemical Society, Chemical Communications, (1992) 965-967.
[35] Introduction: Ionic Liquids, Chemical Reviews, 117 (2017) 6633-6635.

[36] L. Zhang, H. Dong, S. Zeng, Z. Hu, S. Hussain, X. Zhang, An Overview of Ammonia Separation by Ionic Liquids, Industrial & Engineering Chemistry Research, 60 (2021) 6908-6924.
[37] S. Zeng, Y. Cao, P. Li, X. Liu, X. Zhang, Ionic liquid–based green processes for ammonia separation and recovery, Current Opinion in Green and Sustainable Chemistry, 25 (2020) 100354.
[38] O.M. Basha, Y.J. Heintz, M.J. Keller, D.R. Luebke, K.P. Resnik, B.I. Morsi, Development of a Conceptual Process for Selective Capture of CO2 from Fuel Gas Streams Using Two TEGO Ionic Liquids as Physical Solvents, Industrial & Engineering Chemistry Research, 53 (2014) 3184-3195.
[39] M.B. Shiflett, D.W. Drew, R. Cantini, A.J.E. Yokozeki, Fuels, Carbon Dioxide Capture Using Ionic Liquid 1-Butyl-3-methylimidazolium Acetate, 24 (2010) 5781-5789.
[40] Y. Huang, H. Dong, X. Zhang, C. Li, S. Zhang, A new fragment contribution-corresponding states method for physicochemical properties prediction of ionic liquids, AIChE Journal, 59 (2013) 1348-1359.
[41] E. Ruiz, V.R. Ferro, J. de Riva, D. Moreno, J. Palomar, Evaluation of ionic liquids as absorbents for ammonia absorption refrigeration cycles using COSMO-based process simulations, Applied Energy, 123 (2014) 281-291.
[42] C.A.o. Sciences, https://www.cas.cn/syky/202205/t20220517_4834888.shtml, in, 2022.
[43] U.G. Assembly, Transforming our world : the 2030 Agenda for Sustainable Development, in: D.o.e.a.s. affairs (Ed.), 2015, pp. 1–41.
[44] A. Yokozeki, M.B. Shiflett, Ammonia Solubilities in Room-Temperature Ionic Liquids, Industrial & Engineering Chemistry Research, 46 (2007) 1605-1610.
[45] W.-J. Jiang, F.-Y. Zhong, Y. Liu, K. Huang, Effective and Reversible Capture of NH3 by Ethylamine Hydrochloride Plus Glycerol Deep Eutectic Solvents, ACS Sustain. Chem. Eng., 7 (2019) 10552-10560.
[46] K. Li, H. Fang, X. Duan, D. Deng, Efficient uptake of NH3 by dual active sites NH4SCN-imidazole deep eutectic solvents with low viscosity, Journal of Molecular Liquids, 339 (2021) 116724.
[47] E.l. Pagans, X. Font, A. Sánchez, Biofiltration for ammonia removal from composting exhaust gases, Chemical Engineering Journal, 113 (2005) 105-110.
[48] J. Gong, R.A. Ojifinni, T.S. Kim, J.M. White, C.B. Mullins, Selective Catalytic Oxidation of Ammonia to Nitrogen on Atomic Oxygen Precovered Au(111), Journal of the American Chemical Society, 128 (2006) 9012-9013.
[49] M. Karatok, E.I. Vovk, A.V. Koc, E. Ozensoy, Selective Catalytic Ammonia Oxidation to Nitrogen by Atomic Oxygen Species on Ag(111), The Journal of Physical Chemistry C, 121 (2017) 22985-22994.
[50] K.N. Ruckart, Y. Zhang, W.M. Reichert, G.W. Peterson, T.G.J.I. Glover, E.C. Research, Sorption of Ammonia in Mesoporous-Silica Ionic Liquid Composites, 55 (2016) 12191-12204.
[51] H.K. Knuutila, R. Rennemo, A.F. Ciftja, New solvent blends for post-combustion CO_2 capture, Green Energy & Environment, 4 (2019) 439-452.
[52] H. Weiss, Rectisol wash for purification of partial oxidation gases, Gas Separation & Purification, 2 (1988) 171-176.
[53] N. Ghasem, Chapter 21 - CO2 removal from natural gas, in: M.R. Rahimpour, M. Farsi, M.A. Makarem (Eds.) Advances in Carbon Capture, Woodhead Publishing, 2020, pp. 479-501.
[54] M. Stec, A. Tatarczuk, L. Więcław-Solny, A. Krótki, T. Spietz, A. Wilk, D. Śpiewak, Demonstration of a post-combustion carbon capture pilot plant using amine-based solvents at the

Aaziska Power Plant in Poland, Clean technologies and Environmental Policy, 18 (2016) 151-160.
[55] R. Sakwattanapong, A. Aroonwilas, A. Veawab, Behavior of Reboiler Heat Duty for CO2 Capture Plants Using Regenerable Single and Blended Alkanolamines, Industrial & Engineering Chemistry Research, 44 (2005) 4465-4473.
[56] M. Xiao, L. Wang, Y. Wu, C. Cheng, L. Chen, H. Chen, C. Xue, Hybrid dilute sulfuric acid and aqueous ammonia pretreatment for improving butanol production from corn stover with reduced wastewater generation, Bioresource technology, 278 (2019) 460-463.
[57] L. Marrone, P. Bertini, A process for the synthesis of urea, in, Casale SA, 2019.
[58] T. Shen, G. Zhu, Y. Yao, B. Yang, L. Ma, Carbonization method for co-production of ammonium bicarbonate through one-step melamine tail gas, in, Nantong Zixin Ind Co Ltd, 2011.
[59] G. Li, Q. Zhou, X. Zhang, LeiWang, S. Zhang, J. Li, Solubilities of ammonia in basic imidazolium ionic liquids, Fluid Phase Equilibria, 297 (2010) 34-39.
[60] W. Chen, S. Liang, Y. Guo, X. Gui, D. Tang, Investigation on vapor–liquid equilibria for binary systems of metal ion-containing ionic liquid [bmim]Zn2Cl5/NH3 by experiment and modified UNIFAC model, Fluid Phase Equilibria, 360 (2013) 1-6.
[61] S. Zeng, L. Liu, D. Shang, J. Feng, H. Dong, Q. Xu, X. Zhang, S. Zhang, Efficient and reversible absorption of ammonia by cobalt ionic liquids through Lewis acid–base and cooperative hydrogen bond interactions, Green Chemistry, 20 (2018) 2075-2083.
[62] D. Shang, X. Zhang, S. Zeng, K. Jiang, H. Gao, H. Dong, Q. Yang, S. Zhang, Protic ionic liquid [Bim][NTf_2] with strong hydrogen bond donating ability for highly efficient ammonia absorption, Green Chemistry, 19 (2017) 937-945.
[63] P. Li, D. Shang, W. Tu, S. Zeng, Y. Nie, L. Bai, H. Dong, X. Zhang, NH_3 absorption performance and reversible absorption mechanisms of protic ionic liquids with six-membered N-heterocyclic cations, Sep. Purif. Technol., 248 (2020) 117087.
[64] L. Luo, J. Li, X. Chen, X. Cao, Y. Liu, Z. Wu, X. Luo, C. Wang, Superhigh and reversible NH_3 uptake of cobaltous thiocyanate functionalized porous poly ionic liquids through competitive and cooperative interactions, Chemical Engineering Journal, 427 (2022) 131638.
[65] D. Deng, X. Deng, K. Li, H. Fang, Protic ionic liquid ethanolamine thiocyanate with multiple sites for highly efficient NH3 uptake and NH3/CO2 separation, Sep. Purif. Technol., 276 (2021) 119298.
[66] L. Yuan, X. Zhang, B. Ren, Y. Yang, Y. Bai, L. Bai, H. Gao, S. Zeng, Dual-functionalized protic ionic liquids for efficient absorption of NH3 through synergistically physicochemical interaction, 95 (2020) 1815-1824.
[67] Y. Chen, Y. Yao, X. Zhang, B. Ren, L. Wang, H. Dong, X. Tian, Simulation and Optimizaiton of Ammonia Recovery with Ionic Liquid from Purge Gas in Ammonia Synthesis Plant, The Chinese Journal of Process Engineering, 11 (2011) 644-651.
[68] X. Liu, Y. Chen, S. Zeng, X. Zhang, X. Liang, R. Gani, G.M. Kontogeorgis, Separation of NH_3/CO_2 from melamine tail gas with ionic liquid: Process evaluation and thermodynamic properties modelling, Sep. Purif. Technol., 274 (2021) 119007.
[69] S. Zeng, H. Dong, Y. Bai, X. Zhang, S. Zhang, New technology of ionic liquid-based NH_3/CO_2 separation from melamine tail gas, Green Chemical Engineering, 1 (2020) 5.
[70] G.P. Rangaiah, Z. Feng, A.F. Hoadley, Multi-Objective Optimization Applications in Chemical Process Engineering: Tutorial and Review, Processes, 8 (2020) 508.
[71] S. Sharma, G.P. Rangaiah, Mathematical Modeling, Simulation and Optimization for Process

Design, in: Chemical Process Retrofitting and Revamping, 2016, pp. 97-127.
[72] J. Fontalvo, Using user models in Matlab® within the Aspen Plus® interface with an Excel® link, Ingeniería e Investigación, 34 (2014) 39-43.
[73] G. Pour, Software Component Technologies: JavaBeans and ActiveX, in: Proceedings of the Technology of Object-Oriented Languages and Systems, IEEE Computer Society, Los Alamitos, CA, USA, 1998.
[74] N. Asprion, S. Blagov, O. Ryll, R. Welke, A. Winterfeld, A. Dittel, M. Bortz, K.-H. Küfer, J. Burger, A. Scheithauer, H. Hasse, Pareto-Navigation in Chemical Engineering, in: E.N. Pistikopoulos, M.C. Georgiadis, A.C. Kokossis (Eds.) Computer Aided Chemical Engineering, Elsevier, 2011, pp. 422-426.
[75] S. Gass, T. Saaty, The computational algorithm for the parametric objective function, Naval Research Logistics Quarterly, 2 (1955) 39-45.
[76] A.M. Geoffrion, Solving Bicriterion Mathematical Programs, Operations Research, 15 (1967) 39-54.
[77] C.A.C. Coello, G.B. Lamont, D.A.V. Veldhuizen, Evolutionary Algorithms for Solving Multi-Objective Problems, Springer New York, NY, 2007.
[78] K. Deb, A. Pratap, S. Agarwal, T.A.M.T. Meyarivan, A fast and elitist multiobjective genetic algorithm: NSGA-II, IEEE Transactions on Evolutionary Computation, 6 (2002) 182-197.
[79] S. Lin, NGPM -- A NSGA-II Program in Matlab v1.4 in, 2022.
[80] PyGMO, in, 2019.
[81] L.E. Perez, P. Sarkar, A. Rajendran, Experimental validation of multi-objective optimization techniques for design of vacuum swing adsorption processes, Sep. Purif. Technol., 224 (2019) 553-563.
[82] J. Yan, J. Liu, J. Ren, Y. Wu, X. Li, T. Sun, L. Sun, Design and multi-objective optimization of hybrid reactive-extractive distillation process for separating wastewater containing benzene and isopropanol, Sep. Purif. Technol., 290 (2022) 120915.
[83] Y. Wang, X. Liu, H. Zhang, Y. Liu, P. Cui, Z. Zhu, Y. Ma, J. Gao, Comprehensive 3E analysis and multi-objective optimization of a novel process for CO_2 capture and separation process from syngas, Journal of Cleaner Production, 274 (2020) 122871.
[84] S. MohsenHosseini-Ardali, MajidHazrati-Kalbibaki, MoslemFattahi, FerencLezsovits, Multi-objective optimization of post combustion CO_2 capture using methyldiethanolamine (MDEA) and piperazine (PZ) bi-solvent, Energy, 211 (2020) 119035.
[85] M. Panu, K. Topolski, S. Abrash, M. M.El-Halwagi, CO_2 footprint reduction via the optimal design of Carbon-Hydrogen-Oxygen SYmbiosis Networks (CHOSYNs), Chemical Engineering Science, 203 (2019) 1-11.
[86] E. Martelli, M. Gatti, F. Maréchal, S. Consonni, Multi-objective Optimization of a Selexol® Process for the Selective Removal of CO_2 and H_2S from Coal-derived Syngas, in: Proceedings of ECOS Internetional Conference, Pau, France, 2015.
[87] S. Ma, X. Shang, M. Zhu, J. Li, L. Sun, Design, optimization and control of extractive distillation for the separation of isopropanol-water using ionic liquids, Sep. Purif. Technol., 209 (2019) 833-850.
[88] X. Tian, X. Zhang, S. Zeng, Y. Xu, Y. Yao, Y. Chen, L. Huang, Y. Zhao, S. Zhang, Process Analysis and Multi-Objective Optimization of Ionic Liquid-Containing Acetonitrile Process to Produce 1,3-Butadiene, Chemical Engineering & Technology, 34 (2011) 927-936.

[89] G. Zhan, F. Cao, L. Bai, F. Chang, B. Zhou, Y. Duan, S. Zeng, H. Dong, Z. Li, X. Zhang, Process Simulation and Optimization of Ammonia-Containing Gas Separation and Ammonia Recovery with Ionic Liquids, ACS Sustain. Chem. Eng., 9 (2021) 312-325.
[90] S. Skogestad, Control structure design for complete chemical plants, Computers & Chemical Engineering, 28 (2004) 219-234.
[91] R. Jagtap, N. Kaistha, S. Skogestad, Economic Plantwide Control Over a Wide Throughput Range: A Systematic Design Procedure, 59 (2013) 2407-2426.
[92] P. Dorato, A historical review of robust control, IEEE Control Systems Magazine, 7 (1987) 44-47.
[93] M. Ellis, H. Durand, P.D. Christofides, A tutorial review of economic model predictive control methods, Journal of Process Control, 24 (2014) 1156-1178.
[94] M. Heidarinejad, J. Liu, P.D. Christofides, Economic model predictive control of nonlinear process systems using Lyapunov techniques, 58 (2012) 855-870.
[95] J. Li, L. Li, R. Li, Z. Yang, Z. Ma, L. Sun, N. Zhang, Investigation of multi-objective optimization for integrating design and control of ionic liquid-based extractive distillation, Chemical Engineering Research and Design, 170 (2021) 134-146.
[96] D. Valencia-Marquez, A. Flores-Tlacuahuac, L. Ricardez-Sandoval, Technoeconomic and dynamical analysis of a CO2 capture pilot-scale plant using ionic liquids, Industrial & Engineering Chemistry Research, 54 (2015) 11360–11370.
[97] K.M.S. Salvinder, H. Zabiri, S.A. Taqvi, M. Ramasamy, F. Isa, N.E.M. Rozali, H. Suleman, A. Maulud, A.M. Shariff, An overview on control strategies for CO2 capture using absorption/stripping system, Chemical Engineering Research and Design, 147 (2019) 319-337.
[98] S. Gao, C. Bo, J. Li, C. Niu, X. Lu, Multi-objective optimization and dynamic control of biogas pressurized water scrubbing process, Renewable Energy, 147 (2020) 2335-2344.
[99] M. Hossein Sahraei, L.A. Ricardez-Sandoval, Controllability and optimal scheduling of a CO2 capture plant using model predictive control, International Journal of Greenhouse Gas Control, 30 (2014) 58-71.
[100] Y.-J. Lin, T.-H. Pan, D.S.-H. Wong, S.-S. Jang, Y.-W. Chi, C.-H. Yeh, Plantwide Control of CO2 Capture by Absorption and Stripping Using Monoethanolamine Solution, Industrial & Engineering Chemistry Research, 50 (2011) 1338-1345.
[101] X. He, Y. Wang, D. Bhattacharyya, F.V. Lima, R. Turton, Dynamic modeling and advanced control of post-combustion CO2 capture plants, Chemical Engineering Research and Design, 131 (2018) 430-439.
[102] J. Palomar, M. Gonzalez-Miquel, A. Polo, F. Rodriguez, Understanding the Physical Absorption of CO2 in Ionic Liquids Using the COSMO-RS Method, Industrial & Engineering Chemistry Research, 50 (2011) 3452-3463.
[103] Z. Lei, C. Dai, W. Wang, B. Chen, UNIFAC model for ionic liquid-CO2 systems, 60 (2014) 716-729.
[104] R. Anantharaj, T. Banerjee, COSMO-RS-Based Screening of Ionic Liquids as Green Solvents in Denitrification Studies, Industrial & Engineering Chemistry Research, 49 (2010) 8705-8725.
[105] J. Han, C. Dai, G. Yu, Z. Lei, Parameterization of COSMO-RS model for ionic liquids, Green Energy & Environment, 3 (2018) 247-265.
[106] D. Shang, L. Bai, S. Zeng, H. Dong, H. Gao, X. Zhang, S. Zhang, Enhanced NH_3 capture by imidazolium-based protic ionic liquids with different anions and cation substituents, Journal of

Chemical Technology & Biotechnology, 93 (2018) 1228-1236.
[107] W. Tu, L. Bai, S. Zeng, H. Gao, S. Zhang, X. Zhang, An ionic fragments contribution-COSMO method to predict the surface charge density profiles of ionic liquids, Journal of Molecular Liquids, 282 (2019) 292-302.
[108] H. Chen, Y. He, J. Zhu, H. Alias, Y. Ding, P. Nancarrow, C. Hardacre, D. Rooney, C. Tan, Rheological and heat transfer behaviour of the ionic liquid, [C4mim][NTf2], International Journal of Heat and Fluid Flow, 29 (2008) 149-155.
[109] G. Prasad, K. Muralidhar Reddy, R. Padamasuvarna, T. Madhu Mohan, T. Vijaya Krishna, V. Ramesh Kumar, Thermophysical properties of 1-butyl-3-methylimidazolium bis (trifluoromethylsulfonyl) imide with 2-ethoxyethanol from T=(298.15 to 323.15) K at atmospheric pressure, Journal of Molecular Liquids, 251 (2018) 335-344.
[110] X. Liu, Y. Huang, Y. Zhao, R. Gani, X. Zhang, S.J. Zhang, Ionic Liquid Design and Process Simulation for Decarbonization of Shale Gas, Industrial & Engineering Chemistry Research, 55 (2017) 5931-5944.
[111] C.-C. Chen, L.B. Evans, A local composition model for the excess Gibbs energy of aqueous electrolyte systems, Aiche Journal, 32 (1986) 444-454.
[112] Aspen plus V11, in, Aspen Technology Inc., 2017.
[113] W.L. Luyben, Setting Up A Steady-State Simulation, in: Distillation Design and Control Using Aspen™ Simulation, 2013, pp. 39-80.
[114] S.M. Walas, Chemical Process Equipemnt: Selection and Design, Butterworth-Heinemann, Newton, MA, 1990.
[115] T. Ma, J. Wang, Z. Du, A.A. Abdeltawab, A.M. Al-Enizi, X. Chen, G. Yu, A process simulation study of CO_2 capture by ionic liquids, International Journal of Greenhouse Gas Control, 58 (2017) 223-231.
[116] C.K. Seng, G.P. Rangaiah, Multi-Objective Optimization in Food Engineering, Taylor and Francis/CRC Press, Boca Raton, 2009.
[117] A. Konak, D. W.Coit, A. E.Smith, Multi-objective optimization using genetic algorithms: A tutorial, Reliability Engineering & System Safety, 91 (2006) 992-1007.
[118] G.P.Rangaiah, S. Sharma, H.W.Lin, Evaluation of two termination criteria in evolutionary algorithms for multi-objective optimization of complex chemical processes, Chemical Engineering Research and Design, 124 (2017) 58-65.
[119] C.A.o. Sciences, https://www.cas.cn/syky/202006/t20200623_4750917.shtml, in, 2020.
[120] X. Sun, G. Li, S. Zeng, L. Yuan, L. Bai, X. Zhang, Ultra-high NH3 absorption by triazole cation-functionalized ionic liquids through multiple hydrogen bonding, Sep. Purif. Technol., 307 (2023) 122825.
[121] G. Zhan, F. Cao, J. Chen, Z. Chen, Y. Duan, F. Chang, S. Zeng, Y. Bai, Z. Li, X. Zhang, J. Li, Comprehensive evaluation of an ionic liquid based deep purification process for NH3-containing industrial gas, Journal of Environmental Sciences, 136 (2024) 698-708.
[122] J. Palomar, M. Larriba, J. Lemus, D. Moreno, R. Santiago, C. Moya, J. de Riva, G. Pedrosa, Demonstrating the key role of kinetics over thermodynamics in the selection of ionic liquids for CO2 physical absorption, Sep. Purif. Technol., 213 (2019) 578-586.
[123] Z. Wang, Z. Song, T. Zhou, Machine Learning for Ionic Liquid Toxicity Prediction, 9 (2021) 65.
[124] Z. Song, H. Shi, X. Zhang, T. Zhou, Prediction of CO2 solubility in ionic liquids using

machine learning methods, Chemical Engineering Science, 223 (2020) 115752.
[125] K. Wang, H. Xu, C. Yang, T. Qiu, Machine learning-based ionic liquids design and process simulation for CO2 separation from flue gas, Green Energy & Environment, 6 (2021) 432-443.
[126] A. Slowik, H. Kwasnicka, Evolutionary algorithms and their applications to engineering problems, Neural Computing and Applications, 32 (2020) 12363-12379.

Appendix

Table S1 Total separation cost (TSC) calculation

Item	Calculation Composition
TSC	Total operating cost (TOC), Annualized capital cost (ACC)
TOC	Variable operating cost (VOC), Fixed operating cost (FOC)
ACC	Total capital investment (TCI)
TCI	Fixed capital investment (FCI), Working capital (WC), Startup cost (SUC), Initial solvent cost (ISC)
TCC	Total operation cost (TOC), Annual capital cost (ACC)
FCI	Direct cost (DC), Indirect cost (IC)
DC, IC	Purchased equipment cost (PEC) with a coefficient of the percentage

Table S2 TOC calculation

Item	Equation
TOC	TOC=VOC+TOC

Table S3 The price of utility

Item	Price	Value
LP steam	$/t	20.29
Cooling water	$/t	0.07
Electric	$/kWh	0.07
Solvent	$/t	14286.00

Table S4 VOC calculation

Item	Value
LP steam cost	$20.29\times n_{LPst}$
Cooling water cost	$0.07\times n_{cw}$
Electric cost	$0.07\times n_{ele}$
VOC	Total cost of VOC

Table S5 FOC calculation

Item	Percentage
Local tax cost	1%FCI
Insurance cost	1%FCI
Maintenance cost	3%FCI
Operating labor cost	291060
Laboratory cost	20%OL
Supervision cost	20%OL
Plant overhead cost	50%OL
Operating supply cost	15%M
Administrative cost	15%OL
Distribution and marketing cost	0.5%TOC
R&D cost	5%TOC
FOC	Total cost of FOC

Table S6 The TCI calculation

Item	Equation
FCI	FCI=DC+IC
TCI	TCI=FCI+WC+SC+ISC = FCI×(1+0.16)+ISC

Table S7 The DC and IC calculation

DC	Percentage of PEC
Purchased equipment cost (PEC)	100
Purchased equipment installation cost	10
Instrumentation and control cost	20
Pipe cost	30
Electrical cost	5
Building and building services cost	10
Yard improvements cost	10
Land cost	5
Other cost	2
DC=PEC× (1+0.92)	Total cost of DC
IC	Percentage of DC

Engineering and supervision cost	15
Contingency cost	11
Procurement cost	2
IC=0.28×DC	Total cost of IC

Table S8 Equipment cost of separation process in 1985

Item	Calculation Equation
Absorption column / $	$C=f_1\times C_b+V_p\times C_p+C_{p1}$ $C_{p1}=246.4\times D^{0.7396}L^{0.7068}$ $C_b=\exp(6.629+0.1826\times \ln W+0.02297\times(\ln W)^2$
Distillation column / $	$C=f_1\times C_b+N\times f_2\times f_3\times f_4\times C_t\times C_p+C_{p1}$ $C_{p1}=204.9\times D^{0.6332}L^{0.8016}$ $C_t=375.8\exp(0.1739D)$ $C_b=\exp(7.123+0.1478\times \ln W+0.02488\times(\ln W)^2$
Heat exchanger / $	$C=f_C\times C_b$ $C_b=\exp(8.821-0.30863\times \ln A+0.068\times(\ln A)^2$
Liquid pump / $	$C=F_mF_tC_b$ $C_b=1.55\times\exp(8.833-0.6019(\ln QH^{0.5})+0.0519(\ln QH^{0.5})^2$
Vacuum pump / K$	$C=8.15\times(0.1333X)^{1.03}$
Compressor / K$	$C=6.49\times(HP)^{0.62}$
Flash tank / $	$C=F_m\times C_b+C_a$ $C_b=\exp(8.571-0.2330(\ln W)+0.04333(\ln W)^2)$ $C_a=1370\times D^{0.2029}$

*Vp is volume of packing (cuft), Cp is cost of packing ($/cuft), ; HP is equipment consumption (HP), A is exchanger area (sqft), X is the ratio of pumping speed and suction pressure (lb air/hr·kPa), Q is volume flow (gpm), H is pressure head (ft); f1, f2, f3, f4, fc, Fm, FT are the coefficient of equipment;

Table 9 Result of introducing a heat exchanger network for the IL-0 process.

Item		Value	Unit
Base case	Heating	1110	kW
	Cooling	2132	kW
	Heating exchange area	770	m^2
HEN	Heating	561	kW
	Cooling	1631	kW
	Heating exchange area	867	m^2

Table S10 Result of introducing a heating exchanger network for WS process

Item		Value	Unit
Base case	Heating	11446	kW
	Cooling	11174	kW
	Heating exchange Area	817	m^2
HEN	Heating	11375	kW
	Cooling	7822	kW
	Heating exchange Area	848	m^2

Table S11 The utilities cost distribution in WS, IL-0 and IL-En processes

	Electricity	Cooling water	Heat Stream LP
WS	13.13%	5.88%	80.99%
IL-0	73.03%	10.07%	16.90%
IL-En	79.81%	6.37%	13.82%

Table S12 Operation evaluation results of WS, IL-0 and IL-En processes

Item	WS	IL-0	IL-En
Heating utility, kW	11375.00	560.63	398.92
Cooling utility, kW	7821.61	1631.33	1244.41
Electricity utility, kW	1001.79	897.84	893.58
Total equivalent energy penalty, $kJ \cdot Nm^{-3}$ waste gas	4004.22	879.16	830.25

Table S13 Equipment cost of IL-0 process

Equipment	Modified Cost $	Percentage %	Initial Cost $	Percentage %
Absorption column	50263	2.43	50263	2.59
Heat exchanger	95730	4.63	87594	4.51
Liquid pump	36655	1.77	36655	1.89
Flash tank	509781	24.67	509781	26.22
Feed compressor	431765	20.90	430718	22.16
Vacuum pump	941800	45.59	828936	42.64
Sum	2065993	100.00	1943946	100.00

Table S14 Equipment cost of IL-En process

Equipment	Modified Cost $	Percentage %	Initial Cost $	Percentage %
Absorption column	46088	2.34	46088	2.37
Heat exchanger	96222	4.88	96222	4.95
Liquid pump	66518	3.38	66518	3.42
Flash tank	509781	25.87	509781	26.23
Feed compressor	408147	20.71	408147	21.00
Vacuum pump	811476	41.18	784134	40.35
Stripping column	32399	1.64	32399	1.67
Sum	1970630	100.00	1943288	100.00

Table S15 Equipment cost of WS process

Equipment	Modified Cost $	Percentage %	Initial Cost $	Percentage %
Absorption column	83506	3.92	83506	4.00
Heat exchanger	242223	11.38	201993	9.68
Liquid pump	57926	2.72	57926	2.78
Flash tank	238901	11.23	238901	11.44
Compressor	446552	20.99	446552	21.39
Distillation	1058517	49.75	1058517	50.71
Sum	2127626	100.00	2087396	100.00

Table S16 Hydraulics performance of absorption column tray

Tray	Dry hole DP(kPa)	Static Head(kPa)	Height over weir(mm)	Dry hole DP(mm)	Liq Hght on Tray(mm)	Residence time(secs)
1	0.09	0.88	0.00	6.40	50.00	56.83
2	0.09	0.88	0.00	6.52	50.00	56.73
3	0.09	0.96	0.00	6.75	50.00	30.77
4	0.11	0.96	0.00	8.14	50.00	30.48
5	0.18	0.95	0.00	13.22	50.00	29.53
6	0.26	0.93	0.00	19.76	50.00	28.52
7	0.31	0.92	0.00	23.38	50.00	28.08

Table S17 Hydraulics performance of stripping column tray

Tray	Dry hole DP(kPa)	Static Head(kPa)	Height over weir(mm)	Dry hole DP(mm)	Liq Hght on Tray(mm)	Residence time(secs)
1	0.014	0.87	0.00	1.00	50.00	31.83
2	0.014	0.87	0.00	1.03	50.00	31.81

3	0.014	0.87	0.00	1.06	50.00	31.79
4	0.014	0.84	0.00	1.00	50.00	30.50

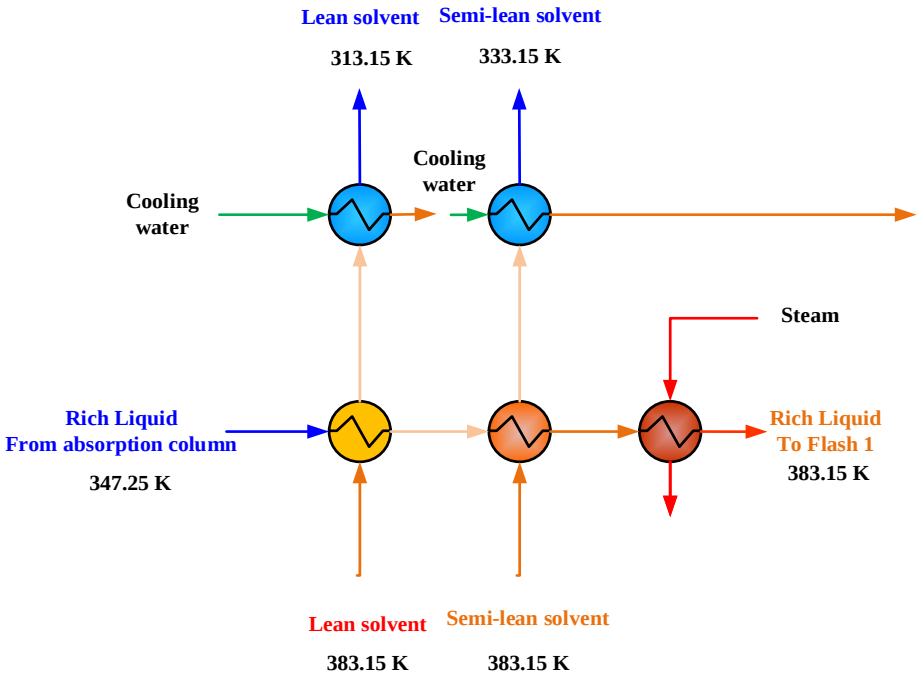

(a)

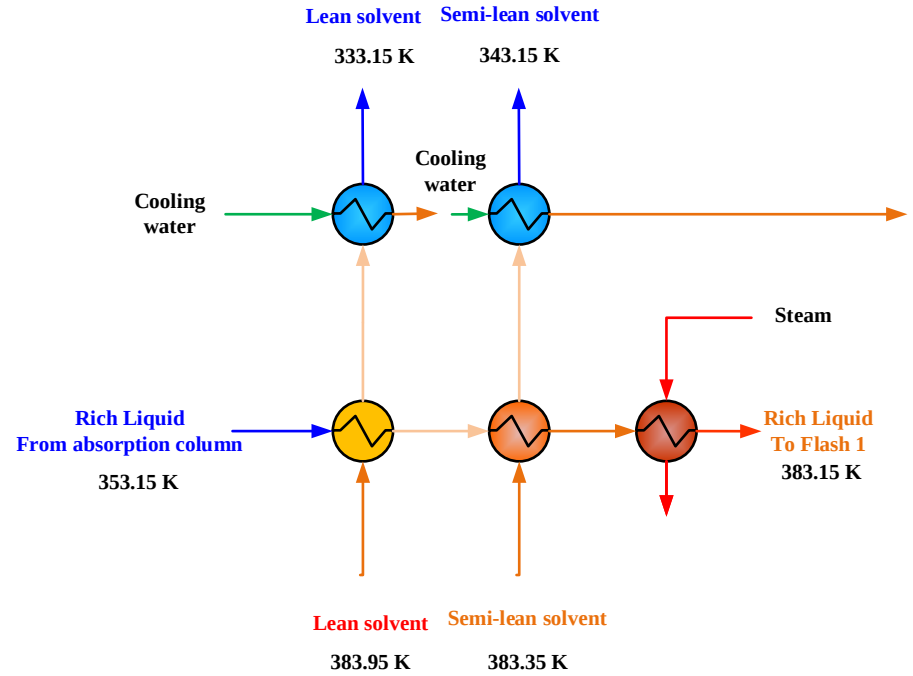

(b)

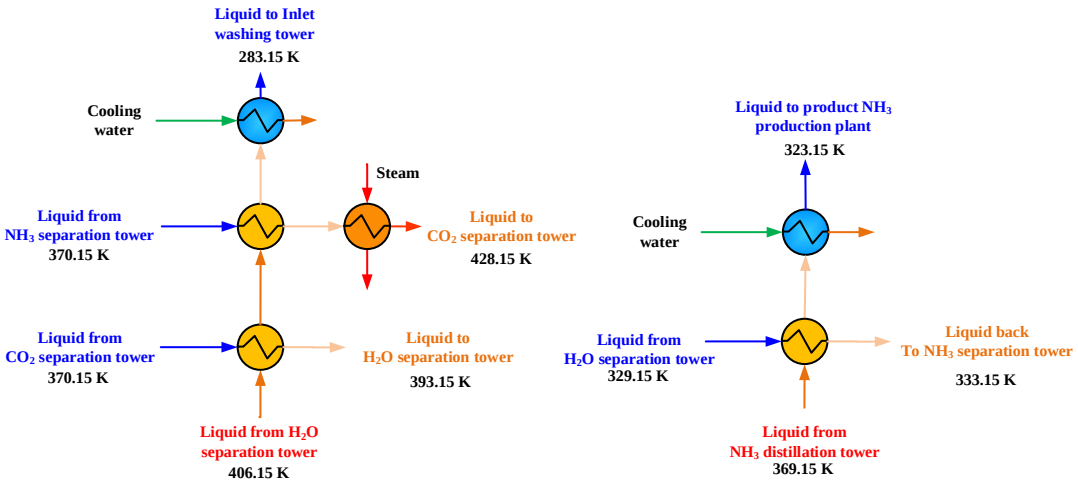

(c)

Figure S1 The flow chart of modification HEN. (a) IL-0 process; (b) IL-En process; (c) WS process.

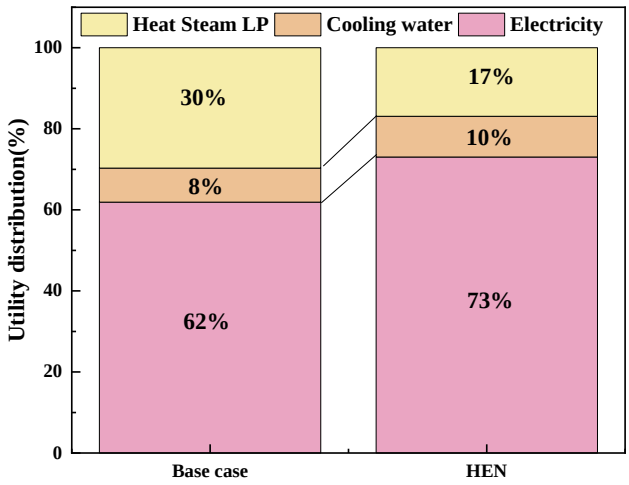

Figure S2 The utilities cost distribution of IL-En process in base case and HEN

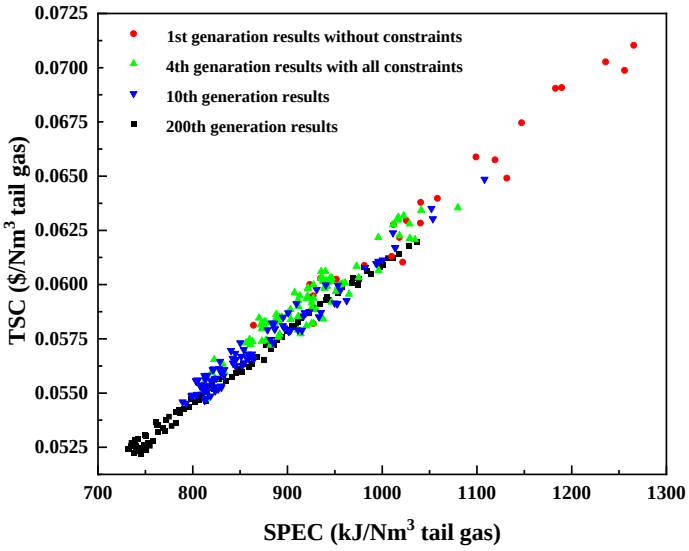
1st genaration results without constraints
4th genaration results with all constraints
10th generation results
200th generation results
TSC ($/Nm3 tail gas)
SPEC (kJ/Nm3 tail gas)
0.0725
0.0700
0.0675
0.0650
0.0625
0.0600
0.0575
0.0550
0.0525
700
800
900
1000
1100
1200
1300

(a)

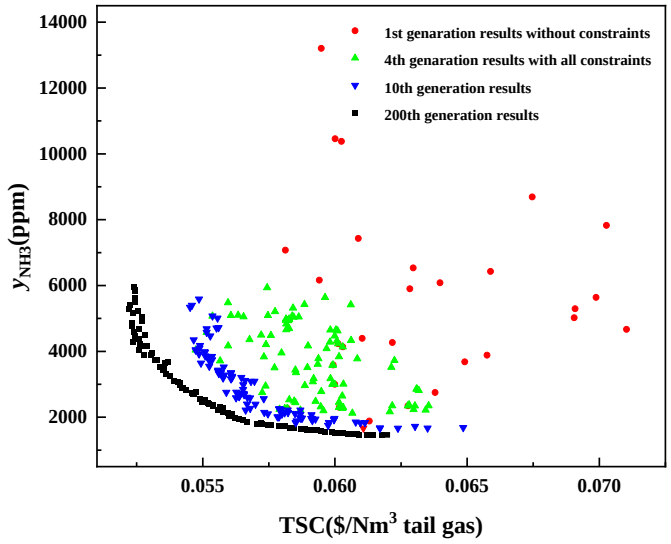
1st genaration results without constraints
4th genaration results with all constraints
10th generation results
200th generation results
yNH3(ppm)
TSC($/Nm3 tail gas)
14000
12000
10000
8000
6000
4000
2000
0.055
0.060
0.065
0.070

(b)

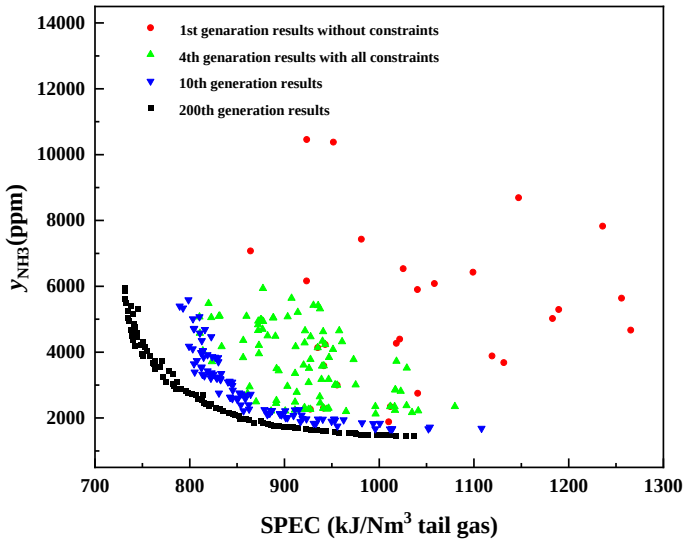

(c)

Figure S3 The relationship between the purified gas of NH_3, SPEC and TSC.